

THREE-DIMENSIONAL ANALYSIS OF MOORED CYLINDERS
USED AS BREAKWATERS

by
Timothy Wayne Mays

Thesis submitted to the Faculty of the
Virginia Polytechnic Institute and State University
in partial fulfillment of the requirements for the degree of
Master of Science
in
Civil Engineering

APPROVED:

Dr. Raymond H. Plaut, Chairman

Dr. Stergios I. Liapis, Co-Chairman

Dr. Kamal B. Rojiani

December, 1997

Blacksburg, Virginia

Keywords: Breakwater, Cylinder, Vibration, Wave, Mooring

THREE-DIMENSIONAL ANALYSIS OF MOORED CYLINDERS USED AS BREAKWATERS

Timothy Wayne Mays

(ABSTRACT)

For oblique and normal water waves at various frequencies, the use of moored cylinders as breakwaters is considered numerically using linear three-dimensional analysis. The breakwater can be used by itself for protection of small structures or as a series of cylinders to protect a harbor, shoreline, or moored vessel from the destructive energy associated with incident water waves. The breakwater is completely submerged below the free surface and is attached to the ocean floor with six symmetrically configured mooring lines. The cylinder is filled with air and the mooring lines remain taut during the structure's motion. Six degrees of freedom describe the motion of the breakwater and additional degrees of freedom are introduced as the cables are modeled with the use of lumped masses connected with springs. The fluid is assumed to be inviscid and incompressible, so that the velocity field can be written as the gradient of the velocity potential. A boundary integral method is used to solve the integral equations that define the external fluid flow. Free vibrations of the cylinder in both air and water are considered and "dry" and "wet" natural frequencies are computed. Motions caused by water waves are studied to establish the effect of certain parameters on the effectiveness of the breakwater. The transmission coefficient is shown to be somewhat misleading when compared to plots that show the spatial variation of the wave amplitude.

ACKNOWLEDGMENTS

There are several individuals who greatly influenced the work of this thesis. Firstly, I would like to thank Dr. Plaut for allowing me to work on this topic and providing me the guidance and assistance which I needed to complete the task. I truly appreciate his patience with me and the “open door” policy he holds for all of his students. Dr. Liapis also helped guide me through the research. His expertise in ocean engineering proved instrumental in helping to efficiently solve problems that often arose. I would also like to thank Dr. Rojiani for being on my graduate committee, Dr. J.Y. Kim for his help with FORTRAN, and Fata Dewi for her help with the fluids code. Lastly, I would like to thank my family for their continued support, faith, and prayers, and God for His continued blessings.

This research was supported by the National Science Foundation under Grant No. BES-9521425. Support from the Via Endowment Fund is also greatly appreciated.

TABLE OF CONTENTS

Chapter 1	Introduction	1
1.1	Purpose	1
1.2	Proposed Breakwater	1
Chapter 2	Literature Review	2
2.1	Floating Breakwaters	2
2.2	Moored Structures Used as Breakwaters	3
2.2.1	Williams and McDougal Breakwater	3
2.2.2	Yamamoto and Yoshido	4
2.3	Moored Cylindrical Breakwaters	5
2.3.1	Evans' Cylinder	5
2.3.2	Bristol Cylinder	6
2.4	Flexible Cylinders Used as Breakwaters	6
2.5	Mooring Systems	7
2.6	Need for Further Research	7
Chapter 3	Static Equilibrium and Lumped Masses	9
3.1	Breakwater Configuration	9
3.2	Mooring Lines Modeled as Massless Springs	9
3.3	Mooring Lines Modeled as Springs with One Mass Per Cable	11
3.4	Mooring Lines Modeled as Springs with N-1 Masses Per Cable	13
3.5	Results	14
Chapter 4	Free Vibration of Breakwater in Air	20
4.1	Initial Configuration	20
4.2	General Configuration	20
4.3	Cylinder Rotation (Euler Angles)	20
4.4	Angular Velocities	23
4.5	Mooring Line Energy	24
4.6	Energy of the Cylinder	25
4.7	Lagrange's Equations	26

4.8	Small Motions About Equilibrium (Linearized Equations)	38
4.9	Standard Case	46
4.10	Case A (Massless Lines)	47
4.11	Case B (One Mass Per Line)	49
4.12	Case C (Two Masses Per Line)	50
Chapter 5	Problem Theory and Development	60
5.1	General Overview	60
5.2	Linear Wave Theory and Fluid Behavior	61
5.3	External Fluid Characteristics	62
5.4	Determination of Force, Added Mass, and Damping Elements	64
5.5	Solving for Response Amplitudes of the Breakwater in Water	64
5.6	Procedure Validation	65
Chapter 6	Analysis of the “Standard Case” Breakwater	75
6.1	Breakwater Modeling	75
6.2	Free Vibration in Water	75
6.3	Forced Vibration of the Breakwater	78
6.4	Hydrodynamic Coefficients: Added Mass and Damping	78
6.5	Hydrodynamic Forces	79
6.6	Structural Response: Response Amplitude Operator (RAO)	79
6.7	Influence of Structure on Water Waves	80
6.8	Free Surface Elevation Amplitude	80
6.9	Free Surface Elevation Plots	82
Chapter 7	Analysis of Two “Standard Case” Breakwaters in Series	186
7.1	Introduction to Using Multiple Cylinders	186
7.2	Transmission Coefficient and Free Surface Elevation Amplitudes	186

7.3	Free Surface Elevation Plots	188
Chapter 8	Conclusions and Recommendations for Further Work	232
References		234
Vita		241

LIST OF FIGURES

Figure 3.1	The Inflatable Breakwater	17
Figure 3.2	System Profile (Massless Mooring Lines)	17
Figure 3.3	System Elevation (Massless Mooring Lines)	18
Figure 3.4	System Profile (One Mass Per Mooring Line)	18
Figure 3.5	System Elevation (One Mass Per Mooring Line)	19
Figure 3.6	Relationship Between Net Buoyant Force and Equilibrium Height for Different Cable Diameters	19
Figure 4.1	“Unstretched Springs” Configuration – General System	52
Figure 4.2	General Configuration During Motion	52
Figure 4.3	Euler Angles	53
Figure 4.4	Cylinder Dimensions	53
Figure 4.5	Mooring Line Identification	54
Figure 4.6	Mode Shape (First Eigenvector – Case A)	54
Figure 4.7	Mode Shape (Second Eigenvector – Case A)	55
Figure 4.8	Mode Shape (Fourth Eigenvector – Case A)	55
Figure 4.9	Mode Shape (Sixth Eigenvector – Case A)	56
Figure 4.10	Natural Frequency (Nondimensional) vs. L/R – Case A	56
Figure 4.11	Natural Frequency (Nondimensional) vs. K (Nondimensional) – Case A	57
Figure 4.12	Mode Shape (First Eigenvector – Case B)	57
Figure 4.13	Mode Shape (Second Eigenvector – Case B)	58
Figure 4.14	Mode Shape (Fourth Eigenvector – Case B)	58
Figure 4.15	Mode Shape (Fifth Eigenvector – Case B)	59
Figure 4.16	Mode Shape (Sixth Eigenvector – Case B)	59
Figure 5.1	New Coordinate System for Breakwater Showing Incident Wave Direction β	67
Figure 5.2	Amplitude of Free Surface Elevation for $\omega=\omega_n=1.25$ rad/s (304.8 m Breakwater, $\beta=0^\circ$)	68
Figure 5.3	Free Surface Elevation for $\omega=\omega_n=1.25$ rad/s (304.8 m Breakwater, $\beta=0^\circ$)	69

Figure 6.1	Nondimensional Added Mass Matrix Element A(1,1) vs. kR	85
Figure 6.2	Nondimensional Added Mass Matrix Element A(2,2) vs. kR	86
Figure 6.3	Nondimensional Added Mass Matrix Element A(3,3) vs. kR	87
Figure 6.4	Nondimensional Added Mass Matrix Element A(4,4) vs. kR	88
Figure 6.5	Nondimensional Added Mass Matrix Element A(5,5) vs. kR	89
Figure 6.6	Nondimensional Damping Matrix Element C(1,1) vs. kR	90
Figure 6.7	Nondimensional Damping Matrix Element C(2,2) vs. kR	91
Figure 6.8	Nondimensional Damping Matrix Element C(3,3) vs. kR	92
Figure 6.9	Nondimensional Damping Matrix Element C(4,4) vs. kR	93
Figure 6.10	Nondimensional Damping Matrix Element C(5,5) vs. kR	94
Figure 6.11	Nondimensional Hydrodynamic Forces vs. kR, $\beta=0^\circ$	95
Figure 6.12	Nondimensional Hydrodynamic Forces vs. kR, $\beta=15^\circ$	96
Figure 6.13	Nondimensional Hydrodynamic Forces vs. kR, $\beta=30^\circ$	97
Figure 6.14	RAO's vs. kR, $\beta=0^\circ$	98
Figure 6.15	RAO's vs. kR, $\beta=15^\circ$	99
Figure 6.16	RAO's vs. kR, $\beta=30^\circ$	100
Figure 6.17	Transmission Coefficient vs. kR	101
Figure 6.18	Amplitude of Free Surface Elevation for $\omega=\omega_n=1.25$ rad/s (9.144 m Breakwater, $\beta=0^\circ$)	102
Figure 6.19	Amplitude of Free Surface Elevation for $\omega=1.85$ rad/s (9.144 m Breakwater, $\beta=0^\circ$)	103

Figure 6.20	Amplitude of Free Surface Elevation for $\omega=2.05$ rad/s (9.144 m Breakwater, $\beta=0^\circ$)	104
Figure 6.21	Amplitude of Free Surface Elevation for $\omega=\pi/2$ rad/s (9.144 m Breakwater, $\beta=0^\circ$)	105
Figure 6.22	Amplitude of Free Surface Elevation for $\omega=\omega_n=1.25$ rad/s (9.144 m Breakwater, $\beta=15^\circ$)	106
Figure 6.23	Amplitude of Free Surface Elevation for $\omega=1.85$ rad/s (9.144 m Breakwater, $\beta=15^\circ$)	107
Figure 6.24	Amplitude of Free Surface Elevation for $\omega=2.05$ rad/s (9.144 m Breakwater, $\beta=15^\circ$)	108
Figure 6.25	Amplitude of Free Surface Elevation for $\omega=\pi/2$ rad/s (9.144 m Breakwater, $\beta=15^\circ$)	109
Figure 6.26	Amplitude of Free Surface Elevation for $\omega=\omega_n=1.25$ rad/s (9.144 m Breakwater, $\beta=30^\circ$)	110
Figure 6.27	Amplitude of Free Surface Elevation for $\omega=1.85$ rad/s (9.144 m Breakwater, $\beta=30^\circ$)	111
Figure 6.28	Amplitude of Free Surface Elevation for $\omega=2.05$ rad/s (9.144 m Breakwater, $\beta=30^\circ$)	112
Figure 6.29	Amplitude of Free Surface Elevation for $\omega=\pi/2$ rad/s (9.144 m Breakwater, $\beta=30^\circ$)	113
Figure 6.30	Free Surface Elevation for $\omega=\omega_n=1.25$ rad/s (9.144 m Breakwater, $\beta=0^\circ$)	114
Figure 6.31	Free Surface Elevation for $\omega=1.85$ rad/s (9.144 m Breakwater, $\beta=0^\circ$)	120
Figure 6.32	Free Surface Elevation for $\omega=2.05$ rad/s (9.144 m Breakwater, $\beta=0^\circ$)	126
Figure 6.33	Free Surface Elevation for $\omega=\pi/2$ rad/s (9.144 m Breakwater, $\beta=0^\circ$)	132
Figure 6.34	Free Surface Elevation for $\omega=\omega_n=1.25$ rad/s (9.144 m Breakwater, $\beta=15^\circ$)	138

Figure 6.35	Free Surface Elevation for $\omega=1.85$ rad/s (9.144 m Breakwater, $\beta=15^\circ$)	144
Figure 6.36	Free Surface Elevation for $\omega=2.05$ rad/s (9.144 m Breakwater, $\beta=15^\circ$)	150
Figure 6.37	Free Surface Elevation for $\omega=\pi/2$ rad/s (9.144 m Breakwater, $\beta=15^\circ$)	156
Figure 6.38	Free Surface Elevation for $\omega=\omega_n=1.25$ rad/s (9.144 m Breakwater, $\beta=30^\circ$)	162
Figure 6.39	Free Surface Elevation for $\omega=1.85$ rad/s (9.144 m Breakwater, $\beta=30^\circ$)	168
Figure 6.40	Free Surface Elevation for $\omega=2.05$ rad/s (9.144 m Breakwater, $\beta=30^\circ$)	174
Figure 6.41	Free Surface Elevation for $\omega=\pi/2$ rad/s (9.144 m Breakwater, $\beta=30^\circ$)	180
Figure 7.1	Two Breakwaters in Series Showing Incident Wave Angle β	189
Figure 7.2	Amplitude of Free Surface Elevation for $\omega=\omega_n=1.25$ rad/s (Two 9.144 m Breakwaters, 1.22 m Gap, $\beta=0^\circ$)	190
Figure 7.3	Amplitude of Free Surface Elevation for $\omega=\omega_n=1.25$ rad/s (Two 9.144 m Breakwaters, 1.22 m Gap, $\beta=15^\circ$)	191
Figure 7.4	Amplitude of Free Surface Elevation for $\omega=\omega_n=1.25$ rad/s (Two 9.144 m Breakwaters, 1.22 m Gap, $\beta=30^\circ$)	192
Figure 7.5	Amplitude of Free Surface Elevation for $\omega=\omega_n=1.25$ rad/s (Two 9.144 m Breakwaters, 6.1 m Gap, $\beta=0^\circ$)	193
Figure 7.6	Amplitude of Free Surface Elevation for $\omega=\omega_n=1.25$ rad/s (Two 9.144 m Breakwaters,	194

	6.1 m Gap, $\beta=15^\circ$)	
Figure 7.7	Amplitude of Free Surface Elevation for $\omega=\omega_n=1.25$ rad/s (Two 9.144 m Breakwaters, 6.1 m Gap, $\beta=30^\circ$)	195
Figure 7.8	Free Surface Elevation for $\omega=\omega_n=1.25$ rad/s (Two 9.144 m Breakwaters, 1.22 m Gap, $\beta=0^\circ$)	196
Figure 7.9	Free Surface Elevation for $\omega=\omega_n=1.25$ rad/s (Two 9.144 m Breakwaters, 1.22 m Gap, $\beta=15^\circ$)	202
Figure 7.10	Free Surface Elevation for $\omega=\omega_n=1.25$ rad/s (Two 9.144 m Breakwaters, 1.22 m Gap, $\beta=30^\circ$)	208
Figure 7.11	Free Surface Elevation for $\omega=\omega_n=1.25$ rad/s (Two 9.144 m Breakwaters, 6.1 m Gap, $\beta=0^\circ$)	214
Figure 7.12	Free Surface Elevation for $\omega=\omega_n=1.25$ rad/s (Two 9.144 m Breakwaters, 6.1 m Gap, $\beta=15^\circ$)	220
Figure 7.13	Free Surface Elevation for $\omega=\omega_n=1.25$ rad/s (Two 9.144 m Breakwaters, 6.1 m Gap, $\beta=30^\circ$)	226

LIST OF TABLES

Table 3.1	Equilibrium Height ($D=0.75$ inches, $W/W_0=150$)	14
Table 3.2	Angles Made with Horizontal by Cables Shown in Figure 4.5	15
Table 6.1	Comparison of Dry and Wet Natural Frequencies	76
Table 7.1	Transmission Coefficients for $\omega=1.25$ rad/s	187

CHAPTER 1 INTRODUCTION

1.1 PURPOSE

This thesis considers the feasibility of using inflatable, submerged, moored structures as breakwaters. These structures can be used to protect the shoreline from erosion, and near-shore and offshore structures from damaging waves caused by severe storms. They can be used continuously or, when not in use, deflated and out of the way.

Although most existing breakwaters are rigid structures that are fixed to the ocean floor and project above the water surface, the shift has been towards more temporary, transportable breakwaters. Inflatable breakwaters have numerous advantages. They are easy to install, cost-efficient, and can be filled with air, water, or some combination of the two.

1.2 PROPOSED BREAKWATER

The structural configuration and components of the proposed breakwater are defined in Chapter 3. Nevertheless, it is necessary to briefly describe the subject of this thesis here to make the literature review of Chapter 2 more relevant.

Ideally, the structure will be a cylindrical breakwater tied to the ocean floor with six symmetrically attached mooring lines. The structure is completely submerged and it is assumed that the structure is under sufficient internal pressure to act as a rigid body. It is filled with air.

CHAPTER 2 LITERATURE REVIEW

2.1 FLOATING BREAKWATERS

A floating breakwater is one of several types of structures that can be used for wave control. The first floating breakwater appeared in 1811 at Plymouth Port in England. During World War II, Bombardon floating breakwaters were used along the Normandy coast (Sawaragi 1995). The structures were designed, tested, and readied for use in a relatively short period of time. Until a severe storm reached the area, the breakwaters performed as intended (Naval Facilities 1971). In 1930, Japan placed the first floating breakwater in Aomori Port to test the structure's resistance to waves and the wave dissipation function (Sawaragi 1995).

There are several types of floating breakwaters, which include box, pontoon, mat, and tethered float. Box-type breakwaters are usually constructed of reinforced concrete. They generally act as barges, which dissipate energy at the wave surface. Advantages of this type of breakwater are numerous and include a fifty-year design life, simple construction, proven performance, and effectiveness under "moderate" wave conditions. The only major disadvantage of the box-type breakwater is its relatively high cost in comparison to the other types of floating breakwaters (McCartney 1985).

The pontoon breakwater, which is often referred to as the Alaska or ladder type (for its ladder-like appearance on the water surface), is smaller, less effective, and generally less expensive than most types of floating breakwaters. Tests on these structures caution the designer to avoid certain length-to-width ratios, which could yield a very inefficient structure.

The Maze, Goodyear, and Wave-Guard tire mat breakwaters have been constructed and tested. As the name implies, the interlocked tire layout looks like a mat on the ocean surface. These structures have a relatively low cost, are easily removable for maintenance, and only require unskilled labor for their construction. On the other hand, they have a short design life, frequently lose buoyancy due to the loss of air in the tire crown, and are only effective under mild wave conditions. In addition, litter entrapment is a major drawback with this type of breakwater (McCartney 1985).

The final type of breakwater, and subject of this thesis, is the tethered (moored) floating breakwater, which McCartney claims lacks sufficient prototype experience for a

detailed analysis. For reference, McCartney's paper concludes with costs and designs for prototype installation of the aforementioned types of breakwaters. This includes the most effective layout pattern in a bay or basin (McCartney 1985).

The preceding breakwater classifications primarily concern rigid structures. However, Sawaragi (1995) includes inflatable (flexible) structures and further categorizes them by their functions, which include wave reflection, wave breaking, friction, jet mixing, and establishing resonance.

The aim of this section was to familiarize the reader with the numerous portable devices used as breakwaters. However, the list of structures described in the literature is quite exhaustive and rather than focus on these structures, it is more beneficial to examine certain configurations more similar to the submerged, cylindrical breakwater investigated in this thesis.

2.2 MOORED STRUCTURES USED AS BREAKWATERS

There are several papers dealing with moored structures used for dissipating wave energy. However, most consider structures that are floating on the surface and are only partially submerged in water. Also, many of the structures described do not have a circular cross-section. Nevertheless, given their applicability to the material discussed herein, two such models are considered in detail.

Frederiksen (1971), Williams, et al. (1997), Harms (1979), Thompson, et al. (1992), Murakami, et al. (1996), Atzeni, et al. (1996), Williams (1996), Ren, et al. (1994), Lau, et al. (1990), Triantafyllou, et al. (1994), Isaacson, et al. (1996), Kato, et al. (1969), Saito, et al. (1996), Murali, et al. (1997), Lipsett, et al. (1991), Nagata, et al. (1983), Idris, et al. (1996), Vethamony (1995), and Valioulis (1990) deal primarily with the performance and effectiveness of various moored structures used for wave attenuation. Other papers that deal with moored structures, but are primarily concerned with the effect of various mooring systems, include Wilson, et al. (1971), Gottlieb, et al. (1992), Gottlieb, et al. (1993), Gottlieb, et al. (1997), Chung (1997), Szelangiewicz (1991), Masuda, et al. (1995), and Headland, et al. (1991).

2.2.1 WILLIAMS AND McDUGAL BREAKWATER

Williams and McDougal (1996) consider a long, tethered breakwater that has a rectangular cross section and can be either submerged or surface-piercing (partially

floating). Only surge, heave, and pitch motions of the structure in two dimensions are considered. Small-scale tests are used to verify the theory and “reasonable” agreement is found.

The prismatic breakwater is located some distance from the ocean surface. In addition, the breakwater is attached to the ocean floor by linear springs. The major assumption made by the authors deals with the structure’s degrees of freedom. It is assumed that the structure will respond linearly only in surge, heave, and pitch. The structure is excited by a series of small amplitude waves.

The main conclusions found in this paper deal with the surge response of the structure. The lowest transmission coefficient (ratio of incident wave amplitude to wave amplitude behind the structure), around 0.5, is found when the structure is excited near the surge natural frequency of the structure. However, this nominal effectiveness is concluded to only exist for a narrow band of wave periods. As a result, this structure is deemed effective only if the stiffness of the structure (mooring lines) could be altered readily for various incident wave frequencies.

2.2.2 YAMAMOTO AND YOSHIDA

Yamamoto and Yoshida (1979) experimentally consider two specific cases and examine the wave attenuation characteristics of each structure. Neither of the two structures considered is completely submerged. The first case is a three-circle cylinder (three different circular cross-sections along its length) with various mooring configurations. In contrast to the cylindrical structures that will be discussed in the following section, and the breakwater of this thesis, the longitudinal axis of the cylinder is in the direction of wave propagation. Springs are used to attach the structure to the floor. Various mooring line configurations are considered and even cross-mooring is used in one instance. The second structure is a rectangular cylinder, which is moored to the floor as well.

For the circular breakwater, the large “sway and roll” motion of the structure contributes to its effectiveness. Zero transmission coefficients occur at low frequencies. However, the bandwidth is once again very small. The rectangular breakwater is very effective at the frequencies corresponding to heave and to combined sway and roll. The system is effective for waves shorter than five times the length of the breakwater.

2.3 MOORED CYLINDRICAL BREAKWATERS

Several authors have considered the feasibility of using both rigid and flexible cylinders as breakwaters and have commented on their eminent wave-dissipating characteristics. Some studies are concerned with surface-piercing cylinders, while others deal with breakwaters completely submerged some distance below the ocean surface. However, most of the research done in these areas is either primarily experimental or considers two-dimensional motions analytically for an infinitely long cylinder. Three-dimensional effects are neglected and only heave, sway, and sometimes surge are considered as displacement modes. These two assumptions are readily questioned for oblique seas. In addition, in order to use submerged cylinders as breakwaters, they must be short enough to be effectively tied to the ocean floor and they must be placed in series with one another to provide enough protection to a given area. Nevertheless, the following papers serve well as an introduction to these breakwaters and manifest the possibilities such structures bring to the rapidly-growing breakwater industry.

2.3.1 EVANS' CYLINDER

Using a two-dimensional analysis, Evans (1979) considers a long, submerged, cylindrical breakwater that is constrained by springs and dampers so that only small oscillations are possible. Linear water wave theory is used, along with the assumption that the structure only exhibits heave and sway. Experimental results are included in the paper, which verify most conclusions.

It is effectively shown that a submerged cylinder can, under a broad bandwidth, be very efficient in absorbing wave energy. In fact, a maximum efficiency of 100% is found for an infinitely long cylinder, which corresponds to a transmission coefficient of zero. The paper also focuses on the fact that the structure is most effective at the “tuning frequency” (when the wave frequency is equal to a natural frequency of the cylinder in water).

Although this paper makes various rudimentary assumptions, it still serves well as a validation for the work included in this thesis. In fact, Section 4.4 deals primarily with this procedure.

2.3.2 BRISTOL CYLINDER

Davis, et al. (1981) consider a moored horizontal breakwater normal to the incident waves as an energy-dissipating device. Two-dimensional linear wave theory is used alongside both two and three-dimensional experimental results. The efficiency of the cylinder is determined as a function of the wave period for several clearances (defined as the distance between the top of the cylinder and the ocean surface). The results show that the structure is most effective close to the surface. However, the authors openly admit that the experimental results are only a fair validation of theoretical results at best.

2.4 FLEXIBLE STRUCTURES USED AS BREAKWATERS

Although this thesis considers the effectiveness of rigid cylinders used as breakwaters, it is still useful to examine some of the research dealing with flexible structures. The breakwater described in Section 1.1 is inflatable and out of the way when not in use. It is assumed that the structure is under enough internal pressure that the structure's dominant modes are rigid body displacements. This is discussed in more detail later.

Lo (1981) considers a horizontal cylinder of infinite length filled with a fluid of specific gravity 0.9 and completely submerged in water. The cylinder is treated as a membrane and is pressurized. Heave and sway are considered, along with the flexible vibration modes. However, no radiation effects due to rigid body motion are included and the dissertation focuses primarily on the flexibility of the structure.

Kim and Kee (1997) consider oblique waves interacting with a tensioned, vertical flexible membrane using two-dimensional, linear water wave theory. Both submerged and surface-piercing buoys are considered. Although the authors consider effective, practical structures, a two-dimensional analysis is insufficient for such small structures.

Ergin, et al. (1992) provide a very complete examination of the dynamic characteristics of a flexible cylinder vibrating in water at some finite depth. The theoretical derivations are made using three-dimensional analysis. The paper manifests the effect that water plays in natural frequency values and mode shapes.

Dewi (1997) considers the effectiveness of a flexible semi-cylindrical bottom-mounted breakwater under certain depths of water. The structure is submerged and has a radius of 4 m and a length of 150 m. The response of the structure is considered for both

normal and oblique waves using a three-dimensional analysis. The results show that this structure can be effective in dissipating energy and thus in reducing incident wave intensity. By considering a structure of finite length using three-dimensional analysis, the author shows clearly the importance that end effects have on wave dissipation for oblique and normal waves.

Liapis, et al. (1996) examine the effectiveness of a flexible mound acting as a wave attenuation device. The structure is hemicircular and a two-dimensional analysis is used. The results are compared to those obtained by using the same structure modeled as a rigid body and it is found that the flexible membrane is more effective.

2.5 MOORING SYSTEMS

There are numerous methods used to model mooring lines and their characteristics. For the breakwater of this thesis, the mooring lines that are part of the configuration are modeled as both massless springs and a series of lumped masses connected by springs. The effects are discussed in Chapters 3 and 4.

Several papers speak of the effectiveness of cable systems as mooring components and include Dercksen, et al. (1994), Ansari (1980), Bernitsas, et al. (1995), Szelangiewicz (1996), and Chaplin, et al. (1992). Studies dealing with modeling mooring lines with lumped masses include Berteaux (1976), Van Den Boom, et al. (1987), Driscoll, et al. (1996), Thomas, et al. (1994), Huang, et al. (1994), Kato, et al. (1986), Nakajima (1986), Ansari, et al. (1986), Chen et al. (1986), Nath, et al. (1975), McLauchlan, et al. (1973), Inoue, et al. (1991), Thresher, et al. (1975), Leonard, et al. (1981), Nuckolls, et al. (1977), Nakajima, et al. (1982), Van Den Boom (1985), Choo, et al. (1973), Migliore, et al. (1979), and Takikawa (1995).

2.6 NEED FOR FURTHER RESEARCH

The previously discussed papers show clearly the possibilities that abound for the use of moored cylindrical breakwaters for ocean wave control. However, most experimental results do not replicate numerical calculations. This is due primarily to the assumptions made by most researchers. For a two-dimensional analysis to be adequate for a moored cylindrical breakwater, the structure must be very long so that end effects are negligible and the structure primarily undergoes heave and sway. In addition, very little is said about oblique incidence angles, which are commonly encountered by

breakwaters. In this case, end effects are quite important. Finally, the structure should be small enough so that its implementation is feasible. However, more than just one breakwater is usually required to protect a specific region. In this case they should be placed side by side where their motions are coupled and they tend to act more like one long cylinder.

CHAPTER 3 STATIC EQUILIBRIUM AND LUMPED MASSES

3.1 BREAKWATER CONFIGURATION

Given that all motion undertaken by the inflatable breakwater will be considered relative to its static equilibrium position, this configuration should first be established. The analysis will also serve as a means of determining proper theoretical assumptions which in turn will help provide efficient design considerations. The structure shown in Figure 3.1 consists of a rigid cylindrical body tied to the ocean floor by six mooring lines connected symmetrically to the structure. As suggested in Figure 3.1, the two cables attached to the bottom of the cylinder remain in a vertical plane that cuts through the cylinder's axis. Also, the other lines remain in the plane established by their independent cylinder's end. More simply put, a top view of the system would seemingly present two cables perpendicular to the other four, yet collinear with each other. The structure is considered as if in air with an upward force equal to a net buoyant force acting through the object's center of mass.

This leads to the question of how the mooring lines should be modeled. It is assumed that for a large net buoyant force as will most definitely result, a discrete system using a relatively small number of masses will suffice. In fact, it may be proven equally valid that the lines themselves can be considered massless while not altering the equilibrium results significantly. This hypothesis can be easily verified by considering three discrete models. Case A (Section 3.2) assumes the lines are massless and that they provide a linearly elastic resistance to the structure's motion. Cases B and C (Sections 3.3 and 3.4, respectively) provide lumped masses along the length of the mooring line. Finally, a program developed in FORTRAN is used to solve for the equilibrium configurations of each case, and the results are compared.

3.2 MOORING LINES MODELED AS MASSLESS SPRINGS

Case A assumes that the weight of the mooring lines can be neglected and that the lines can be modeled by linear springs. This is somewhat counter-intuitive, given that the shape of lines often used in offshore projects is a catenary (i.e., an anchor line). However, the large net upward force acting on the structure may prove the assumption's validity. On the other hand, it should be noted at this point that even if the assumption is

valid for determining the static equilibrium configuration, the assumption must be reconsidered for structural motion. The drag forces that act on the mooring lines will cause the lines to deflect nonlinearly. Nevertheless, the drag force acting on the much larger cylindrical body, along with the extremely large net buoyant force, could make the assumption valid for both cases.

Figures 3.2 and 3.3 show the profile and elevation views of the system, respectively. The cylinder of radius R and length L is tied symmetrically to the floor by six springs. Four of the springs have a stiffness K_{21} and the other two have a stiffness K_{11} . The lengths a , b , and h along with the angles β and γ are also shown in Figures 3.2 and 3.3. In all three cases to be considered, when the cylinder's weight and the buoyancy are assumed to be inactive, the springs are unstretched and a subscript 0 is added to some geometrical quantities (e.g., the bottom of the cylinder has a height h_0 in case A) to specify the initial condition.

Under the net buoyant force, the symmetrical tension in the cables, T_{11} and T_{21} , can be obtained by

$$T_{11} = k_{11}(\sqrt{h^2 + a^2} - \sqrt{h_0^2 + a^2}) \quad (3.1)$$

$$T_{21} = k_{21}(\sqrt{(h+R)^2 + b^2} - \sqrt{(h_0+R)^2 + b^2}) \quad (3.2)$$

In addition, the resulting angles of static equilibrium can be found as

$$\tan \gamma = \frac{h}{a} \quad (3.3)$$

$$\tan \beta = \frac{h+R}{b} \quad (3.4)$$

Now, applying the net buoyancy acting on the structure, w , and summing vertical forces acting on the cylinder yields

$$w = 2T_{11} \frac{h}{\sqrt{h^2 + a^2}} + 4T_{21} \frac{h+R}{\sqrt{(h+R)^2 + b^2}} \quad (3.5)$$

In order to nondimensionalize (3.5), the following terms are introduced:

$$A = \frac{a}{R}, B = \frac{b}{R}, H_0 = \frac{h_0}{R}, H = \frac{h}{R}, W = \frac{w}{w_n}, K_{ij} = \frac{k_{ij}R}{w_n} \quad (3.6)$$

where the cylinder radius R and a nominal standard weight w_n are used to make the transformation which results in

$$W = 2K_{11}(\sqrt{H^2 + A^2} - \sqrt{H_0^2 + A^2}) \frac{H}{\sqrt{H^2 + A^2}} + 4K_{21}(\sqrt{(H+1)^2 + B^2} - \sqrt{(H_0+1)^2 + B^2}) \frac{H+1}{\sqrt{(H+1)^2 + B^2}} \quad (3.7)$$

3.3 MOORING LINES MODELED AS SPRINGS WITH ONE MASS PER CABLE

For Case B, the total mass of each cable is replaced by a point mass at the line's midpoint. Figures 3.4 and 3.5 show the structure's configuration and can be used to develop the modeling equations. The lengths a_1 , a_2 , b_1 , b_2 , and L , along with the angles γ_1 , γ_2 , β_1 , and β_2 , describe the structural configuration. It should be noted here that in the equations that follow, capital letters simply denote the variables' aforementioned nondimensional counterpart. Since the development of the cable tension was discussed in the previous section, it will be skipped here.

A summation of vertical forces on the cylinder results in the following equation:

$$W = 2K_{12}(\sqrt{H_{12}^2 + A_2^2} - \sqrt{H_{120}^2 + A_{20}^2}) \frac{H_{12}}{\sqrt{H_{12}^2 + A_2^2}} + 4K_{22}(\sqrt{H_{22}^2 + B_2^2} - \sqrt{H_{220}^2 + B_{20}^2}) \frac{H_{22}}{\sqrt{H_{22}^2 + B_2^2}} \quad (3.8)$$

where the following variables are unknown: H_{12} , H_{22} , A_2 , B_2 .

The masses each provide two new unknowns, but these can be easily determined using simple force summation. Summing vertical forces acting on mass M_{11} results in

$$M_{11} = K_{12}(\sqrt{H_{12}^2 + A_2^2} - \sqrt{H_{120}^2 + A_{20}^2}) \frac{H_{12}}{\sqrt{H_{12}^2 + A_2^2}} - K_{11}(\sqrt{H_{11}^2 + A_1^2} - \sqrt{H_{110}^2 + A_{10}^2}) \frac{H_{11}}{\sqrt{H_{11}^2 + A_1^2}} \quad (3.9)$$

and likewise for mass M_{21} ,

$$\begin{aligned}
M_{21} &= K_{22}(\sqrt{H_{22}^2 + B_2^2} - \sqrt{H_{220}^2 + B_{20}^2}) \frac{H_{22}}{\sqrt{H_{22}^2 + B_2^2}} \\
&- K_{21}(\sqrt{H_{21}^2 + B_1^2} - \sqrt{H_{210}^2 + B_{10}^2}) \frac{H_{21}}{\sqrt{H_{21}^2 + B_1^2}}
\end{aligned} \tag{3.10}$$

where

$$M_{11} = \frac{m_{11}g}{w_n}, M_{21} = \frac{m_{21}g}{w_n} \tag{3.11}$$

Now, a summation of horizontal forces acting on each of the two masses will yield two more equilibrium equations, namely,

$$\begin{aligned}
0 &= K_{12}(\sqrt{H_{12}^2 + A_2^2} - \sqrt{H_{120}^2 + A_{20}^2}) \frac{A_2}{\sqrt{H_{12}^2 + A_2^2}} \\
&- K_{11}(\sqrt{H_{11}^2 + A_1^2} - \sqrt{H_{110}^2 + A_{10}^2}) \frac{A_1}{\sqrt{H_{11}^2 + A_1^2}}
\end{aligned} \tag{3.12}$$

and

$$\begin{aligned}
0 &= K_{22}(\sqrt{H_{22}^2 + B_2^2} - \sqrt{H_{220}^2 + B_{20}^2}) \frac{B_2}{\sqrt{H_{22}^2 + B_2^2}} \\
&- K_{21}(\sqrt{H_{21}^2 + B_1^2} - \sqrt{H_{210}^2 + B_{10}^2}) \frac{B_1}{\sqrt{H_{21}^2 + B_1^2}}
\end{aligned} \tag{3.13}$$

for masses M_{11} and M_{21} , respectively.

The final three required equations can be obtained from the defined system parameters as shown in Figures 3.4 and 3.5:

$$\begin{aligned}
A_1 + A_2 &= A_T \\
B_1 + B_2 &= B_T \\
H_{11} + H_{12} + 1 &= H_{21} + H_{22}
\end{aligned} \tag{3.14}$$

where the subscript T simply denotes the sum of the lengths in the direction considered.

For example, a_T would be equal to the sum of the values a_1 and a_2 shown in Figure 3.4.

3.4 MOORING LINES MODELED AS SPRINGS WITH N-1 MASSES PER CABLE

For Case C, where each cable is composed of n-1 masses, the derivation of the equations required for determining static equilibrium can be seen simply as an extension of Section 3.3. The summation of vertical forces on the cylinder yields

$$W = 2K_{1n}(\sqrt{H_{1n}^2 + A_n^2} - \sqrt{H_{1n0}^2 + A_{n0}^2}) \frac{H_{1n}}{\sqrt{H_{1n}^2 + A_n^2}} + 4K_{2n}(\sqrt{H_{2n}^2 + B_n^2} - \sqrt{H_{2n0}^2 + B_{n0}^2}) \frac{H_{2n}}{\sqrt{H_{2n}^2 + B_n^2}} \quad (3.15)$$

where the following variables are unknown: H_{1n}, H_{2n}, A_n, B_n .

Next the equilibrium equations for each mass must be obtained. Therefore, letting i alternate between 1 and 2 and j vary from 1 to n, the resulting vertical and horizontal equilibrium equations for mass M_{ij} can be found as (3.16) and (3.17), respectively:

$$M_{i(j-1)} = K_{ij}(\sqrt{H_{ij}^2 + A_j^2} - \sqrt{H_{ij0}^2 + A_{j0}^2}) \frac{H_{ij}}{\sqrt{H_{ij}^2 + A_j^2}} - K_{i(j-1)}(\sqrt{H_{i(j-1)}^2 + A_{j-1}^2} - \sqrt{H_{i(j-1)0}^2 + A_{(j-1)0}^2}) \frac{H_{i(j-1)}}{\sqrt{H_{i(j-1)}^2 + A_{j-1}^2}} \quad (3.16)$$

$$0 = K(\sqrt{H_{ij}^2 + A_j^2} - \sqrt{H_{ij0}^2 + A_{j0}^2}) \frac{A_j}{\sqrt{H_{ij}^2 + A_j^2}} - K(\sqrt{H_{i(j-1)}^2 + A_{j-1}^2} - \sqrt{H_{i(j-1)0}^2 + A_{(j-1)0}^2}) \frac{A_{j-1}}{\sqrt{H_{i(j-1)}^2 + A_{j-1}^2}} \quad (3.17)$$

Once again, the final three required equations can be obtained from the defined system parameters:

$$\sum_{i=1}^n A_i = A_T$$

$$\sum_{i=1}^n B_i = B_T \quad (3.18)$$

$$1 + \sum_{j=1}^n H_{1j} = \sum_{j=1}^n H_{2j}$$

3.5 RESULTS

The typical system used to compare the applicability of all three cases consists of a cylinder 30 feet long and 6 feet in diameter tied to the floor using mooring lines made of Kevlar. The initial height of the cylinder from the floor to the cylinder's axis was chosen to be 10 feet. In addition, a_T and b_T were chosen to be 7 feet and 10 feet, respectively, putting all cables at an initial angle of 45° with the floor. For cases B and C, the lumped masses account for the line's total weight and are spread equally along the length of the line. In addition, each spring on a line has a stiffness equal to the other springs on that particular line. Once again, due to the symmetry of the structure, only two different sets of values of masses and springs are specified under these conditions. The FORTRAN program used to solve for the equilibrium positions of the system calls the IMSL subroutine NEQNF which sends back the solutions to the unknowns in the user-provided equations. By changing the diameter D of the cable and specifying initial conditions as required, the program can be used for many different conditions. By considering the typical material properties of both the mooring lines and the cylinder itself, it is easy to see how the net buoyant force on the structure can exceed 50,000 lbs. Therefore, for loads varying from 0 to 225,000 lbs, the static equilibrium configuration of the system was obtained. It should be noted that a value of eight was arbitrarily chosen for n , corresponding to seven masses per cable for Case C. The results show clearly that for the loads considered, the cable's mass plays no significant role on the equilibrium height and the line can be efficiently modeled as a massless spring. Typical values are shown in Table 3.1.

Table 3.1 - Equilibrium Height ($D=0.75$ inches, $W/W_0=150$)

Case Number	Equilibrium Height of Cylinder, H
A	2.4601
B	2.4601
C	2.4601

As expected, however, the lumped mass model does slightly alter the angle of each spring segment. This is established using the same data as above and is shown in Table 3.2.

Table 3.2 - Angles Made with Horizontal by Cables Shown in Figure 3.5

Segment Number, i	Angle, β_i
1	46.5121°
2	46.5129°
3	46.5137°
4	46.5144°
5	46.5152°
6	46.5160°
7	46.5168°
8	46.5176°

Indeed, each segment's angle increases with increasing elevation. Nevertheless, this minute change is trivial and thus justifies neglecting the weight of the cables for equilibrium purposes. Once again, it should be pointed out that this conclusion is only valid for obtaining the equilibrium configuration. Dynamic considerations could prove this assumption invalid.

The effect of the net buoyant force on the equilibrium height is plotted in Figure 3.6 for three values of cable diameter. The curves are almost linear. If the cable diameter is decreased, the equilibrium height increases as expected.

Finally, it is warranted that the reliability of the material in question be considered and limitations be placed on the diameter of the cable and thickness of the cylinder. From the previously derived equilibrium equations, the force in each cable can be easily obtained. For W/W_0 (ratio of net buoyant force to weight of structure in air) equal to 50, which is close to the expected value, and a cable diameter of one inch, a maximum stress of 18,690 psi is obtained. This is acceptable for the material in question, Kevlar.

Nevertheless, for very small diameter cables or large lightweight cylinders, the maximum stress in the cables should always be checked for the applicability of Hooke's Law.

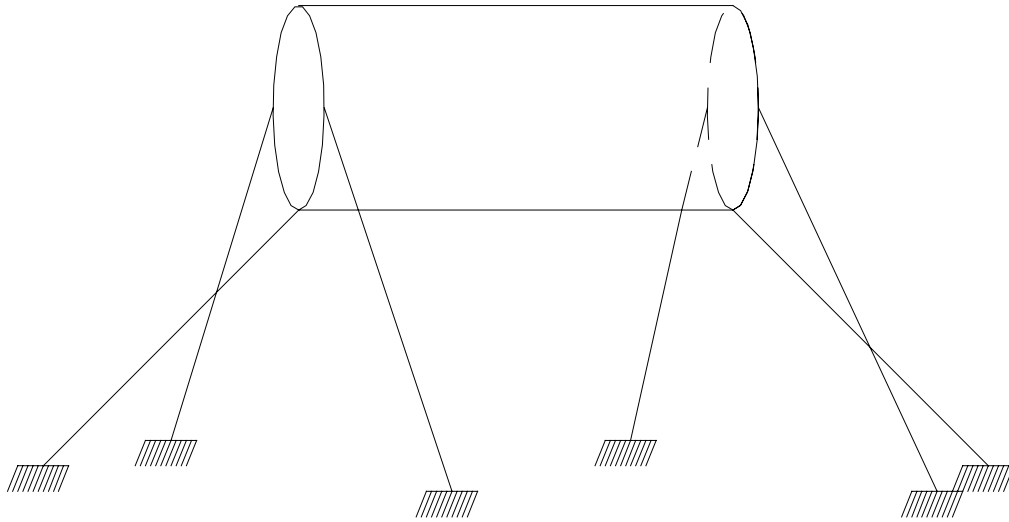


Figure 3.1 – The Inflatable Breakwater

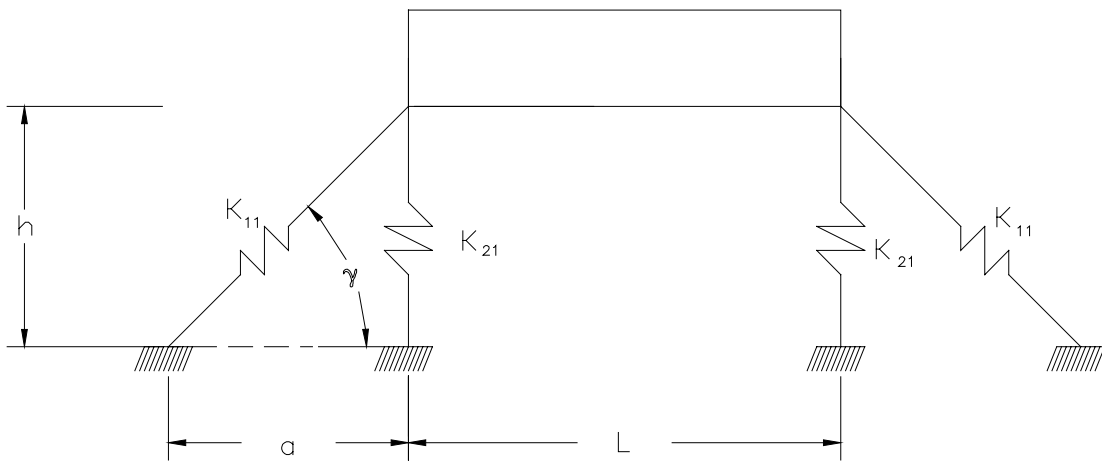


Figure 3.2 – System Profile (Massless Mooring Lines)

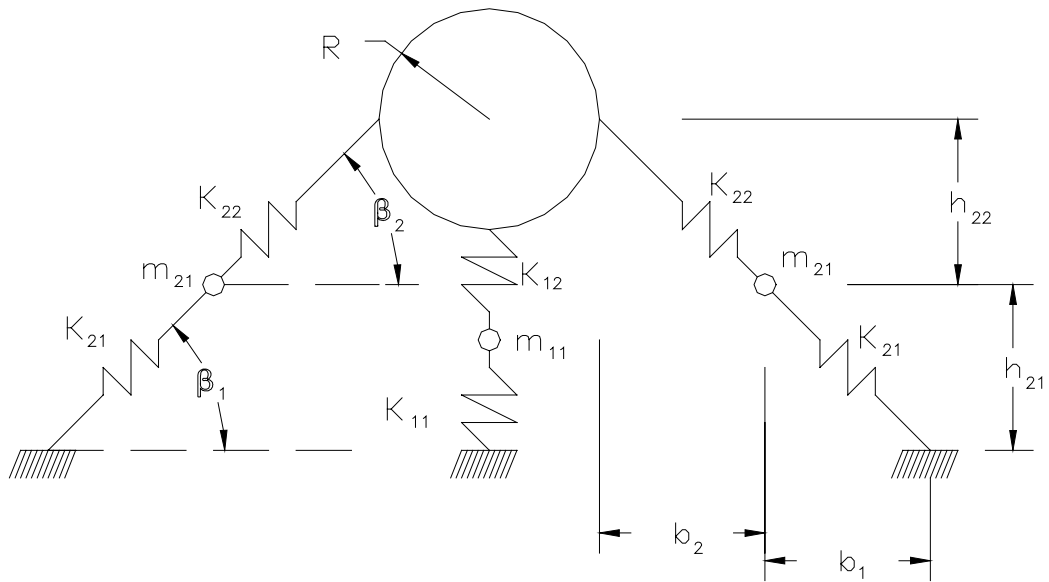


Figure 3.5 – System Elevation (One Mass Per Mooring Line)

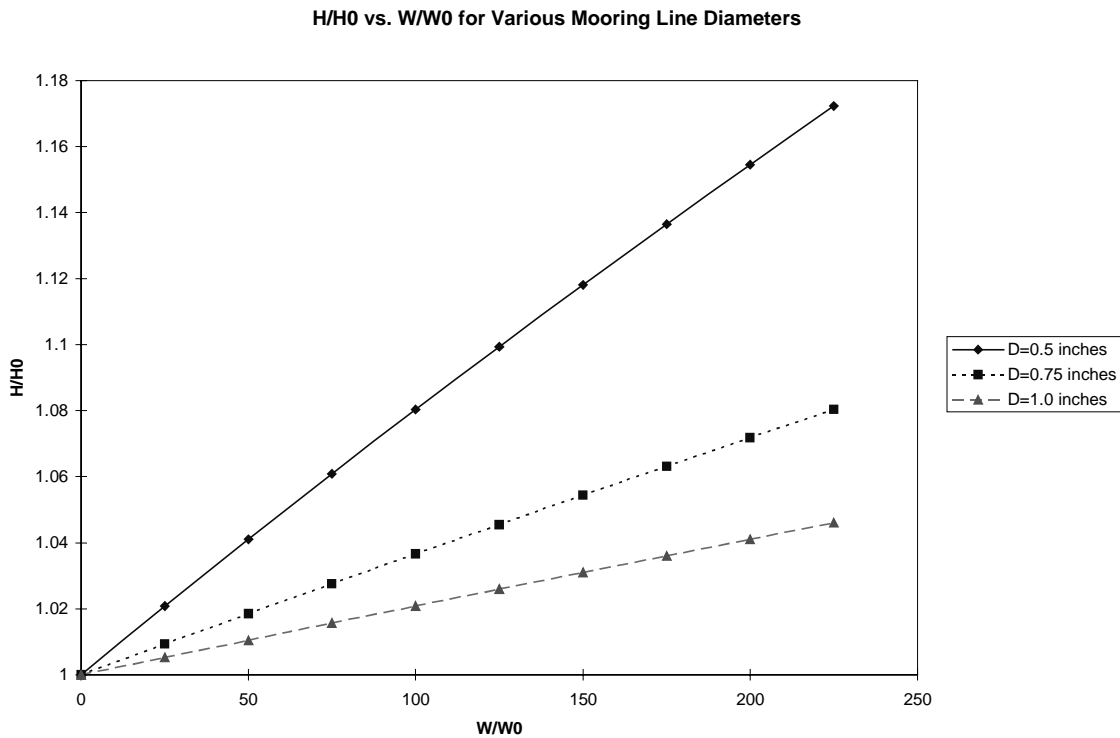


Figure 3.6 - Relationship Between Net Buoyant Force and Equilibrium Height for Different Cable Diameters

CHAPTER 4 FREE VIBRATION OF BREAKWATER IN AIR

4.1 INITIAL CONFIGURATION

Before considering the motion of the standard case discussed in Chapter 3, a general case will be adopted to provide more flexibility in design alterations and to serve as an introduction to the dynamic characteristics. The general system consists of a cylindrical breakwater of length L , radius R , thickness t_l along the longitudinal axis, and end thickness t_e , along with one mooring line modeled by $n-1$ masses and n springs. Figure 4.1 shows the initial or “unstretched springs” configuration of the system. The XYZ system is fixed in space and is used to trace the motion of the cylinder’s center of gravity and the point masses making up the mooring line. The xyz system is fixed to the cylinder with its origin at the cylinder’s center of gravity and thus participates in the cylinder’s motion. The vector $\mathbf{r}_{c,0}$ denotes the initial position of the cylinder’s center of gravity, while the vector $\mathbf{r}_{i,j,0}$ describes the location of mass j for mooring line i . Mass $m_{i,j}$ is described by the initial location $(X_{i,j,0}, Y_{i,j,0}, Z_{i,j,0})$ where i and j indicate the line and mass number, respectively. As shown in Figure 4.1, point A , which corresponds to the location where the cylinder and mooring line connect, can also be described as the sum of the two vectors $\mathbf{r}_{c,0}$ and \mathbf{A}_0 or $(X_{c0}+A1, Y_{c0}+A2, Z_{c0}+A3)$ where vector \mathbf{A} consists of the \mathbf{I} , \mathbf{J} , and \mathbf{K} components $A1$, $A2$, and $A3$, respectively. This will be discussed further in Section 4.3 where a specific correlation between these vectors will be derived.

4.2 GENERAL CONFIGURATION

Figure 4.2 portrays the general configuration of the system using the same axes described in Section 4.1 where the subscript 0 has been removed from the coordinates to represent a new configuration. Thus, a description of the elements of Figure 4.2 will not be provided here.

4.3 CYLINDER ROTATION (EULER ANGLES)

It has been previously established that the XYZ and xyz axes can be used simultaneously to locate any point on the moving structure. Nevertheless, since the xyz system is allowed to rotate and translate with the cylinder, the orientation of this system must first be established. Hence, to trace the rotational motion of the body and likewise any point on the body other than the center of gravity, the Euler angles ψ , θ , and ϕ will be

used. It is important to note here that the rotations will be performed independently and always in the order stated above. Should the rotations be performed inconsistently, the results would be misleading if not entirely invalid. Therefore, the six variables X_C , Y_C , Z_C , ψ , θ , and ϕ will be used to trace the body's motion.

Let the axes $x_0y_0z_0$ represent the initial or "unstretched springs" orientation of the xyz system. Now, consider the three successive rotations shown in Figure 4.3 as (A), (B), and (C) which result in the final xyz orientation of $x_3y_3z_3$. From (A) the transformation from $x_0y_0z_0$ to $x_1y_1z_1$ (a rotation of angle ψ about the z_0 axis) yields

$$\begin{aligned}x_1 &= x_0 \cos \psi + y_0 \sin \psi \\y_1 &= y_0 \cos \psi - x_0 \sin \psi \\z_1 &= z_0\end{aligned}\tag{4.1}$$

or,

$$\begin{Bmatrix} x_1 \\ y_1 \\ z_1 \end{Bmatrix} = \begin{bmatrix} \cos \psi & \sin \psi & 0 \\ -\sin \psi & \cos \psi & 0 \\ 0 & 0 & 1 \end{bmatrix} \begin{Bmatrix} x_0 \\ y_0 \\ z_0 \end{Bmatrix} = [R_1(\psi)] \begin{Bmatrix} x_0 \\ y_0 \\ z_0 \end{Bmatrix}\tag{4.2}$$

where $R_1(\psi)$ denotes the first rotational matrix. Similarly, the second rotation, θ , about the y_1 axis, provides

$$\begin{aligned}x_2 &= x_1 \cos \theta - z_1 \sin \theta \\y_2 &= y_1 \\z_2 &= z_1 \cos \theta + x_1 \sin \theta\end{aligned}\tag{4.3}$$

or,

$$\begin{Bmatrix} x_2 \\ y_2 \\ z_2 \end{Bmatrix} = \begin{bmatrix} \cos \theta & 0 & -\sin \theta \\ 0 & 1 & 0 \\ \sin \theta & 0 & \cos \theta \end{bmatrix} \begin{Bmatrix} x_1 \\ y_1 \\ z_1 \end{Bmatrix} = [R_2(\theta)] \begin{Bmatrix} x_1 \\ y_1 \\ z_1 \end{Bmatrix}\tag{4.4}$$

and the final rotation ϕ about the x_2 axis gives

$$\begin{aligned}x_3 &= x_2 \\y_3 &= y_2 \cos \phi + z_2 \sin \phi \\z_3 &= z_2 \cos \phi - y_2 \sin \phi\end{aligned}\tag{4.5}$$

or,

$$\begin{Bmatrix} x_3 \\ y_3 \\ z_3 \end{Bmatrix} = \begin{bmatrix} 1 & 0 & 0 \\ 0 & \cos \phi & \sin \phi \\ 0 & -\sin \phi & \cos \phi \end{bmatrix} \begin{Bmatrix} x_2 \\ y_2 \\ z_2 \end{Bmatrix} = [\mathbf{R}_3(\phi)] \begin{Bmatrix} x_2 \\ y_2 \\ z_2 \end{Bmatrix} \quad (4.6)$$

The complete transformation from $x_0y_0z_0$ to $x_3y_3z_3$ is simply

$$\begin{Bmatrix} x_3 \\ y_3 \\ z_3 \end{Bmatrix} = [\mathbf{R}_3][\mathbf{R}_2][\mathbf{R}_1] \begin{Bmatrix} x_0 \\ y_0 \\ z_0 \end{Bmatrix} = [\mathbf{R}] \begin{Bmatrix} x_0 \\ y_0 \\ z_0 \end{Bmatrix} \quad (4.7)$$

or in expanded form,

$$\begin{Bmatrix} x_3 \\ y_3 \\ z_3 \end{Bmatrix} = \begin{bmatrix} \cos \theta \cos \psi & \sin \psi \cos \theta & -\sin \theta \\ \sin \phi \sin \theta \cos \psi - \sin \psi \cos \phi & \sin \psi \sin \phi \sin \theta + \cos \phi \cos \psi & \sin \phi \cos \theta \\ \sin \theta \cos \phi \cos \psi + \sin \phi \sin \psi & \sin \theta \cos \phi \sin \psi - \sin \phi \cos \psi & \cos \theta \cos \phi \end{bmatrix} \begin{Bmatrix} x_0 \\ y_0 \\ z_0 \end{Bmatrix} \quad (4.8)$$

As a result, any point on the cylinder can be written as a function of the three aforementioned Euler angles alone using the original xyz system position. Hence, point A with coordinates a_1, a_2, a_3 in the xyz system can now be expressed mathematically as a function of the variables $X_C, Y_C, Z_C, \psi, \theta,$ and ϕ by simply adding the motion of the center of gravity of the cylinder to the transformed position of point A. However, this assumes that the initial configuration of the system is known and can be expressed using vectors. This is fine for our purpose, where the equilibrium or unstretched position of the springs causes the xyz axes to be parallel to the XYZ system. The vector relationship should now be written as

$$\bar{\mathbf{r}}_A = \bar{\mathbf{r}}_C + [\mathbf{R}]^T \begin{Bmatrix} a_1 \\ a_2 \\ a_3 \end{Bmatrix} \quad (4.9)$$

Since the rotation matrices have been previously defined, \mathbf{r}_A can be written in terms of the six unknowns:

$$\begin{aligned}
\bar{\mathbf{r}}_A = & [X_c + a_1(\cos \theta \cos \psi) + a_2(\sin \phi \sin \theta \cos \psi - \sin \psi \cos \phi) \\
& + a_3(\sin \theta \cos \phi \cos \psi + \sin \phi \sin \psi)]\hat{\mathbf{i}} + [Y_c + a_1(\sin \psi \cos \theta) \\
& + a_2(\sin \psi \sin \phi \sin \theta + \cos \phi \cos \psi) + a_3(\sin \theta \cos \phi \sin \psi - \sin \phi \cos \psi)]\hat{\mathbf{j}} \\
& + [Z_c + a_1(-\sin \theta) + a_2(\sin \phi \cos \theta) + a_3(\cos \theta \cos \phi)]\hat{\mathbf{k}}
\end{aligned} \tag{4.10}$$

4.4 ANGULAR VELOCITIES

To begin, it should first be assumed that the angular velocity of the cylinder can be written as

$$\boldsymbol{\Omega} = P\hat{\mathbf{i}}_3 + Q\hat{\mathbf{j}}_3 + R\hat{\mathbf{k}}_3 \tag{4.11}$$

where P, Q, and R are simply functions of the Euler angles and \mathbf{i}_3 , \mathbf{j}_3 , and \mathbf{k}_3 are unit vectors along the x_3 , y_3 , and z_3 axes, respectively. (Similar notations will be used for the $x_2y_2z_2$ and $x_1y_1z_1$ systems). Remembering the order of the rotations, the angular velocities can be written relative to the previous transformation. In other words, the angular velocity of $x_3y_3z_3$ relative to $x_2y_2z_2$ is

$$\boldsymbol{\Omega}_{x_3y_3z_3 / x_2y_2z_2} = \dot{\phi}\hat{\mathbf{i}}_3 \tag{4.12}$$

Similarly, the other angular velocities can be written as:

$$\boldsymbol{\Omega}_{x_2y_2z_2 / x_1y_1z_1} = \dot{\theta}\hat{\mathbf{j}}_2 \tag{4.13}$$

$$\boldsymbol{\Omega}_{x_1y_1z_1 / x_0y_0z_0} = \dot{\psi}\hat{\mathbf{k}}_1 \tag{4.14}$$

Now, the angular velocities should be expressed in terms of the final position of the xyz system. This can be done by transforming the angular velocities utilizing the previously determined rotation matrices. Letting $\mathbf{j}_2 = a\mathbf{i}_3 + b\mathbf{j}_3 + c\mathbf{k}_3$, one can see that the unknowns a, b, and c can be obtained from

$$[\mathbf{R}_3] \begin{Bmatrix} 0 \\ 1 \\ 0 \end{Bmatrix} = \begin{Bmatrix} a \\ b \\ c \end{Bmatrix} \tag{4.15}$$

which results in

$$\begin{Bmatrix} a \\ b \\ c \end{Bmatrix} = \begin{Bmatrix} 0 \\ \cos \phi \\ -\sin \phi \end{Bmatrix} \tag{4.16}$$

Likewise, letting $\mathbf{k}_1 = d\mathbf{i}_3 + e\mathbf{j}_3 + f\mathbf{k}_3$ yields

$$[R_3][R_2] \begin{Bmatrix} 0 \\ 0 \\ 1 \end{Bmatrix} = \begin{Bmatrix} d \\ e \\ f \end{Bmatrix} \quad (4.17)$$

which results in

$$\begin{Bmatrix} d \\ e \\ f \end{Bmatrix} = \begin{Bmatrix} -\sin\theta \\ \sin\phi\cos\theta \\ \cos\theta\cos\phi \end{Bmatrix} \quad (4.18)$$

So the resulting angular velocity is

$$\Omega = (\dot{\phi} - \dot{\psi}\sin\theta)\hat{i}_3 + (\dot{\theta}\cos\phi + \dot{\psi}\sin\phi\cos\theta)\hat{j}_3 + (\dot{\psi}\cos\theta\cos\phi - \dot{\theta}\sin\phi)\hat{k}_3 \quad (4.19)$$

or in matrix form

$$\begin{Bmatrix} \Omega_{x_3} \\ \Omega_{y_3} \\ \Omega_{z_3} \end{Bmatrix} = \begin{bmatrix} 1 & 0 & -\sin\theta \\ 0 & \cos\phi & \sin\phi\cos\theta \\ 0 & -\sin\phi & \cos\theta\cos\phi \end{bmatrix} \begin{Bmatrix} \dot{\phi} \\ \dot{\theta} \\ \dot{\psi} \end{Bmatrix} \quad (4.20)$$

Derivations similar to those of Sections 4.3 and 4.4 are considered by Clayton, et al. (1982) and Chakrabarti (1990).

4.5 MOORING LINE ENERGY

For the mooring line shown in Figures 4.1 and 4.2 made up of $n-1$ masses, the kinetic energy of the line, T_i , is described by

$$T_i = \frac{1}{2} \sum_{j=1}^{n-1} (m_{i,j}) (\dot{X}_{i,j}^2 + \dot{Y}_{i,j}^2 + \dot{Z}_{i,j}^2) \quad (4.21)$$

The potential energy of the line, V_i , is found as

$$\begin{aligned} V_i &= \sum_{j=1}^n \frac{1}{2} K_j (|\bar{r}_{i,j} - \bar{r}_{i,j-1}| - l_j)^2 - \sum_{j=1}^{n-1} w_{i,j} Y_{i,j} \\ &= \sum_{j=1}^n \frac{1}{2} K_j \{ (X_{i,j} - X_{i,j-1})^2 + (Y_{i,j} - Y_{i,j-1})^2 + (Z_{i,j} - Z_{i,j-1})^2 + l_j^2 \\ &\quad - 2l_j [(X_{i,j} - X_{i,j-1})^2 + (Y_{i,j} - Y_{i,j-1})^2 + (Z_{i,j} - Z_{i,j-1})^2]^{\frac{1}{2}} \} - \sum_{j=1}^{n-1} w_{i,j} Y_{i,j} \end{aligned} \quad (4.22)$$

where $w_{i,j}$ represents the nominal net buoyant force on mass $m_{i,j}$ and l_j is the length of spring j . It should be recalled that vector $\mathbf{r}_{i,n}$ can be written as the sum of the vectors \mathbf{r}_c and \mathbf{A} . Thus V_i can also be written as

$$\begin{aligned}
V_i = & \sum_{j=1}^{n-1} \frac{1}{2} K_j \{ (X_{i,j} - X_{i,j-1})^2 + (Y_{i,j} - Y_{i,j-1})^2 + (Z_{i,j} - Z_{i,j-1})^2 + I_j^2 \\
& - 2I_j [(X_{i,j} - X_{i,j-1})^2 + (Y_{i,j} - Y_{i,j-1})^2 + (Z_{i,j} - Z_{i,j-1})^2]^{\frac{1}{2}} \} \\
& + \frac{1}{2} K_n \{ [X_c + a_1(\cos \theta \cos \psi) + a_2(\sin \phi \sin \theta \cos \psi - \sin \psi \cos \phi) \\
& + a_3(\sin \theta \cos \phi \cos \psi + \sin \phi \sin \psi) - X_{i,n-1}]^2 + [Y_c + a_1(\sin \psi \cos \theta) \\
& + a_2(\sin \psi \sin \phi \sin \theta + \cos \phi \cos \psi) + a_3(\sin \theta \cos \phi \sin \psi - \sin \phi \cos \psi) \\
& - Y_{i,n-1}]^2 + [Z_c + a_1(-\sin \theta) + a_2(\sin \phi \cos \theta) + a_3(\cos \theta \cos \phi) - Z_{i,n-1}]^2 + I_n^2 \\
& - 2I_n \{ [X_c + a_1(\cos \theta \cos \psi) + a_2(\sin \phi \sin \theta \cos \psi - \sin \psi \cos \phi) \\
& + a_3(\sin \theta \cos \phi \cos \psi + \sin \phi \sin \psi) - X_{i,n-1}]^2 + [Y_c + a_1(\sin \psi \cos \theta) \\
& + a_2(\sin \psi \sin \phi \sin \theta + \cos \phi \cos \psi) + a_3(\sin \theta \cos \phi \sin \psi - \sin \phi \cos \psi) \\
& - Y_{i,n-1}]^2 + [Z_c + a_1(-\sin \theta) + a_2(\sin \phi \cos \theta) + a_3(\cos \theta \cos \phi) - Z_{i,n-1}]^2 \}^{\frac{1}{2}} \} \\
& - \sum_{j=1}^{n-1} w_{i,j} Y_{i,j}
\end{aligned} \tag{4.23}$$

4.6 ENERGY OF THE CYLINDER

The potential energy, V_c , of the cylinder can be found as

$$V_c = -w_c Y_c \tag{4.24}$$

where w_c denotes the net buoyant force on the cylinder.

The kinetic energy of the cylinder is more complicated as it involves not only translation but rotation as well. The xyz axes are the principal axes of inertia of the cylinder, with the corresponding principal moments of inertia I_{xx} , I_{yy} , and I_{zz} , respectively. Thus the kinetic energy, T_c , of the cylinder is found as

$$\begin{aligned}
T_c = & \frac{1}{2} [m_c (\dot{X}_c^2 + \dot{Y}_c^2 + \dot{Z}_c^2) + I_{xx} (\dot{\phi} - \dot{\psi} \sin \theta)^2 + I_{yy} (\dot{\theta} \cos \phi + \dot{\psi} \sin \phi \cos \theta)^2 \\
& + I_{zz} (\dot{\psi} \cos \theta \cos \phi - \dot{\theta} \sin \phi)^2]
\end{aligned} \tag{4.25}$$

where I_{xx} , I_{yy} , and I_{zz} are all found with reference to Figure 4.4 as

$$I_{xx} = \frac{1}{2} M_0 R^2 - \frac{1}{2} M_1 (R - t_L)^2 \tag{4.26}$$

$$I_{yy} = I_{zz} = \frac{1}{4} M_0 R^2 + \frac{1}{12} M_0 L^2 - \left[\frac{1}{4} M_1 (R - t_L)^2 + \frac{1}{12} M_1 (L - 2t_e)^2 \right] \tag{4.27}$$

where M_0 is the mass of a solid cylinder of radius R and length L , and M_1 is the mass of a solid cylinder of radius $R-t_l$ and length $L-2t_e$, i.e.,

$$M_0 = \pi R^2 L \rho_c \quad (4.28)$$

and

$$M_1 = \pi (R - t_l)^2 (L - 2t_e) \rho_c \quad (4.29)$$

where the density, ρ_c , of the cylinder is known.

4.7 LAGRANGE'S EQUATIONS

Given the complexity of equations (4.21) through (4.25) along with the variations in point masses along the mooring line, the Lagrangian, L_i , for the mooring line will be found independently from the Lagrangian, L_c , of the cylinder. However, a summation of these and the development of Lagrange's equations will conclude this section.

Referencing Meirovitch (1986), for any system, the Lagrangian can be found by

$$L = T - V \quad (4.30)$$

where T and V are the kinetic and potential energies of the system, respectively. Now, for a conservative system defined by n degrees of freedom, Lagrange's Equations are found directly from

$$\frac{d}{dt} \left(\frac{\partial L}{\partial \dot{Q}_j} \right) - \frac{\partial L}{\partial Q_j} = 0 \quad j = 1, 2, 3, \dots, N \quad (4.31)$$

where each Q_j represents an independent variable. However, for the case of the inflatable breakwater,

$$L = L_i + L_c \quad (4.32)$$

and

$$\frac{d}{dt} \left(\frac{\partial L_i}{\partial \dot{Q}_j} \right) - \frac{\partial L_i}{\partial Q_j} + \frac{d}{dt} \left(\frac{\partial L_c}{\partial \dot{Q}_j} \right) - \frac{\partial L_c}{\partial Q_j} = 0 \quad j = 1, 2, 3, \dots, N \quad (4.33)$$

where N degrees of freedom define the system, which includes both the structure and the mooring lines (lumped masses).

For mooring line i made of $n-1$ masses, the Lagrangian, L_i , can be written as

$$\begin{aligned}
L_i = T_i - V_i = & \frac{1}{2} \sum_{j=1}^{n-1} (m_{i,j}) (\dot{X}_{i,j}^2 + \dot{Y}_{i,j}^2 + \dot{Z}_{i,j}^2) - \sum_{j=1}^{n-1} \frac{1}{2} K_j \{ (X_{i,j} - X_{i,j-1})^2 \\
& + (Y_{i,j} - Y_{i,j-1})^2 + (Z_{i,j} - Z_{i,j-1})^2 + I_j^2 \\
& - 2I_j [(X_{i,j} - X_{i,j-1})^2 + (Y_{i,j} - Y_{i,j-1})^2 + (Z_{i,j} - Z_{i,j-1})^2]^{\frac{1}{2}} \} \\
& - \frac{1}{2} K_n \{ [X_c + a_1(\cos \theta \cos \psi) + a_2(\sin \phi \sin \theta \cos \psi - \sin \psi \cos \phi) \\
& + a_3(\sin \theta \cos \phi \cos \psi + \sin \phi \sin \psi) - X_{i,n-1}]^2 + [Y_c + a_1(\sin \psi \cos \theta) \\
& + a_2(\sin \psi \sin \phi \sin \theta + \cos \phi \cos \psi) + a_3(\sin \theta \cos \phi \sin \psi - \sin \phi \cos \psi) \\
& - Y_{i,n-1}]^2 + [Z_c + a_1(-\sin \theta) + a_2(\sin \phi \cos \theta) + a_3(\cos \theta \cos \phi) - Z_{i,n-1}]^2 \\
& + I_n^2 - 2I_n \{ [X_c + a_1(\cos \theta \cos \psi) + a_2(\sin \phi \sin \theta \cos \psi - \sin \psi \cos \phi) \\
& + a_3(\sin \theta \cos \phi \cos \psi + \sin \phi \sin \psi) - X_{i,n-1}]^2 + [Y_c + a_1(\sin \psi \cos \theta) \\
& + a_2(\sin \psi \sin \phi \sin \theta + \cos \phi \cos \psi) + a_3(\sin \theta \cos \phi \sin \psi - \sin \phi \cos \psi) \\
& - Y_{i,n-1}]^2 + [Z_c + a_1(-\sin \theta) + a_2(\sin \phi \cos \theta) + a_3(\cos \theta \cos \phi) - Z_{i,n-1}]^2 \}^{\frac{1}{2}} \} \\
& + \sum_{j=1}^{n-1} w_{i,j} Y_{i,j} \tag{4.34}
\end{aligned}$$

For each mooring line mass, it can be shown that the accompanying Lagrange's equations only involve L_i (i.e., $X_{i,j}$, $Y_{i,j}$, and $Z_{i,j}$ will not be associated with the energy equations developed for the cylinder).

Hence, Lagrange's equations are obtained directly from L_i for each of the point masses $m_{i,j}$ as

$$\frac{d}{dt} \left(\frac{\partial L_i}{\partial \dot{X}_{i,j}} \right) - \frac{\partial L_i}{\partial X_{i,j}} = 0 \tag{4.35}$$

or,

$$\begin{aligned}
m_{i,j} \ddot{X}_{i,j} + K_j (X_{i,j} - X_{i,j-1}) - K_j I_j [(X_{i,j} - X_{i,j-1})^2 + (Y_{i,j} - Y_{i,j-1})^2 \\
+ (Z_{i,j} - Z_{i,j-1})^2]^{\frac{1}{2}} (X_{i,j} - X_{i,j-1}) - K_{j+1} (X_{i,j+1} - X_{i,j}) + \tag{4.36}
\end{aligned}$$

$$K_{j+1} I_{j+1} [(X_{i,j+1} - X_{i,j})^2 + (Y_{i,j+1} - Y_{i,j})^2 + (Z_{i,j+1} - Z_{i,j})^2]^{\frac{1}{2}} (X_{i,j+1} - X_{i,j}) = 0;$$

$$\frac{d}{dt} \left(\frac{\partial L_i}{\partial \dot{Y}_{i,j}} \right) - \frac{\partial L_i}{\partial Y_{i,j}} = 0 \tag{4.37}$$

or,

$$\begin{aligned}
& m_{i,j} \ddot{Y}_{i,j} + K_j (Y_{i,j} - Y_{i,j-1}) - K_j l_j [(X_{i,j} - X_{i,j-1})^2 + (Y_{i,j} - Y_{i,j-1})^2 \\
& + (Z_{i,j} - Z_{i,j-1})^2]^{-\frac{1}{2}} (Y_{i,j} - Y_{i,j-1}) - K_{j+1} (Y_{i,j+1} - Y_{i,j}) + \\
& K_{j+1} l_{j+1} [(X_{i,j+1} - X_{i,j})^2 + (Y_{i,j+1} - Y_{i,j})^2 + (Z_{i,j+1} - Z_{i,j})^2]^{-\frac{1}{2}} (Y_{i,j+1} - Y_{i,j}) \\
& - w_{i,j} = 0
\end{aligned} \tag{4.38}$$

and

$$\frac{d}{dt} \left(\frac{\partial L_i}{\partial \dot{Z}_{i,j}} \right) - \frac{\partial L_i}{\partial Z_{i,j}} = 0 \tag{4.39}$$

or,

$$\begin{aligned}
& m_{i,j} \ddot{Z}_{i,j} + K_j (Z_{i,j} - Z_{i,j-1}) - K_j l_j [(X_{i,j} - X_{i,j-1})^2 + (Y_{i,j} - Y_{i,j-1})^2 \\
& + (Z_{i,j} - Z_{i,j-1})^2]^{-\frac{1}{2}} (Z_{i,j} - Z_{i,j-1}) - K_{j+1} (Z_{i,j+1} - Z_{i,j}) + \\
& K_{j+1} l_{j+1} [(X_{i,j+1} - X_{i,j})^2 + (Y_{i,j+1} - Y_{i,j})^2 + (Z_{i,j+1} - Z_{i,j})^2]^{-\frac{1}{2}} (Z_{i,j+1} - Z_{i,j}) = 0
\end{aligned} \tag{4.40}$$

from $j=1$ to $n-2$ making up mooring line i .

However, for mass $n-1$, equation (4.23) leads to the equations

$$\begin{aligned}
& m_{i,n-1} \ddot{X}_{i,n-1} + K_{n-1} (X_{i,n-1} - X_{i,n-2}) - K_{n-1} l_{n-1} [(X_{i,n-1} - X_{i,n-2})^2 \\
& + (Y_{i,n-1} - Y_{i,n-2})^2 + (Z_{i,n-1} - Z_{i,n-2})^2]^{-\frac{1}{2}} (X_{i,n-1} - X_{i,n-2}) - K_n [X_c + a_1 (\cos \theta \cos \psi) \\
& + a_2 (\sin \phi \sin \theta \cos \psi - \sin \psi \cos \phi) + a_3 (\sin \theta \cos \phi \cos \psi + \sin \phi \sin \psi) \\
& - X_{i,n-1}] + K_n l_n \{ [X_c + a_1 (\cos \theta \cos \psi) + a_2 (\sin \phi \sin \theta \cos \psi - \sin \psi \cos \phi) \\
& + a_3 (\sin \theta \cos \phi \cos \psi + \sin \phi \sin \psi) - X_{i,n-1}]^2 + [Y_c + a_1 (\sin \psi \cos \theta) \\
& + a_2 (\sin \psi \sin \phi \sin \theta + \cos \phi \cos \psi) + a_3 (\sin \theta \cos \phi \sin \psi - \sin \phi \cos \psi) - Y_{i,n-1}]^2 \\
& + [Z_c + a_1 (-\sin \theta) + a_2 (\sin \phi \cos \theta) + a_3 (\cos \theta \cos \phi) - Z_{i,n-1}]^2 \}^{-\frac{1}{2}} [X_c \\
& + a_1 (\cos \theta \cos \psi) + a_2 (\sin \phi \sin \theta \cos \psi - \sin \psi \cos \phi) \\
& + a_3 (\sin \theta \cos \phi \cos \psi + \sin \phi \sin \psi) - X_{i,n-1}] = 0;
\end{aligned} \tag{4.41}$$

$$\begin{aligned}
& m_{i,n-1} \ddot{Y}_{i,n-1} + K_{n-1} (Y_{i,n-1} - Y_{i,n-2}) - K_{n-1} l_{n-1} [(X_{i,n-1} - X_{i,n-2})^2 + (Y_{i,n-1} - Y_{i,n-2})^2 \\
& + (Z_{i,n-1} - Z_{i,n-2})^2]^{-\frac{1}{2}} (Y_{i,n-1} - Y_{i,n-2}) - K_n [Y_c + a_1 (\sin \psi \cos \theta) \\
& + a_2 (\sin \psi \sin \phi \sin \theta + \cos \phi \cos \psi) + a_3 (\sin \theta \cos \phi \sin \psi - \sin \phi \cos \psi) \\
& - Y_{i,n-1}] + K_n l_n \{ [X_c + a_1 (\cos \theta \cos \psi) + a_2 (\sin \phi \sin \theta \cos \psi - \sin \psi \cos \phi) \\
& + a_3 (\sin \theta \cos \phi \cos \psi + \sin \phi \sin \psi) - X_{i,n-1}]^2 + [Y_c + a_1 (\sin \psi \cos \theta) \\
& + a_2 (\sin \psi \sin \phi \sin \theta + \cos \phi \cos \psi) + a_3 (\sin \theta \cos \phi \sin \psi - \sin \phi \cos \psi) - Y_{i,n-1}]^2 \\
& + [Z_c + a_1 (-\sin \theta) + a_2 (\sin \phi \cos \theta) + a_3 (\cos \theta \cos \phi) - Z_{i,n-1}]^2 \}^{-\frac{1}{2}} [Y_c \\
& + a_1 (\sin \psi \cos \theta) + a_2 (\sin \psi \sin \phi \sin \theta + \cos \phi \cos \psi) + a_3 (\sin \theta \cos \phi \sin \psi \\
& - \sin \phi \cos \psi) - Y_{i,n-1}] - w_{i,n-1} = 0
\end{aligned} \tag{4.42}$$

and

$$\begin{aligned}
& m_{i,n-1} \ddot{Z}_{i,n-1} + K_{n-1} (Z_{i,n-1} - Z_{i,n-2}) - K_{n-1} l_{n-1} [(X_{i,n-1} - X_{i,n-2})^2 + (Y_{i,n-1} - Y_{i,n-2})^2 \\
& + (Z_{i,n-1} - Z_{i,n-2})^2]^{-\frac{1}{2}} (Z_{i,n-1} - Z_{i,n-2}) - K_n [Z_c + a_1 (-\sin \theta) + a_2 (\sin \phi \cos \theta) \\
& + a_3 (\cos \theta \cos \phi) - Z_{i,n-1}] + K_n l_n \{ [X_c + a_1 (\cos \theta \cos \psi) + a_2 (\sin \phi \sin \theta \cos \psi \\
& - \sin \psi \cos \phi) + a_3 (\sin \theta \cos \phi \cos \psi + \sin \phi \sin \psi) - X_{i,n-1}]^2 + [Y_c \\
& + a_1 (\sin \psi \cos \theta) + a_2 (\sin \psi \sin \phi \sin \theta + \cos \phi \cos \psi) + a_3 (\sin \theta \cos \phi \sin \psi \\
& - \sin \phi \cos \psi) - Y_{i,n-1}]^2 + [Z_c + a_1 (-\sin \theta) + a_2 (\sin \phi \cos \theta) + a_3 (\cos \theta \cos \phi) \\
& - Z_{i,n-1}]^2 \}^{-\frac{1}{2}} [Z_c + a_1 (-\sin \theta) + a_2 (\sin \phi \cos \theta) + a_3 (\cos \theta \cos \phi) - Z_{i,n-1}] = 0
\end{aligned} \tag{4.43}$$

For the rest of the variables, the Lagrangians for both the cylinder, L_c , and the mooring line, L_i , contribute to the general equation

$$\frac{d}{dt} \left(\frac{\partial L}{\partial \dot{Q}} \right) - \frac{\partial L}{\partial Q} = 0 \tag{4.44}$$

where Q denotes any of the unknowns X_c , Y_c , Z_c , ψ , θ , or ϕ .

The parts of Lagrange's equations (33) involving L_i are found as

$$\frac{d}{dt} \left(\frac{\partial L_i}{\partial \dot{X}_c} \right) - \frac{\partial L_i}{\partial X_c} \tag{4.45}$$

or,

$$\begin{aligned}
& K_n [X_c + a_1 (\cos \theta \cos \psi) + a_2 (\sin \phi \sin \theta \cos \psi - \sin \psi \cos \phi) \\
& + a_3 (\sin \theta \cos \phi \cos \psi + \sin \phi \sin \psi) - X_{i,n-1}] - K_n I_n \{ [X_c + a_1 (\cos \theta \cos \psi) \\
& + a_2 (\sin \phi \sin \theta \cos \psi - \sin \psi \cos \phi) \\
& + a_3 (\sin \theta \cos \phi \cos \psi + \sin \phi \sin \psi) - X_{i,n-1}]^2 + [Y_c + a_1 (\sin \psi \cos \theta) \\
& + a_2 (\sin \psi \sin \phi \sin \theta + \cos \phi \cos \psi) + a_3 (\sin \theta \cos \phi \sin \psi - \sin \phi \cos \psi) - Y_{i,n-1}]^2 \} \\
& + [Z_c + a_1 (-\sin \theta) + a_2 (\sin \phi \cos \theta) + a_3 (\cos \theta \cos \phi) - Z_{i,n-1}]^2 \}^{\frac{1}{2}} [X_c \\
& + a_1 (\cos \theta \cos \psi) + a_2 (\sin \phi \sin \theta \cos \psi - \sin \psi \cos \phi) \\
& + a_3 (\sin \theta \cos \phi \cos \psi + \sin \phi \sin \psi) - X_{i,n-1}];
\end{aligned}$$

$$\frac{d}{dt} \left(\frac{\partial L_i}{\partial \dot{Y}_c} \right) - \frac{\partial L_i}{\partial Y_c} \quad (4.47)$$

or,

$$\begin{aligned}
& K_n [Y_c + a_1 (\sin \psi \cos \theta) + a_2 (\sin \psi \sin \phi \sin \theta + \cos \phi \cos \psi) \\
& + a_3 (\sin \theta \cos \phi \sin \psi - \sin \phi \cos \psi) - Y_{i,n-1}] - K_n I_n \{ [X_c + a_1 (\cos \theta \cos \psi) \\
& + a_2 (\sin \phi \sin \theta \cos \psi - \sin \psi \cos \phi) \\
& + a_3 (\sin \theta \cos \phi \cos \psi + \sin \phi \sin \psi) - X_{i,n-1}]^2 + [Y_c + a_1 (\sin \psi \cos \theta) \\
& + a_2 (\sin \psi \sin \phi \sin \theta + \cos \phi \cos \psi) + a_3 (\sin \theta \cos \phi \sin \psi - \sin \phi \cos \psi) \\
& - Y_{i,n-1}]^2 + [Z_c + a_1 (-\sin \theta) + a_2 (\sin \phi \cos \theta) + a_3 (\cos \theta \cos \phi) - Z_{i,n-1}]^2 \}^{\frac{1}{2}} [Y_c \\
& + a_1 (\sin \psi \cos \theta) + a_2 (\sin \psi \sin \phi \sin \theta + \cos \phi \cos \psi) + a_3 (\sin \theta \cos \phi \sin \psi \\
& - \sin \phi \cos \psi) - Y_{i,n-1}];
\end{aligned}$$

$$\frac{d}{dt} \left(\frac{\partial L_i}{\partial \dot{Z}_c} \right) - \frac{\partial L_i}{\partial Z_c} \quad (4.49)$$

or,

$$\begin{aligned}
& K_n [Z_c + a_1 (-\sin \theta) + a_2 (\sin \phi \cos \theta) + a_3 (\cos \theta \cos \phi) - Z_{i,n-1}] - K_n I_n \{ [X_c \\
& + a_1 (\cos \theta \cos \psi) + a_2 (\sin \phi \sin \theta \cos \psi - \sin \psi \cos \phi) \\
& + a_3 (\sin \theta \cos \phi \cos \psi + \sin \phi \sin \psi) - X_{i,n-1}]^2 + [Y_c + a_1 (\sin \psi \cos \theta) \\
& + a_2 (\sin \psi \sin \phi \sin \theta + \cos \phi \cos \psi) + a_3 (\sin \theta \cos \phi \sin \psi - \sin \phi \cos \psi) \\
& - Y_{i,n-1}]^2 + [Z_c + a_1 (-\sin \theta) + a_2 (\sin \phi \cos \theta) + a_3 (\cos \theta \cos \phi) \\
& - Z_{i,n-1}]^2 \}^{\frac{1}{2}} [Z_c + a_1 (-\sin \theta) + a_2 (\sin \phi \cos \theta) + a_3 (\cos \theta \cos \phi) - Z_{i,n-1}];
\end{aligned}$$

$$\frac{d}{dt} \left(\frac{\partial L_i}{\partial \dot{\psi}} \right) - \frac{\partial L_i}{\partial \psi} \quad (4.51)$$

or,

$$\begin{aligned}
& K_n [X_c + a_1 (\cos \theta \cos \psi) + a_2 (\sin \phi \sin \theta \cos \psi - \sin \psi \cos \phi) \\
& + a_3 (\sin \theta \cos \phi \cos \psi + \sin \phi \sin \psi) - X_{i,n-1}] [-a_1 \cos \theta \sin \psi \\
& - a_2 (\sin \phi \sin \theta \sin \psi + \cos \psi \cos \phi) - a_3 (\sin \theta \cos \phi \sin \psi - \sin \phi \cos \psi)] + K_n [Y_c \\
& + a_1 (\sin \psi \cos \theta) + a_2 (\sin \psi \sin \phi \sin \theta + \cos \phi \cos \psi) + a_3 (\sin \theta \cos \phi \sin \psi \\
& - \sin \phi \cos \psi) - Y_{i,n-1}] [a_1 \cos \theta \cos \psi + a_2 (\cos \psi \sin \phi \sin \theta - \cos \phi \sin \psi) \\
& + a_3 (\sin \theta \cos \phi \cos \psi + \sin \phi \sin \psi)] - K_n I_n \{ [X_c + a_1 (\cos \theta \cos \psi) + \\
& a_2 (\sin \phi \sin \theta \cos \psi - \sin \psi \cos \phi) \\
& + a_3 (\sin \theta \cos \phi \cos \psi + \sin \phi \sin \psi) - X_{i,n-1}]^2 + [Y_c + a_1 (\sin \psi \cos \theta) \\
& + a_2 (\sin \psi \sin \phi \sin \theta + \cos \phi \cos \psi) + a_3 (\sin \theta \cos \phi \sin \psi - \sin \phi \cos \psi) \\
& - Y_{i,n-1}]^2 + [Z_c + a_1 (-\sin \theta) + a_2 (\sin \phi \cos \theta) + a_3 (\cos \theta \cos \phi) - Z_{i,n-1}]^2 \}^{\frac{1}{2}} \{ [X_c \\
& + a_1 (\cos \theta \cos \psi) + a_2 (\sin \phi \sin \theta \cos \psi - \sin \psi \cos \phi) \\
& + a_3 (\sin \theta \cos \phi \cos \psi + \sin \phi \sin \psi) - X_{i,n-1}] [-a_1 \cos \theta \sin \psi \\
& - a_2 (\sin \phi \sin \theta \sin \psi + \cos \psi \cos \phi) - a_3 (\sin \theta \cos \phi \sin \psi - \sin \phi \cos \psi)] \\
& + [Y_c + a_1 (\sin \psi \cos \theta) + a_2 (\sin \psi \sin \phi \sin \theta + \cos \phi \cos \psi) \\
& + a_3 (\sin \theta \cos \phi \sin \psi - \sin \phi \cos \psi) - Y_{i,n-1}] [a_1 \cos \theta \cos \psi \\
& + a_2 (\cos \psi \sin \phi \sin \theta - \cos \phi \sin \psi) + a_3 (\sin \theta \cos \phi \cos \psi + \sin \phi \sin \psi)] \}; \tag{4.52}
\end{aligned}$$

$$\frac{d}{dt} \left(\frac{\partial L_i}{\partial \dot{\theta}} \right) - \frac{\partial L_i}{\partial \theta} \tag{4.53}$$

or,

$$\begin{aligned}
& K_n [X_c + a_1(\cos \theta \cos \psi) + a_2(\sin \phi \sin \theta \cos \psi - \sin \psi \cos \phi) \\
& + a_3(\sin \theta \cos \phi \cos \psi + \sin \phi \sin \psi) - X_{i,n-1}] [-a_1 \cos \psi \sin \theta \\
& + a_2(\sin \phi \cos \theta \cos \psi) + a_3(\cos \theta \cos \phi \cos \psi)] + K_n [Y_c + a_1(\sin \psi \cos \theta) \\
& + a_2(\sin \psi \sin \phi \sin \theta + \cos \phi \cos \psi) + a_3(\sin \theta \cos \phi \sin \psi - \sin \phi \cos \psi) \\
& - Y_{i,n-1}] [-a_1 \sin \psi \sin \theta + a_2 \sin \psi \sin \phi \cos \theta + a_3(\cos \theta \cos \phi \sin \psi)] \\
& + K_n [Z_c + a_1(-\sin \theta) + a_2(\sin \phi \cos \theta) + a_3(\cos \theta \cos \phi) - Z_{i,n-1}] (-a_1 \cos \theta \\
& - a_2 \sin \phi \sin \theta - a_3 \sin \theta \cos \phi) - K_n I_n \{ [X_c + a_1(\cos \theta \cos \psi) + \\
& a_2(\sin \phi \sin \theta \cos \psi - \sin \psi \cos \phi) \\
& + a_3(\sin \theta \cos \phi \cos \psi + \sin \phi \sin \psi) - X_{i,n-1}]^2 + [Y_c + a_1(\sin \psi \cos \theta) \\
& + a_2(\sin \psi \sin \phi \sin \theta + \cos \phi \cos \psi) + a_3(\sin \theta \cos \phi \sin \psi - \sin \phi \cos \psi) \\
& - Y_{i,n-1}]^2 + [Z_c + a_1(-\sin \theta) + a_2(\sin \phi \cos \theta) + a_3(\cos \theta \cos \phi) \\
& - Z_{i,n-1}]^2 \}^{\frac{1}{2}} \{ [X_c + a_1(\cos \theta \cos \psi) + a_2(\sin \phi \sin \theta \cos \psi - \sin \psi \cos \phi) \\
& + a_3(\sin \theta \cos \phi \cos \psi + \sin \phi \sin \psi) - X_{i,n-1}] [-a_1 \cos \psi \sin \theta \\
& + a_2(\sin \phi \cos \theta \cos \psi) + a_3(\cos \theta \cos \phi \cos \psi)] + [Y_c + a_1(\sin \psi \cos \theta) \\
& + a_2(\sin \psi \sin \phi \sin \theta + \cos \phi \cos \psi) + a_3(\sin \theta \cos \phi \sin \psi - \sin \phi \cos \psi) \\
& - Y_{i,n-1}] [-a_1 \sin \psi \sin \theta + a_2 \sin \psi \sin \phi \cos \theta + a_3(\cos \theta \cos \phi \sin \psi)] \\
& + [Z_c + a_1(-\sin \theta) + a_2(\sin \phi \cos \theta) + a_3(\cos \theta \cos \phi) - Z_{i,n-1}] (-a_1 \cos \theta \\
& - a_2 \sin \phi \sin \theta - a_3 \sin \theta \cos \phi) \};
\end{aligned} \tag{4.54}$$

and

$$\frac{d}{dt} \left(\frac{\partial L_i}{\partial \dot{\phi}} \right) - \frac{\partial L_i}{\partial \phi} \tag{4.55}$$

or,

$$\begin{aligned}
& K_n [X_c + a_1 (\cos \theta \cos \psi) + a_2 (\sin \phi \sin \theta \cos \psi - \sin \psi \cos \phi) \\
& + a_3 (\sin \theta \cos \phi \cos \psi + \sin \phi \sin \psi) - X_{i,n-1}] [a_2 (\cos \phi \sin \theta \cos \psi \\
& + \sin \psi \sin \phi) + a_3 (-\sin \theta \sin \phi \cos \psi)] + K_n [Y_c + a_1 (\sin \psi \cos \theta) \\
& + a_2 (\sin \psi \sin \phi \sin \theta + \cos \phi \cos \psi) + a_3 (\sin \theta \cos \phi \sin \psi \\
& - \sin \phi \cos \psi) - Y_{i,n-1}] [a_2 (\sin \psi \cos \phi \sin \theta - \sin \phi \cos \psi) \\
& - a_3 (\sin \theta \sin \phi \sin \psi + \cos \phi \cos \psi)] + K_n [Z_c + a_1 (-\sin \theta) \\
& + a_2 (\sin \phi \cos \theta) + a_3 (\cos \theta \cos \phi) - Z_{i,n-1}] [a_2 \cos \phi \cos \theta \\
& - a_3 \cos \theta \sin \phi] - K_n I_n \{ [X_c + a_1 (\cos \theta \cos \psi) + a_2 (\sin \phi \sin \theta \cos \psi \\
& - \sin \psi \cos \phi) + a_3 (\sin \theta \cos \phi \cos \psi + \sin \phi \sin \psi) - X_{i,n-1}]^2 + [Y_c \\
& + a_1 (\sin \psi \cos \theta) + a_2 (\sin \psi \sin \phi \sin \theta + \cos \phi \cos \psi) \\
& + a_3 (\sin \theta \cos \phi \sin \psi - \sin \phi \cos \psi) - Y_{i,n-1}]^2 + [Z_c + a_1 (-\sin \theta) \\
& + a_2 (\sin \phi \cos \theta) + a_3 (\cos \theta \cos \phi) - Z_{i,n-1}]^2 \}^{\frac{1}{2}} \{ [X_c \\
& + a_1 (\cos \theta \cos \psi) + a_2 (\sin \phi \sin \theta \cos \psi - \sin \psi \cos \phi) \\
& + a_3 (\sin \theta \cos \phi \cos \psi + \sin \phi \sin \psi) - X_{i,n-1}] [a_2 (\cos \phi \sin \theta \cos \psi + \sin \psi \sin \phi) \\
& + a_3 (-\sin \theta \sin \phi \cos \psi)] + [Y_c + a_1 (\sin \psi \cos \theta) \\
& + a_2 (\sin \psi \sin \phi \sin \theta + \cos \phi \cos \psi) + a_3 (\sin \theta \cos \phi \sin \psi \\
& - \sin \phi \cos \psi) - Y_{i,n-1}] [a_2 (\sin \psi \cos \phi \sin \theta - \sin \phi \cos \psi) - a_3 (\sin \theta \sin \phi \sin \psi \\
& + \cos \phi \cos \psi)] + [Z_c + a_1 (-\sin \theta) + a_2 (\sin \phi \cos \theta) \\
& + a_3 (\cos \theta \cos \phi) - Z_{i,n-1}] [a_2 \cos \phi \cos \theta - a_3 \cos \theta \sin \phi] \} \quad (4.56)
\end{aligned}$$

For the cylinder, the Lagrangian, L_c , can be written as

$$\begin{aligned}
L_c = T_c - V_c = \frac{1}{2} [m_c (\dot{X}_c^2 + \dot{Y}_c^2 + \dot{Z}_c^2) + I_{xx} (\dot{\phi} - \dot{\psi} \sin \theta)^2 + I_{yy} (\dot{\theta} \cos \phi \\
+ \dot{\psi} \sin \phi \cos \theta)^2 + I_{zz} (\dot{\psi} \cos \theta \cos \phi - \dot{\theta} \sin \phi)^2] + w_c Y_c \quad (4.57)
\end{aligned}$$

from which the following parts of the Lagrange's equations are obtained:

$$\frac{d}{dt} \left(\frac{\partial L_c}{\partial \dot{X}_c} \right) - \frac{\partial L_c}{\partial X_c} \quad (4.58)$$

or,

$$m_c \ddot{X}_c; \quad (4.59)$$

$$\frac{d}{dt} \left(\frac{\partial L_c}{\partial \dot{Y}_c} \right) - \frac{\partial L_c}{\partial Y_c} \quad (4.60)$$

or,

$$m_c \ddot{Y}_c - w_c ; \quad (4.61)$$

$$\frac{d}{dt} \left(\frac{\partial L_c}{\partial \dot{Z}_c} \right) - \frac{\partial L_c}{\partial Z_c} \quad (4.62)$$

or,

$$m_c \ddot{Z}_c ; \quad (4.63)$$

$$\frac{d}{dt} \left(\frac{\partial L_c}{\partial \dot{\psi}} \right) - \frac{\partial L_c}{\partial \psi} \quad (4.64)$$

or,

$$\begin{aligned} & -I_{xx} [\dot{\phi} \dot{\theta} \cos \theta + \ddot{\phi} \sin \theta - 2\dot{\psi} \dot{\theta} \sin \theta \cos \theta - \ddot{\psi} \sin^2 \theta] \\ & + I_{yy} [\dot{\theta} \cos \phi (-\dot{\theta} \sin \phi \sin \theta + \dot{\phi} \cos \theta \cos \phi) + \sin \phi \cos \theta (-\dot{\phi} \dot{\theta} \sin \phi \\ & + \ddot{\theta} \cos \phi) + \dot{\psi} \sin^2 \phi \cos^2 \theta + \dot{\psi} (-2\dot{\theta} \sin^2 \phi \cos \theta \sin \theta \\ & + 2\dot{\phi} \sin \phi \cos \phi \cos^2 \theta)] + I_{zz} [\dot{\psi} (-2\dot{\phi} \cos \phi \sin \phi \cos^2 \theta \\ & - 2\dot{\theta} \cos \theta \sin \theta \cos^2 \phi) + \dot{\psi} \cos^2 \theta \cos^2 \phi + (\dot{\theta} \sin \phi)(\dot{\phi} \cos \theta \sin \phi \\ & + \dot{\theta} \cos \phi \sin \theta) - \cos \theta \cos \phi (\dot{\phi} \dot{\theta} \cos \phi + \ddot{\theta} \sin \phi)]; \end{aligned} \quad (4.65)$$

$$\frac{d}{dt} \left(\frac{\partial L_c}{\partial \dot{\theta}} \right) - \frac{\partial L_c}{\partial \theta} \quad (4.66)$$

or,

$$\begin{aligned} & I_{yy} [(-2\dot{\phi} \dot{\theta} \cos \phi \sin \phi + \ddot{\theta} \cos^2 \theta - \dot{\psi} \sin \phi (\dot{\phi} \cos \theta \sin \phi + \dot{\theta} \cos \phi \sin \theta) \\ & + \cos \theta \cos \phi (\dot{\psi} \dot{\phi} \cos \phi + \dot{\psi} \sin \phi))] - I_{zz} [\dot{\psi} \cos \theta (\dot{\phi} \cos^2 \phi - \dot{\phi} \sin^2 \phi) \\ & + \cos \phi \sin \phi (\dot{\psi} \cos \theta - \dot{\theta} \dot{\psi} \sin \theta) - 2\dot{\phi} \dot{\theta} \cos \phi \sin \phi - \ddot{\theta} \sin^2 \theta] \\ & - [I_{xx} (\dot{\phi} - \dot{\psi} \sin \theta) (-\dot{\psi} \cos \theta) + I_{yy} (\dot{\theta} \cos \phi + \dot{\psi} \sin \phi \cos \theta) (-\dot{\psi} \sin \phi \sin \theta) \\ & + I_{zz} (\dot{\psi} \cos \theta \cos \phi - \dot{\theta} \sin \phi) (-\dot{\psi} \cos \phi \sin \theta)]; \end{aligned} \quad (4.67)$$

and

$$\frac{d}{dt} \left(\frac{\partial L_c}{\partial \dot{\phi}} \right) - \frac{\partial L_c}{\partial \phi} \quad (4.68)$$

or,

$$\begin{aligned} & I_{xx} (\ddot{\phi} - \dot{\psi} \dot{\theta} \cos \theta - \dot{\psi} \sin \theta) - [I_{yy} (\dot{\theta} \cos \phi + \dot{\psi} \sin \phi \cos \theta) (\dot{\psi} \cos \theta \cos \phi - \dot{\theta} \sin \phi) \\ & - I_{zz} (\dot{\psi} \cos \theta \cos \phi - \dot{\theta} \sin \phi) (\dot{\psi} \cos \theta \sin \phi + \dot{\theta} \cos \phi)] \end{aligned} \quad (4.69)$$

Hence, the resulting Lagrange's equations include

$$\frac{d}{dt} \left(\frac{\partial L}{\partial \dot{X}_c} \right) - \frac{\partial L}{\partial X_c} = 0 \quad (4.70)$$

or,

$$\begin{aligned} m_c \ddot{X}_c + K_n [X_c + a_1(\cos \theta \cos \psi) + a_2(\sin \phi \sin \theta \cos \psi - \sin \psi \cos \phi) \\ + a_3(\sin \theta \cos \phi \cos \psi + \sin \phi \sin \psi) - X_{i,n-1}] - K_n I_n \{ [X_c + a_1(\cos \theta \cos \psi) \\ + a_2(\sin \phi \sin \theta \cos \psi - \sin \psi \cos \phi) \\ + a_3(\sin \theta \cos \phi \cos \psi + \sin \phi \sin \psi) - X_{i,n-1}]^2 + [Y_c + a_1(\sin \psi \cos \theta) \\ + a_2(\sin \psi \sin \phi \sin \theta + \cos \phi \cos \psi) + a_3(\sin \theta \cos \phi \sin \psi - \sin \phi \cos \psi) \\ - Y_{i,n-1}]^2 + [Z_c + a_1(-\sin \theta) + a_2(\sin \phi \cos \theta) + a_3(\cos \theta \cos \phi) \\ - Z_{i,n-1}]^2 \}^{\frac{1}{2}} [X_c + a_1(\cos \theta \cos \psi) + a_2(\sin \phi \sin \theta \cos \psi - \sin \psi \cos \phi) \\ + a_3(\sin \theta \cos \phi \cos \psi + \sin \phi \sin \psi) - X_{i,n-1}] = 0; \end{aligned} \quad (4.71)$$

$$\frac{d}{dt} \left(\frac{\partial L}{\partial \dot{Y}_c} \right) - \frac{\partial L}{\partial Y_c} = 0 \quad (4.72)$$

or,

$$\begin{aligned} m_c \ddot{Y}_c - w_c + K_n [Y_c + a_1(\sin \psi \cos \theta) + a_2(\sin \psi \sin \phi \sin \theta + \cos \phi \cos \psi) \\ + a_3(\sin \theta \cos \phi \sin \psi - \sin \phi \cos \psi) - Y_{i,n-1}] - K_n I_n \{ [X_c + a_1(\cos \theta \cos \psi) \\ + a_2(\sin \phi \sin \theta \cos \psi - \sin \psi \cos \phi) \\ + a_3(\sin \theta \cos \phi \cos \psi + \sin \phi \sin \psi) - X_{i,n-1}]^2 + [Y_c + a_1(\sin \psi \cos \theta) \\ + a_2(\sin \psi \sin \phi \sin \theta + \cos \phi \cos \psi) + a_3(\sin \theta \cos \phi \sin \psi - \sin \phi \cos \psi) \\ - Y_{i,n-1}]^2 + [Z_c + a_1(-\sin \theta) + a_2(\sin \phi \cos \theta) + a_3(\cos \theta \cos \phi) - Z_{i,n-1}]^2 \}^{\frac{1}{2}} [Y_c \\ + a_1(\sin \psi \cos \theta) + a_2(\sin \psi \sin \phi \sin \theta + \cos \phi \cos \psi) + a_3(\sin \theta \cos \phi \sin \psi \\ - \sin \phi \cos \psi) - Y_{i,n-1}] = 0; \end{aligned} \quad (4.73)$$

$$\frac{d}{dt} \left(\frac{\partial L}{\partial \dot{Z}_c} \right) - \frac{\partial L}{\partial Z_c} = 0 \quad (4.74)$$

or,

$$\begin{aligned}
& m_c \ddot{Z}_c + K_n [Z_c + a_1(-\sin \theta) + a_2(\sin \phi \cos \theta) + a_3(\cos \theta \cos \phi) \\
& - Z_{i,n-1}] - K_n I_n \{ [X_c + a_1(\cos \theta \cos \psi) + a_2(\sin \phi \sin \theta \cos \psi - \sin \psi \cos \phi) \\
& + a_3(\sin \theta \cos \phi \cos \psi + \sin \phi \sin \psi) - X_{i,n-1}]^2 + [Y_c + a_1(\sin \psi \cos \theta) \\
& + a_2(\sin \psi \sin \phi \sin \theta + \cos \phi \cos \psi) + a_3(\sin \theta \cos \phi \sin \psi - \sin \phi \cos \psi) \\
& - Y_{i,n-1}]^2 + [Z_c + a_1(-\sin \theta) + a_2(\sin \phi \cos \theta) + a_3(\cos \theta \cos \phi) - Z_{i,n-1}]^2 \}^{\frac{1}{2}} [Z_c \\
& + a_1(-\sin \theta) + a_2(\sin \phi \cos \theta) + a_3(\cos \theta \cos \phi) - Z_{i,n-1}] = 0;
\end{aligned} \tag{4.75}$$

$$\frac{d}{dt} \left(\frac{\partial L}{\partial \dot{\psi}} \right) - \frac{\partial L}{\partial \psi} = 0, \tag{4.76}$$

or,

$$\begin{aligned}
& -I_{xx} [\dot{\phi} \dot{\theta} \cos \theta + \ddot{\phi} \sin \theta - 2\dot{\psi} \dot{\theta} \sin \theta \cos \theta - \ddot{\psi} \sin^2 \theta] + I_{yy} [\dot{\theta} \cos \phi (-\dot{\theta} \sin \phi \sin \theta \\
& + \dot{\phi} \cos \theta \cos \phi) + \sin \phi \cos \theta (-\dot{\phi} \dot{\theta} \sin \phi + \ddot{\theta} \cos \phi) + \ddot{\psi} \sin^2 \phi \cos^2 \theta \\
& + \dot{\psi} (-2\dot{\theta} \sin^2 \phi \cos \theta \sin \theta + 2\dot{\phi} \sin \phi \cos \phi \cos^2 \theta)] + I_{zz} [\dot{\psi} (-2\dot{\phi} \cos \phi \sin \phi \cos^2 \theta \\
& - 2\dot{\theta} \cos \theta \sin \theta \cos^2 \phi) + \ddot{\psi} \cos^2 \theta \cos^2 \phi + (\dot{\theta} \sin \phi)(\dot{\phi} \cos \theta \sin \phi + \dot{\theta} \cos \phi \sin \theta) \\
& - \cos \theta \cos \phi (\dot{\phi} \dot{\theta} \cos \phi + \ddot{\theta} \sin \phi)] + K_n [X_c + a_1(\cos \theta \cos \psi) + a_2(\sin \phi \sin \theta \cos \psi \\
& - \sin \psi \cos \phi) + a_3(\sin \theta \cos \phi \cos \psi + \sin \phi \sin \psi) - X_{i,n-1}] [-a_1 \cos \theta \sin \psi \\
& - a_2(\sin \phi \sin \theta \sin \psi + \cos \psi \cos \phi) - a_3(\sin \theta \cos \phi \sin \psi - \sin \phi \cos \psi)] \\
& + K_n [Y_c + a_1(\sin \psi \cos \theta) + a_2(\sin \psi \sin \phi \sin \theta + \cos \phi \cos \psi) + a_3(\sin \theta \cos \phi \sin \psi \\
& - \sin \phi \cos \psi) - Y_{i,n-1}] [a_1 \cos \theta \cos \psi + a_2(\cos \psi \sin \phi \sin \theta - \cos \phi \sin \psi) \\
& + a_3(\sin \theta \cos \phi \cos \psi + \sin \phi \sin \psi)] - K_n I_n \{ [X_c + a_1(\cos \theta \cos \psi) + \\
& a_2(\sin \phi \sin \theta \cos \psi - \sin \psi \cos \phi) \\
& + a_3(\sin \theta \cos \phi \cos \psi + \sin \phi \sin \psi) - X_{i,n-1}]^2 + [Y_c + a_1(\sin \psi \cos \theta) \\
& + a_2(\sin \psi \sin \phi \sin \theta + \cos \phi \cos \psi) + a_3(\sin \theta \cos \phi \sin \psi - \sin \phi \cos \psi) - Y_{i,n-1}]^2 \\
& + [Z_c + a_1(-\sin \theta) + a_2(\sin \phi \cos \theta) + a_3(\cos \theta \cos \phi) - Z_{i,n-1}]^2 \}^{\frac{1}{2}} \{ [X_c \\
& + a_1(\cos \theta \cos \psi) + a_2(\sin \phi \sin \theta \cos \psi - \sin \psi \cos \phi) \\
& + a_3(\sin \theta \cos \phi \cos \psi + \sin \phi \sin \psi) - X_{i,n-1}] [-a_1 \cos \theta \sin \psi - a_2(\sin \phi \sin \theta \sin \psi \\
& + \cos \psi \cos \phi) - a_3(\sin \theta \cos \phi \sin \psi - \sin \phi \cos \psi)] + [Y_c + a_1(\sin \psi \cos \theta) \\
& + a_2(\sin \psi \sin \phi \sin \theta + \cos \phi \cos \psi) + a_3(\sin \theta \cos \phi \sin \psi \\
& - \sin \phi \cos \psi) - Y_{i,n-1}] [a_1 \cos \theta \cos \psi + a_2(\cos \psi \sin \phi \sin \theta - \cos \phi \sin \psi) \\
& + a_3(\sin \theta \cos \phi \cos \psi + \sin \phi \sin \psi)] \} = 0;
\end{aligned} \tag{4.77}$$

$$\frac{d}{dt} \left(\frac{\partial L}{\partial \dot{\theta}} \right) - \frac{\partial L}{\partial \theta} = 0 \quad (4.78)$$

or,

$$\begin{aligned} & I_{yy} [-2\dot{\phi}\dot{\theta} \cos \phi \sin \phi + \ddot{\theta} \cos^2 \theta - \dot{\psi} \sin \phi (\dot{\phi} \cos \theta \sin \phi + \dot{\theta} \cos \phi \sin \theta) \\ & + \cos \theta \cos \phi (\dot{\psi} \dot{\phi} \cos \phi + \dot{\psi} \sin \phi)] - I_{zz} [\dot{\psi} \cos \theta (\dot{\phi} \cos^2 \phi - \dot{\phi} \sin^2 \phi) \\ & + \cos \phi \sin \phi (\dot{\psi} \cos \theta - \dot{\theta} \dot{\psi} \sin \theta) - 2\dot{\phi}\dot{\theta} \cos \phi \sin \phi - \ddot{\theta} \sin^2 \theta] - [I_{xx} (\dot{\phi} \\ & - \dot{\psi} \sin \theta)(-\dot{\psi} \cos \theta) + I_{yy} (\dot{\theta} \cos \phi + \dot{\psi} \sin \phi \cos \theta)(-\dot{\psi} \sin \phi \sin \theta) + I_{zz} (\dot{\psi} \cos \theta \cos \phi \\ & - \dot{\theta} \sin \phi)(-\dot{\psi} \cos \phi \sin \theta)] + K_n [X_c + a_1 (\cos \theta \cos \psi) + a_2 (\sin \phi \sin \theta \cos \psi \\ & - \sin \psi \cos \phi) + a_3 (\sin \theta \cos \phi \cos \psi + \sin \phi \sin \psi) - X_{i,n-1}] [-a_1 \cos \psi \sin \theta \\ & + a_2 (\sin \phi \cos \theta \cos \psi) + a_3 (\cos \theta \cos \phi \cos \psi)] + K_n [Y_c + a_1 (\sin \psi \cos \theta) \\ & + a_2 (\sin \psi \sin \phi \sin \theta + \cos \phi \cos \psi) + a_3 (\sin \theta \cos \phi \sin \psi - \sin \phi \cos \psi) - Y_{i,n-1}] \\ & [-a_1 \sin \psi \sin \theta + a_2 \sin \psi \sin \phi \cos \theta + a_3 (\cos \theta \cos \phi \sin \psi)] \\ & + K_n [Z_c + a_1 (-\sin \theta) + a_2 (\sin \phi \cos \theta) + a_3 (\cos \theta \cos \phi) - Z_{i,n-1}] (-a_1 \cos \theta \\ & - a_2 \sin \phi \sin \theta - a_3 \sin \theta \cos \phi) - K_n I_n \{ [X_c + a_1 (\cos \theta \cos \psi) + \\ & a_2 (\sin \phi \sin \theta \cos \psi - \sin \psi \cos \phi) \\ & + a_3 (\sin \theta \cos \phi \cos \psi + \sin \phi \sin \psi) - X_{i,n-1}]^2 + [Y_c + a_1 (\sin \psi \cos \theta) \\ & + a_2 (\sin \psi \sin \phi \sin \theta + \cos \phi \cos \psi) + a_3 (\sin \theta \cos \phi \sin \psi - \sin \phi \cos \psi) - Y_{i,n-1}]^2 \\ & + [Z_c + a_1 (-\sin \theta) + a_2 (\sin \phi \cos \theta) + a_3 (\cos \theta \cos \phi) - Z_{i,n-1}]^2 \}^{\frac{1}{2}} \{ [X_c + \\ & a_1 (\cos \theta \cos \psi) + a_2 (\sin \phi \sin \theta \cos \psi - \sin \psi \cos \phi) \\ & + a_3 (\sin \theta \cos \phi \cos \psi + \sin \phi \sin \psi) - X_{i,n-1}] [-a_1 \cos \psi \sin \theta + a_2 (\sin \phi \cos \theta \cos \psi) \\ & + a_3 (\cos \theta \cos \phi \cos \psi)] + [Y_c + a_1 (\sin \psi \cos \theta) \\ & + a_2 (\sin \psi \sin \phi \sin \theta + \cos \phi \cos \psi) + a_3 (\sin \theta \cos \phi \sin \psi - \sin \phi \cos \psi) - Y_{i,n-1}] \\ & [-a_1 \sin \psi \sin \theta + a_2 \sin \psi \sin \phi \cos \theta + a_3 (\cos \theta \cos \phi \sin \psi)] \\ & + [Z_c + a_1 (-\sin \theta) + a_2 (\sin \phi \cos \theta) + a_3 (\cos \theta \cos \phi) - Z_{i,n-1}] (-a_1 \cos \theta \\ & - a_2 \sin \phi \sin \theta - a_3 \sin \theta \cos \phi) \} = 0; \end{aligned} \quad (4.79)$$

and

$$\frac{d}{dt} \left(\frac{\partial L}{\partial \dot{\phi}} \right) - \frac{\partial L}{\partial \phi} = 0 \quad (4.80)$$

or,

$$\begin{aligned}
& I_{xx}(\ddot{\phi} - \dot{\psi}\dot{\theta}\cos\theta - \ddot{\psi}\sin\theta) - [I_{yy}(\dot{\theta}\cos\phi + \dot{\psi}\sin\phi\cos\theta)(\dot{\psi}\cos\theta\cos\phi - \dot{\theta}\sin\phi) \\
& - I_{zz}(\dot{\psi}\cos\theta\cos\phi - \dot{\theta}\sin\phi)(\dot{\psi}\cos\theta\sin\phi + \dot{\theta}\cos\phi)] \\
& + K_n[X_c + a_1(\cos\theta\cos\psi) + a_2(\sin\phi\sin\theta\cos\psi - \sin\psi\cos\phi) \\
& + a_3(\sin\theta\cos\phi\cos\psi + \sin\phi\sin\psi) - X_{i,n-1}][a_2(\cos\phi\sin\theta\cos\psi + \sin\psi\sin\phi) \\
& + a_3(-\sin\theta\sin\phi\cos\psi)] + K_n[Y_c + a_1(\sin\psi\cos\theta) \\
& + a_2(\sin\psi\sin\phi\sin\theta + \cos\phi\cos\psi) + a_3(\sin\theta\cos\phi\sin\psi \\
& - \sin\phi\cos\psi) - Y_{i,n-1}][a_2(\sin\psi\cos\phi\sin\theta - \sin\phi\cos\psi) - a_3(\sin\theta\sin\phi\sin\psi \\
& + \cos\phi\cos\psi)] + K_n[Z_c + a_1(-\sin\theta) + a_2(\sin\phi\cos\theta) \\
& + a_3(\cos\theta\cos\phi) - Z_{i,n-1}][a_2\cos\phi\cos\theta - a_3\cos\theta\sin\phi] - K_n I_n \{ [X_c \\
& + a_1(\cos\theta\cos\psi) + a_2(\sin\phi\sin\theta\cos\psi - \sin\psi\cos\phi) \\
& + a_3(\sin\theta\cos\phi\cos\psi + \sin\phi\sin\psi) - X_{i,n-1}]^2 + [Y_c + a_1(\sin\psi\cos\theta) \\
& + a_2(\sin\psi\sin\phi\sin\theta + \cos\phi\cos\psi) + a_3(\sin\theta\cos\phi\sin\psi - \sin\phi\cos\psi) - Y_{i,n-1}]^2 \\
& + [Z_c + a_1(-\sin\theta) + a_2(\sin\phi\cos\theta) + a_3(\cos\theta\cos\phi) - Z_{i,n-1}]^2 \}^{\frac{1}{2}} \{ [X_c \\
& + a_1(\cos\theta\cos\psi) + a_2(\sin\phi\sin\theta\cos\psi - \sin\psi\cos\phi) \\
& + a_3(\sin\theta\cos\phi\cos\psi + \sin\phi\sin\psi) - X_{i,n-1}][a_2(\cos\phi\sin\theta\cos\psi + \sin\psi\sin\phi) \\
& + a_3(-\sin\theta\sin\phi\cos\psi)] + [Y_c + a_1(\sin\psi\cos\theta) \\
& + a_2(\sin\psi\sin\phi\sin\theta + \cos\phi\cos\psi) + a_3(\sin\theta\cos\phi\sin\psi \\
& - \sin\phi\cos\psi) - Y_{i,n-1}][a_2(\sin\psi\cos\phi\sin\theta - \sin\phi\cos\psi) - a_3(\sin\theta\sin\phi\sin\psi \\
& + \cos\phi\cos\psi)] + [Z_c + a_1(-\sin\theta) + a_2(\sin\phi\cos\theta) \\
& + a_3(\cos\theta\cos\phi) - Z_{i,n-1}][a_2\cos\phi\cos\theta - a_3\cos\theta\sin\phi] \} = 0
\end{aligned}
\tag{4.81}$$

4.8 SMALL MOTIONS ABOUT EQUILIBRIUM (LINEARIZED EQUATIONS)

In contrast to the previously defined complete equations of motion (EOM's) for the system, we now look at the linearized equations in order to more easily examine the behavior of small motions about the equilibrium point. It can be shown from equations (4.36), (4.38), and (4.40) that the EOM's for each of the lowest $n-2$ (to exclude $n-1$) point masses $m_{i,j}$ making up mooring line i , where $X_{i,j}(t) = X_{i,j,\text{new}}(t) + X_{i,j,\text{eq}}$, $Y_{i,j}(t) = Y_{i,j,\text{new}}(t) + Y_{i,j,\text{eq}}$, and $Z_{i,j}(t) = Z_{i,j,\text{new}}(t) + Z_{i,j,\text{eq}}$, are found as

$$\begin{aligned}
& m_{i,j} \ddot{X}_{i,j,\text{new}} + K_{i,j} (X_{i,j,\text{new}} - X_{i,j-1,\text{new}}) \left(1 - \frac{l_{i,j}}{\sqrt{G_{i,j}}}\right) + \\
& \frac{K_{i,j} l_{i,j} H_{i,j}}{2G_{i,j}^{3/2}} (X_{i,j,\text{eq}} - X_{i,j-1,\text{eq}}) - \\
& K_{i,j+1} (X_{i,j+1,\text{new}} - X_{i,j,\text{new}}) \left(1 - \frac{l_{i,j+1}}{\sqrt{G_{i,j+1}}}\right) - \\
& \frac{K_{i,j+1} l_{i,j+1} H_{i,j+1}}{2G_{i,j+1}^{3/2}} (X_{i,j+1,\text{eq}} - X_{i,j,\text{eq}}) = 0;
\end{aligned} \tag{4.82}$$

$$\begin{aligned}
& m_{i,j} \ddot{Y}_{i,j,\text{new}} + K_{i,j} (Y_{i,j,\text{new}} - Y_{i,j-1,\text{new}}) \left(1 - \frac{l_{i,j}}{\sqrt{G_{i,j}}}\right) + \\
& \frac{K_{i,j} l_{i,j} H_{i,j}}{2G_{i,j}^{3/2}} (Y_{i,j,\text{eq}} - Y_{i,j-1,\text{eq}}) - \\
& K_{i,j+1} (Y_{i,j+1,\text{new}} - Y_{i,j,\text{new}}) \left(1 - \frac{l_{i,j+1}}{\sqrt{G_{i,j+1}}}\right) - \\
& \frac{K_{i,j+1} l_{i,j+1} H_{i,j+1}}{2G_{i,j+1}^{3/2}} (Y_{i,j+1,\text{eq}} - Y_{i,j,\text{eq}}) = 0;
\end{aligned} \tag{4.83}$$

and

$$\begin{aligned}
& m_{i,j} \ddot{Z}_{i,j,\text{new}} + K_{i,j} (Z_{i,j,\text{new}} - Z_{i,j-1,\text{new}}) \left(1 - \frac{l_{i,j}}{\sqrt{G_{i,j}}}\right) + \\
& \frac{K_{i,j} l_{i,j} H_{i,j}}{2G_{i,j}^{3/2}} (Z_{i,j,\text{eq}} - Z_{i,j-1,\text{eq}}) - \\
& K_{i,j+1} (Z_{i,j+1,\text{new}} - Z_{i,j,\text{new}}) \left(1 - \frac{l_{i,j+1}}{\sqrt{G_{i,j+1}}}\right) - \\
& \frac{K_{i,j+1} l_{i,j+1} H_{i,j+1}}{2G_{i,j+1}^{3/2}} (Z_{i,j+1,\text{eq}} - Z_{i,j,\text{eq}}) = 0
\end{aligned} \tag{4.84}$$

where

$$\begin{aligned}
G_{i,j} &= X_{i,j,eq}^2 + X_{i,j-1,eq}^2 - 2X_{i,j,eq} X_{i,j-1,eq} + Y_{i,j,eq}^2 + Y_{i,j-1,eq}^2 - 2Y_{i,j,eq} Y_{i,j-1,eq} \\
&Z_{i,j,eq}^2 + Z_{i,j-1,eq}^2 - 2Z_{i,j,eq} Z_{i,j-1,eq} \\
H_{i,j} &= A_{i,j} X_{i,j,new} + B_{i,j} X_{i,j-1,new} + C_{i,j} Y_{i,j,new} + D_{i,j} Y_{i,j-1,new} + E_{i,j} Z_{i,j,new} + F_{i,j} Z_{i,j-1,new} \\
A_{i,j} &= 2(X_{i,j,eq} - X_{i,j-1,eq}) \\
B_{i,j} &= -A_{i,j} \\
C_{i,j} &= 2(Y_{i,j,eq} - Y_{i,j-1,eq}) \\
D_{i,j} &= -C_{i,j} \\
E_{i,j} &= 2(Z_{i,j,eq} - Z_{i,j-1,eq}) \\
F_{i,j} &= -E_{i,j}
\end{aligned} \tag{4.85}$$

for all j except $j=n$. Here the subscript “eq” refers to the equilibrium state under a net bouyant force, and the subscript “new” refers to a quantity relative to the equilibrium state. However, for mass $n-1$, linearizing equations (4.41) through (4.43) by ignoring all higher order terms in the “new” variables and letting $X_c(t) = X_{c,new}(t) + X_{c,eq}$, $Y_c(t) = Y_{c,new}(t) + Y_{c,eq}$, and $Z_c(t) = Z_{c,new}(t) + Z_{c,eq}$ leads to

$$\begin{aligned}
m_{i,n-1} \ddot{X}_{i,n-1,new} + K_{i,n-1} (X_{i,n-1,new} - X_{i,n-2,new}) \left(1 - \frac{l_{i,n-1}}{\sqrt{G_{i,n-1}}}\right) + \\
\frac{K_{i,n-1} l_{i,n-1} H_{i,n-1}}{2G_{i,n-1}^{3/2}} (X_{i,n-1,eq} - X_{i,n-2,eq}) + K_{i,n} (X_{c,new} - a_{i,2} \psi + a_{i,3} \theta \\
- X_{i,n-1,new}) \left(1 - \frac{l_{i,n}}{\sqrt{G_{i,n}}}\right) + \frac{K_{i,n} l_{i,n} H_{i,n}}{2G_{i,n}^{3/2}} (a_{i,1} - X_{i,n-1,eq}) = 0;
\end{aligned} \tag{4.86}$$

$$\begin{aligned}
m_{i,n-1} \ddot{Y}_{i,n-1,new} + K_{i,n-1} (Y_{i,n-1,new} - Y_{i,n-2,new}) \left(1 - \frac{l_{i,n-1}}{\sqrt{G_{i,n-1}}}\right) \\
+ \frac{K_{i,n-1} l_{i,n-1} H_{i,n-1}}{2G_{i,n-1}^{3/2}} (Y_{i,n-1,new} - Y_{i,n-2,new}) + K_{i,n} (Y_{c,new} + a_{i,1} \psi \\
- a_{i,3} \phi - Y_{i,n-1,new}) \left(1 - \frac{l_{i,n}}{\sqrt{G_{i,n}}}\right) + \frac{K_{i,n} l_{i,n} H_{i,n}}{2G_{i,n}^{3/2}} (Y_{c,eq} + a_{i,2} - Y_{i,n-1,eq}) = 0;
\end{aligned} \tag{4.87}$$

and

$$\begin{aligned}
& m_{i,n-1} \ddot{Z}_{i,n-1,new} + K_{i,n-1} (Z_{i,n-1,new} - Z_{i,n-2,new}) \left(1 - \frac{I_{i,n-1}}{\sqrt{G_{i,n-1}}}\right) \\
& + \frac{K_{i,n-1} I_{i,n-1} H_{i,n-1}}{2G_{i,n-1}^{3/2}} (Z_{i,n-1,new} - Z_{i,n-2,new}) + K_{i,n} (Z_{c,new} - a_{i,1} \theta \\
& + a_{i,2} \phi - Z_{i,n-1,new}) \left(1 - \frac{I_{i,n}}{\sqrt{G_{i,n}}}\right) + \frac{K_{i,n} I_{i,n} H_{i,n}}{2G_{i,n}^{3/2}} (a_{i,3} - Z_{i,n-1,eq}) = 0
\end{aligned} \tag{4.88}$$

where

$$\begin{aligned}
G_{i,n} &= a_{i,1}^2 - 2a_{i,1} X_{i,n-1,eq} + X_{i,n-1,eq}^2 + Y_{c,eq}^2 + 2a_{i,2} Y_{c,eq} - 2Y_{c,eq} Y_{i,n-1,eq} + a_{i,2}^2 \\
& - 2a_{i,2} Y_{i,n-1,eq} + Y_{i,n-1,eq}^2 + a_{i,3}^2 - 2a_{i,3} Z_{i,n-1,eq} + Z_{i,n-1,eq}^2 \\
H_{i,n} &= A_{i,n} X_{c,new} + B_{i,n} X_{c,new} + C_{i,n} Y_{c,new} + D_{i,n} \psi + E_{i,n} \theta + F_{i,n} \phi + R_{i,n} X_{i,n-1,new} \\
& + S_{i,n} Y_{i,n-1,new} + T_{i,n} Z_{i,n-1,new} \\
A_{i,n} &= 2(a_{i,1} - X_{i,n-1,eq}) \\
B_{i,n} &= 2(Y_{c,eq} + a_{i,2} - Y_{i,n-1,eq}) \\
C_{i,n} &= 2(a_{i,3} - Z_{i,n-1,eq}) \\
D_{i,n} &= 2(a_{i,2} X_{i,n-1,eq} + a_{i,1} Y_{c,eq} - a_{i,1} Y_{i,n-1,eq}) \\
E_{i,n} &= 2(-a_{i,3} X_{i,n-1,eq} + a_{i,1} Z_{i,n-1,eq}) \\
F_{i,n} &= 2(-a_{i,3} Y_{c,eq} + a_{i,3} Y_{i,n-1,eq} - a_{i,2} Z_{i,n-1,eq}) \\
R_{i,n} &= -A_{i,n} \\
S_{i,n} &= -B_{i,n} \\
T_{i,n} &= -C_{i,n}
\end{aligned} \tag{4.89}$$

Here, it is assumed that the system has sufficient symmetry such that the initial and equilibrium values of θ , ϕ , and ψ are zero. Hence, no subscript “new” will be used for these quantities. Likewise, $X_{c,eq}$ and $Z_{c,eq}$ are zero and these terms are omitted in all equations.

Using the same procedure as above, linearizing equations (4.71), (4.73), (4.75), (4.77), (4.79), and (4.81) yields

$$m_c \ddot{X}_{c,new} + K_{i,n} (X_{c,new} - a_{i,2} \psi + a_{i,3} \theta - X_{i,n-1,new}) \left(1 - \frac{l_{i,n}}{\sqrt{G_{i,n}}}\right) + \frac{K_{i,n} l_{i,n} H_{i,n}}{2G_{i,n}^{3/2}} (a_{i,1} - X_{i,n-1,eq}) = 0; \quad (4.90)$$

$$m_c \ddot{Y}_{c,new} + K_{i,n} (Y_{c,new} + a_{i,1} \psi - a_{i,3} \phi - Y_{i,n-1,new}) \left(1 - \frac{l_{i,n}}{\sqrt{G_{i,n}}}\right) + \frac{K_{i,n} l_{i,n} H_{i,n}}{2G_{i,n}^{3/2}} (Y_{c,eq} + a_{i,2} - Y_{i,n-1,eq}) = 0; \quad (4.91)$$

$$m_c \ddot{Z}_{c,new} + K_{i,n} (Z_{c,new} - a_{i,1} \theta + a_{i,2} \phi - Z_{i,n-1,new}) \left(1 - \frac{l_{i,n}}{\sqrt{G_{i,n}}}\right) + \frac{K_{i,n} l_{i,n} H_{i,n}}{2G_{i,n}^{3/2}} (a_{i,3} - Z_{i,n-1,eq}) = 0; \quad (4.92)$$

$$I_{zz} \ddot{\psi} + K_{i,n} (-a_{i,2} X_{c,new} + a_{i,1} X_{i,n-1,eq} \psi - a_{i,3} X_{i,n-1,eq} \phi + a_{i,2} X_{i,n-1,new} + a_{i,1} Y_{c,new} - a_{i,1} Y_{i,n-1,new} - a_{i,2} \psi Y_{c,eq} + a_{i,3} \theta Y_{c,eq} + a_{i,2} \psi Y_{i,n-1,eq} - a_{i,3} \theta Y_{i,n-1,eq}) \left(1 - \frac{l_{i,n}}{\sqrt{G_{i,n}}}\right) + \frac{K_{i,n} l_{i,n} H_{i,n}}{2G_{i,n}^{3/2}} (a_{i,2} X_{i,n-1,eq} + a_{i,1} Y_{c,eq} - a_{i,1} Y_{i,n-1,eq}) = 0; \quad (4.93)$$

$$I_{yy} \ddot{\theta} + K_{i,n} (a_{i,3} X_{c,new} - a_{i,3} X_{i,n-1,new} + a_{i,1} X_{i,n-1,eq} \theta - a_{i,2} X_{i,n-1,eq} \phi + a_{i,3} Y_{c,eq} \psi - a_{i,3} Y_{i,n-1,eq} \psi - a_{i,1} Z_{c,new} + a_{i,1} Z_{i,n-1,new} + a_{i,3} Z_{i,n-1,eq} \theta) \left(1 - \frac{l_{i,n}}{\sqrt{G_{i,n}}}\right) + \frac{K_{i,n} l_{i,n} H_{i,n}}{2G_{i,n}^{3/2}} (-a_{i,3} X_{i,n-1,eq} + a_{i,1} Z_{i,n-1,eq}) = 0; \quad (4.94)$$

and

$$I_{xx} \ddot{\phi} + K_{i,n} (-a_{i,2} X_{i,n-1,eq} \theta - a_{i,3} Y_{c,new} - a_{i,1} a_{i,3} \psi + a_{i,3} Y_{i,n-1,new} - a_{i,2} Y_{c,eq} \phi + a_{i,2} Y_{i,n-1,eq} \phi - a_{i,2} Z_{c,new} - a_{i,2} Z_{i,n-1,new} + a_{i,3} Z_{i,n-1,eq} \phi) \left(1 - \frac{l_{i,n}}{\sqrt{G_{i,n}}}\right) + \frac{K_{i,n} l_{i,n} H_{i,n}}{2G_{i,n}^{3/2}} (a_{i,3} Y_{i,n-1,eq} - a_{i,3} Y_{c,eq} - a_{i,2} Z_{i,n-1,eq}) = 0 \quad (4.95)$$

Equations (4.82) through (4.84), (4.86) through (4.88), and (4.90) through (4.95) can be nondimensionalized by letting $a_{i,j} = a_{i,j}/R$, $X_{c,new} = X_{c,new}/R$, $Y_{c,new} = Y_{c,new}/R$, $Z_{c,new} = Z_{c,new}/R$, $X_{i,j,new} = X_{i,j,new}/R$, $Y_{i,j,new} = Y_{i,j,new}/R$, $Z_{i,j,new} = Z_{i,j,new}/R$, $m_{i,j} = m_{i,j}/m_c$, $m_c = m_c/m_c = 1$, $K_{i,j} = K_{i,j}R/(m_c g)$, $I_{xx} = I_{xx}/(m_c R^2)$, $I_{yy} = I_{yy}/(m_c R^2)$, $I_{zz} = I_{zz}/(m_c R^2)$, and $\tau = t(g/R)^{1/2}$.

If overdots now represent derivatives with respect to τ , these equations become:

$$\begin{aligned}
& m_{i,j} \ddot{X}_{i,j,new} + K_{i,j} (X_{i,j,new} - X_{i,j-1,new}) \left(1 - \frac{I_{i,j}}{\sqrt{G_{i,j}}}\right) + \\
& \frac{K_{i,j} I_{i,j} H_{i,j}}{2G_{i,j}^{3/2}} (X_{i,j,eq} - X_{i,j-1,eq}) - \\
& K_{i,j+1} (X_{i,j+1,new} - X_{i,j,new}) \left(1 - \frac{I_{i,j+1}}{\sqrt{G_{i,j+1}}}\right) - \\
& \frac{K_{i,j+1} I_{i,j+1} H_{i,j+1}}{2G_{i,j+1}^{3/2}} (X_{i,j+1,eq} - X_{i,j,eq}) = 0;
\end{aligned} \tag{4.96}$$

$$\begin{aligned}
& m_{i,j} \ddot{Y}_{i,j,new} + K_{i,j} (Y_{i,j,new} - Y_{i,j-1,new}) \left(1 - \frac{I_{i,j}}{\sqrt{G_{i,j}}}\right) + \\
& \frac{K_{i,j} I_{i,j} H_{i,j}}{2G_{i,j}^{3/2}} (Y_{i,j,eq} - Y_{i,j-1,eq}) - \\
& K_{i,j+1} (Y_{i,j+1,new} - Y_{i,j,new}) \left(1 - \frac{I_{i,j+1}}{\sqrt{G_{i,j+1}}}\right) - \\
& \frac{K_{i,j+1} I_{i,j+1} H_{i,j+1}}{2G_{i,j+1}^{3/2}} (Y_{i,j+1,eq} - Y_{i,j,eq}) = 0;
\end{aligned} \tag{4.97}$$

$$\begin{aligned}
& m_{i,j} \ddot{Z}_{i,j,new} + K_{i,j} (Z_{i,j,new} - Z_{i,j-1,new}) \left(1 - \frac{I_{i,j}}{\sqrt{G_{i,j}}}\right) + \\
& \frac{K_{i,j} I_{i,j} H_{i,j}}{2G_{i,j}^{3/2}} (Z_{i,j,eq} - Z_{i,j-1,eq}) - \\
& K_{i,j+1} (Z_{i,j+1,new} - Z_{i,j,new}) \left(1 - \frac{I_{i,j+1}}{\sqrt{G_{i,j+1}}}\right) - \\
& \frac{K_{i,j+1} I_{i,j+1} H_{i,j+1}}{2G_{i,j+1}^{3/2}} (Z_{i,j+1,eq} - Z_{i,j,eq}) = 0;
\end{aligned} \tag{4.98}$$

$$\begin{aligned}
& m_{i,n-1} \ddot{X}_{i,n-1,new} + K_{i,n-1} (X_{i,n-1,new} - X_{i,n-2,new}) \left(1 - \frac{I_{i,n-1}}{\sqrt{G_{i,n-1}}}\right) + \\
& \frac{K_{i,n-1} I_{i,n-1} H_{i,n-1}}{2G_{i,n-1}^{3/2}} (X_{i,n-1,eq} - X_{i,n-2,eq}) + K_{i,n} (X_{c,new} - a_{i,2}\psi + a_{i,3}\theta \\
& - X_{i,n-1,new}) \left(1 - \frac{I_{i,n}}{\sqrt{G_{i,n}}}\right) + \frac{K_{i,n} I_{i,n} H_{i,n}}{2G_{i,n}^{3/2}} (a_{i,1} - X_{i,n-1,eq}) = 0;
\end{aligned} \tag{4.99}$$

$$\begin{aligned}
& m_{i,n-1} \ddot{Y}_{i,n-1,new} + K_{i,n-1} (Y_{i,n-1,new} - Y_{i,n-2,new}) \left(1 - \frac{I_{i,n-1}}{\sqrt{G_{i,n-1}}}\right) \\
& + \frac{K_{i,n-1} I_{i,n-1} H_{i,n-1}}{2G_{i,n-1}^{3/2}} (Y_{i,n-1,new} - Y_{i,n-2,new}) + K_{i,n} (Y_{c,new} + a_{i,1}\psi \\
& - a_{i,3}\phi - Y_{i,n-1,new}) \left(1 - \frac{I_{i,n}}{\sqrt{G_{i,n}}}\right) + \frac{K_{i,n} I_{i,n} H_{i,n}}{2G_{i,n}^{3/2}} (Y_{c,eq} + a_{i,2} - Y_{i,n-1,eq}) = 0;
\end{aligned} \tag{4.100}$$

$$\begin{aligned}
& m_{i,n-1} \ddot{Z}_{i,n-1,new} + K_{i,n-1} (Z_{i,n-1,new} - Z_{i,n-2,new}) \left(1 - \frac{I_{i,n-1}}{\sqrt{G_{i,n-1}}}\right) \\
& + \frac{K_{i,n-1} I_{i,n-1} H_{i,n-1}}{2G_{i,n-1}^{3/2}} (Z_{i,n-1,new} - Z_{i,n-2,new}) + K_{i,n} (Z_{c,new} - a_{i,1}\theta \\
& + a_{i,2}\phi - Z_{i,n-1,new}) \left(1 - \frac{I_{i,n}}{\sqrt{G_{i,n}}}\right) + \frac{K_{i,n} I_{i,n} H_{i,n}}{2G_{i,n}^{3/2}} (a_{i,3} - Z_{i,n-1,eq}) = 0;
\end{aligned} \tag{4.101}$$

$$\begin{aligned}
& \ddot{X}_{c,new} + K_{i,n} (X_{c,new} - a_{i,2}\psi + a_{i,3}\theta - X_{i,n-1,new}) \left(1 - \frac{I_{i,n}}{\sqrt{G_{i,n}}}\right) + \\
& \frac{K_{i,n} I_{i,n} H_{i,n}}{2G_{i,n}^{3/2}} (a_{i,1} - X_{i,n-1,eq}) = 0;
\end{aligned} \tag{4.102}$$

$$\begin{aligned}
& \ddot{Y}_{c,new} + K_{i,n} (Y_{c,new} + a_{i,1}\psi - a_{i,3}\phi - Y_{i,n-1,new}) \left(1 - \frac{I_{i,n}}{\sqrt{G_{i,n}}}\right) + \\
& \frac{K_{i,n} I_{i,n} H_{i,n}}{2G_{i,n}^{3/2}} (Y_{c,eq} + a_{i,2} - Y_{i,n-1,eq}) = 0;
\end{aligned} \tag{4.103}$$

$$\begin{aligned}
& \ddot{Z}_{c,new} + K_{i,n} (Z_{c,new} - a_{i,1}\theta + a_{i,2}\phi - Z_{i,n-1,new}) \left(1 - \frac{I_{i,n}}{\sqrt{G_{i,n}}}\right) + \\
& \frac{K_{i,n} I_{i,n} H_{i,n}}{2G_{i,n}^{3/2}} (a_{i,3} - Z_{i,n-1,eq}) = 0;
\end{aligned} \tag{4.104}$$

$$\begin{aligned}
& I_{zz}\ddot{\psi} + K_{i,n}(-a_{i,2}X_{c,new} + a_{i,1}X_{i,n-1,eq}\psi - a_{i,3}X_{i,n-1,eq}\phi + a_{i,2}X_{i,n-1,new} \\
& + a_{i,1}Y_{c,new} - a_{i,1}Y_{i,n-1,new} - a_{i,2}\psi Y_{c,eq} + a_{i,3}\theta Y_{c,eq} + a_{i,2}\psi Y_{i,n-1,eq} \\
& - a_{i,3}\theta Y_{i,n-1,eq})(1 - \frac{I_{i,n}}{\sqrt{G_{i,n}}}) + \frac{K_{i,n}I_{i,n}H_{i,n}}{2G_{i,n}^{3/2}}(a_{i,2}X_{i,n-1,eq} + a_{i,1}Y_{c,eq} \\
& - a_{i,1}Y_{i,n-1,eq}) = 0;
\end{aligned} \tag{4.105}$$

$$\begin{aligned}
& I_{yy}\ddot{\theta} + K_{i,n}(a_{i,3}X_{c,new} - a_{i,3}X_{i,n-1,new} + a_{i,1}X_{i,n-1,eq}\theta - a_{i,2}X_{i,n-1,eq}\phi \\
& + a_{i,3}Y_{c,eq}\psi - a_{i,3}Y_{i,n-1,eq}\psi - a_{i,1}Z_{c,new} + a_{i,1}Z_{i,n-1,new} \\
& + a_{i,3}Z_{i,n-1,eq}\theta)(1 - \frac{I_{i,n}}{\sqrt{G_{i,n}}}) + \frac{K_{i,n}I_{i,n}H_{i,n}}{2G_{i,n}^{3/2}}(-a_{i,3}X_{i,n-1,eq} + a_{i,1}Z_{i,n-1,eq}) = 0;
\end{aligned} \tag{4.106}$$

and

$$\begin{aligned}
& I_{xx}\ddot{\phi} + K_{i,n}(-a_{i,2}X_{i,n-1,eq}\theta - a_{i,3}Y_{c,new} - a_{i,1}a_{i,3}\psi + a_{i,3}Y_{i,n-1,new} - a_{i,2}Y_{c,eq}\phi \\
& + a_{i,2}Y_{i,n-1,eq}\phi - a_{i,2}Z_{c,new} - a_{i,2}Z_{i,n-1,new} + a_{i,3}Z_{i,n-1,eq}\phi)(1 - \frac{I_{i,n}}{\sqrt{G_{i,n}}}) \\
& + \frac{K_{i,n}I_{i,n}H_{i,n}}{2G_{i,n}^{3/2}}(a_{i,3}Y_{i,n-1,eq} - a_{i,3}Y_{c,eq} - a_{i,2}Z_{i,n-1,eq}) = 0
\end{aligned} \tag{4.107}$$

where

$$\begin{aligned}
G_{i,j} &= X_{i,j,eq}^2 + X_{i,j-1,eq}^2 - 2X_{i,j,eq}X_{i,j-1,eq} + Y_{i,j,eq}^2 + Y_{i,j-1,eq}^2 - 2Y_{i,j,eq}Y_{i,j-1,eq} \\
& Z_{i,j,eq}^2 + Z_{i,j-1,eq}^2 - 2Z_{i,j,eq}Z_{i,j-1,eq} \\
H_{i,j} &= A_{i,j}X_{i,j,new} + B_{i,j}X_{i,j-1,new} + C_{i,j}Y_{i,j,new} + D_{i,j}Y_{i,j-1,new} + E_{i,j}Z_{i,j,new} + F_{i,j}Z_{i,j-1,new} \\
A_{i,j} &= 2(X_{i,j,eq} - X_{i,j-1,eq}) \\
B_{i,j} &= -A_{i,j} \\
C_{i,j} &= 2(Y_{i,j,eq} - Y_{i,j-1,eq}) \\
D_{i,j} &= -C_{i,j} \\
E_{i,j} &= 2(Z_{i,j,eq} - Z_{i,j-1,eq}) \\
F_{i,j} &= -E_{i,j}
\end{aligned} \tag{4.108}$$

and

$$\begin{aligned}
G_{i,n} &= a_{i,1}^2 - 2a_{i,1}X_{i,n-1,eq} + X_{i,n-1,eq}^2 + Y_{c,eq}^2 + 2a_{i,2}Y_{c,eq} - 2Y_{c,eq}Y_{i,n-1,eq} + a_{i,2}^2 \\
&\quad - 2a_{i,2}Y_{i,n-1,eq} + Y_{i,n-1,eq}^2 + a_{i,3}^2 - 2a_{i,3}Z_{i,n-1,eq} + Z_{i,n-1,eq}^2 \\
H_{i,n} &= A_{i,n}X_{c,new} + B_{i,n}X_{c,new} + C_{i,n}Y_{c,new} + D_{i,n}\psi + E_{i,n}\theta + F_{i,n}\phi + R_{i,n}X_{i,n-1,new} \\
&\quad + S_{i,n}Y_{i,n-1,new} + T_{i,n}Z_{i,n-1,new} \\
A_{i,n} &= 2(a_{i,1} - X_{i,n-1,eq}) \\
B_{i,n} &= 2(Y_{c,eq} + a_{i,2} - Y_{i,n-1,eq}) \\
C_{i,n} &= 2(a_{i,3} - Z_{i,n-1,eq}) \\
D_{i,n} &= 2(a_{i,2}X_{i,n-1,eq} + a_{i,1}Y_{c,eq} - a_{i,1}Y_{i,n-1,eq}) \\
E_{i,n} &= 2(-a_{i,3}X_{i,n-1,eq} + a_{i,1}Z_{i,n-1,eq}) \\
F_{i,n} &= 2(-a_{i,3}Y_{c,eq} + a_{i,3}Y_{i,n-1,eq} - a_{i,2}Z_{i,n-1,eq}) \\
R_{i,n} &= -A_{i,n} \\
S_{i,n} &= -B_{i,n} \\
T_{i,n} &= -C_{i,n}
\end{aligned} \tag{4.109}$$

4.9 STANDARD CASE

The previously stated linearized equations of motion can now be written in matrix form as an eigenvalue problem from which the vibration frequencies, mode shapes, and small motions of the system about its equilibrium state can be determined. However, given the size of each equation and the number of variables (6 for the cylinder and 3 per mass per mooring line), the procedure will be performed similarly to the one used in Chapter 3 where three separate cases were considered. These include: Case A, where the lines are modeled as massless springs; Case B, where the mass of each mooring line is lumped into one mass; and Case C, where the mass of each mooring line is lumped into some chosen finite number of equal masses. As detailed in Chapter 3, the structure is configured in such a way that only two spring stiffnesses will be considered. Hence, each line will contain a series of springs of a common and known stiffness. K_A will refer to the stiffness of each spring making up lines 1 and 4 (previously tagged i) and K_B will refer to those making up lines 2, 3, 5, and 6 as shown in Figure 4.5. In addition, the points where the mooring lines connect to the cylinder are known to have one value of

each coordinate equal to zero, which will help simplify the EOM's. These are $a_{1,3}$, $a_{2,2}$, $a_{3,2}$, $a_{4,3}$, $a_{5,2}$, and $a_{6,2}$.

4.10 CASE A (MASSLESS LINES)

Case A, the most simple case to be considered, should still show much about the small motion of the cylinder. The system of linearized equations can now be written in matrix form as

$$[m]\{\ddot{q}\} + [s]\{q\} = 0 \quad (4.110)$$

where q represents a general vector of variables and $[m]$ and $[s]$ are the inertia and stiffness matrices, respectively.

First, the vector $\{q\}^T$ is defined as

$$\{q\}^T = \{X_{c,new} \quad Y_{c,new} \quad Z_{c,new} \quad \psi \quad \theta \quad \phi\} \quad (4.111)$$

Here, only six EOM's will be involved, making the eigenvalue problem associated with this condition quite attractive. The inertia matrix $[m]$ is easy to develop from the EOMs (4.102)-(4.107) with $n=1$ and $X_{i,0,new} = Y_{i,0,new} = Z_{i,0,new} = 0$ as

$$[m] = \begin{bmatrix} 1 & 0 & 0 & 0 & 0 & 0 \\ 0 & 1 & 0 & 0 & 0 & 0 \\ 0 & 0 & 1 & 0 & 0 & 0 \\ 0 & 0 & 0 & I_{zz} & 0 & 0 \\ 0 & 0 & 0 & 0 & I_{yy} & 0 \\ 0 & 0 & 0 & 0 & 0 & I_{xx} \end{bmatrix} \quad (4.112)$$

The stiffness matrix $[s]$ can be easily obtained as well, but due to the complexity shown in equations (4.102) – (4.107) for one mooring line, a listing for six mooring lines becomes too exhaustive and only the numerical results will be provided.

The non-dimensional eigenvalues obtained by solving the eigenvalue problem for the standard case ($L=30$ ft, $R=5$ ft, $a_T=10$ ft, $b_T=15$ ft, $K_A=197,970$ plf, and $K_B=131,980$ plf) are found in matrix form to be

$$[\omega^2] = [46.2 \quad 205.3 \quad 675.7 \quad 802.4 \quad 808.5 \quad 1,188.2]^T \quad (4.113)$$

which can be written as dimensional frequencies (rad/s) as

$$[\omega] = [17.3 \quad 36.4 \quad 66.0 \quad 71.9 \quad 72.2 \quad 87.5]^T \quad (4.114)$$

with the following normalized eigenvectors:

$$[u] = \begin{bmatrix} 0 & 0.99 & 0 & 0 & 0 & -0.52 \\ 0 & 0 & 1 & 0 & 0 & 0 \\ 0.74 & 0 & 0 & 0.65 & 0 & 0 \\ 0 & 0.14 & 0 & 0 & 0 & 0.86 \\ 0 & 0 & 0 & 0 & 1 & 0 \\ -0.68 & 0 & 0 & 0.76 & 0 & 0 \end{bmatrix} \quad (4.115)$$

where each column represents the eigenvector corresponding to the matching natural frequency. The sum of the squares of the elements of each eigenvector is unity. It is easy to see that each natural frequency causes the structure to vibrate in a unique, but fairly simple, fashion. The third eigenvalue results in a motion of the cylinder's center of mass only in the Y (heave) direction, whereas the fifth eigenvector describes a rotation only in the θ (pitch) direction. Since these motions are intuitive with reference to Figure 4.1, figures will not be shown here. The coupled motions occur in the first, second, fourth, and sixth eigenvectors, which are shown as Figures 4.6, 4.7, 4.8 and 4.9, respectively. Eigenvectors one and four involve sway and roll, whereas two and six involve surge and pitch. The solid lines represent the equilibrium configuration. Figures 4.6 and 4.8 show end views, while Figures 4.7 and 4.9 show side views.

Non-dimensionalizing the EOM's has allowed for solutions for various cases of L/R in addition to the standard case. As shown graphically in Figure 4.10, the fourth, fifth, and sixth natural frequencies (nondimensional) tend to decrease nonlinearly with respect to increasing L/R . The second and third natural frequencies increase nonlinearly for very low L/R . However, they reach a maximum for L/R less than that of the standard case ($L/R = 6$) and then decrease. The first natural frequency is hardly affected by L/R . For very low L/R values a slight increase can be seen. However, for the most part, it is constant after that. It should be noted that a change in L/R affects the entire inertia matrix. This is probably the reason for such sharp and contrasting curves. A plot of ω vs. $K/(\rho_c g R^2)$ is also shown as Figure 4.11. Here, all six natural frequencies increase nonlinearly with respect to increasing $K/(\rho_c g R^2)$.

4.11 CASE B (ONE MASS PER LINE)

For case B, each mooring line will be modeled as two springs with a central mass representing the weight of the entire line. Each mass contributes three new unknowns to the system, which results in a 24x24 eigenvalue problem. For convenience, only the non-zero elements of the mass matrix will be identified here. Here, the vector $\{q\}^T$ is defined as

$$\{q\}^T = \{ X_{c,new} \quad Y_{c,new} \quad Z_{c,new} \quad \psi \quad \theta \quad \phi \quad X_{1,1,new} \quad Y_{1,1,new} \\ Z_{1,1,new} \quad X_{2,1,new} \quad Y_{2,1,new} \quad Z_{2,1,new} \quad X_{3,1,new} \quad Y_{3,1,new} \quad Z_{3,1,new} \quad X_{4,1,new} \\ Y_{4,1,new} \quad Z_{4,1,new} \quad X_{5,1,new} \quad Y_{5,1,new} \quad Z_{5,1,new} \quad X_{6,1,new} \quad Y_{6,1,new} \quad Z_{6,1,new} \} \quad (4.116)$$

Using (4.99) through (4.107), the inertia matrix in (4.110) contains the elements

$$\begin{aligned} m_{1,1} &= m_c & m_{2,2} &= m_c & m_{3,3} &= m_c & m_{4,4} &= I_{ZZ} & m_{5,5} &= I_{YY} \\ m_{6,6} &= I_{XX} & m_{7,7} &= m_{1,1} & m_{8,8} &= m_{1,1} & m_{9,9} &= m_{1,1} & m_{10,10} &= m_{2,1} \\ m_{11,11} &= m_{2,1} & m_{12,12} &= m_{2,1} & m_{13,13} &= m_{3,1} & m_{14,14} &= m_{3,1} & m_{15,15} &= m_{3,1} \\ m_{16,1} &= m_{4,1} & m_{17,17} &= m_{4,1} & m_{18,18} &= m_{4,1} & m_{19,19} &= m_{5,1} & m_{20,20} &= m_{5,1} \\ m_{21,21} &= m_{5,1} & m_{22,22} &= m_{6,1} & m_{23,23} &= m_{6,1} & m_{24,24} &= m_{6,1} \end{aligned} \quad (4.117)$$

The values of K_A and K_B are twice as high as the corresponding values in Case A, since the springs are half as long. Solving this eigenvalue problem results in the following natural frequencies in rad/s:

$$\begin{aligned} \omega_1 &= 17.21 & \omega_2 &= 36.32 & \omega_3 &= 65.89 & \omega_4 &= 71.83 & \omega_5 &= 71.98 \\ \omega_6 &= 87.28 & \omega_7 &= 191.22 & \omega_8 &= 191.22 & \omega_9 &= 191.22 & \omega_{10} &= 191.29 \\ \omega_{11} &= 191.36 & \omega_{12} &= 191.36 & \omega_{13} &= 191.39 & \omega_{14} &= 191.41 & \omega_{15} &= 286.54 \\ \omega_{16} &= 286.69 & \omega_{17} &= 286.70 & \omega_{18} &= 286.71 & \omega_{19} &= 1180.4 & \omega_{20} &= 1181.0 \\ \omega_{21} &= 1181.0 & \omega_{22} &= 1,881.1 & \omega_{23} &= 2,302.6 & \omega_{24} &= 2,302.9 \end{aligned} \quad (4.118)$$

The non-zero mode shape terms for the first six natural frequencies are as follows:

$$\begin{aligned} u_{3,1} &= 0.42 & u_{6,1} &= -0.39 & u_{9,1} &= 0.041 & u_{11,1} &= -0.20 & u_{12,1} &= 0.21 \\ u_{14,1} &= 0.20 & u_{15,1} &= 0.21 & u_{18,1} &= 0.041 & u_{20,1} &= -0.20 & u_{21,1} &= 0.21 \\ u_{23,1} &= 0.20 & u_{24,1} &= 0.21 & & & & & & \\ u_{1,2} &= 0.57 & u_{4,2} &= 0.08 & u_{7,2} &= 0.33 & u_{8,2} &= -0.12 & u_{10,2} &= 0.30 \\ u_{11,2} &= -0.12 & u_{13,2} &= 0.3 & u_{14,2} &= -0.12 & u_{16,2} &= 0.33 & u_{17,2} &= 0.12 \\ u_{19,2} &= 0.29 & u_{20,2} &= 0.12 & u_{22,2} &= 0.29 & u_{23,2} &= 0.12 & & \end{aligned}$$

$$\begin{array}{ccccc}
u_{2,3}=0.62 & u_{8,3}=0.31 & u_{11,3}=0.32 & u_{14,3}=0.32 & u_{17,3}=0.31 \\
u_{20,3}=0.32 & u_{23,3}=0.32 & & & \\
u_{3,4}=0.45 & u_{6,4}=0.54 & u_{9,4}=-0.04 & u_{11,4}=0.27 & u_{6,4}=0.23 \\
u_{14,4}=-0.27 & u_{15,4}=0.23 & u_{18,4}=-0.04 & u_{20,4}=0.27 & u_{21,4}=0.23 \\
u_{23,4}=-0.27 & u_{24,4}=0.23 & & & \\
u_{5,5}=-0.23 & u_{9,5}=-0.38 & u_{10,5}=0.14 & u_{12,5}=-0.38 & u_{13,5}=-0.14 \\
u_{15,5}=-0.38 & u_{18,5}=0.38 & u_{19,5}=0.14 & u_{21,5}=0.38 & u_{22,5}=-0.14 \\
u_{24,5}=0.38 & & & & \\
u_{1,6}=-0.14 & u_{4,6}=0.23 & u_{7,6}=0.06 & u_{8,6}=-0.37 & u_{10,6}=-0.09 \\
u_{11,6}=-0.39 & u_{13,6}=-0.09 & u_{14,6}=-0.39 & u_{16,6}=0.06 & u_{17,6}=0.37 \\
u_{19,6}=-0.09 & u_{20,6}=0.39 & u_{22,6}=-0.09 & u_{23,6}=0.39 &
\end{array}$$

(4.119)

where for $u_{i,j}$, i and j represent an independent variable and corresponding natural frequency, respectively. Here, given that the relatively high seventh natural frequency and above are of less interest, the mode shapes corresponding to these frequencies are not listed. On the other hand, it should be noted that the first six natural frequencies have decreased slightly as a result of the added masses and splitting a single spring into two springs with half the length and twice the stiffness (so that the total stiffness of the line doesn't change). Excluding the third mode shape where the cylinder and mass vibrate only in the Y direction, plots of the first six mode shapes are shown as Figures 4.12 through 4.16. Again, the solid lines represent the equilibrium configuration of the system. Figures 4.12 and 4.14 show end views, Figures 4.13 and 4.16 show side views, and Figure 4.15 is a top view of the breakwater. The small circles shown in all the figures are the lumped masses that are located at the center of each mooring line. It is helpful to visualize the mooring lines extending from the cylinder's ends through the masses, and to the ocean floor. In all the figures, the masses tend to "go with" the motion of the breakwater as expected.

4.12 CASE C (TWO MASSES PER LINE)

For case C, each mooring line will be modeled as three springs with two equal masses whose weights sum to equal the weight of the entire line. Each mass contributes

three new unknowns to the system, which now yields a 42x42 eigenvalue problem.

Following the same procedure discussed in Sections 4.10 and 4.11, the first six natural frequencies are found in rad/s to be

$$\begin{aligned} \omega_1=17.23 \quad \omega_2=36.34 \quad \omega_3=65.92 \quad \omega_4=71.84 \quad \omega_5=72.01 \\ \omega_6=87.33 \end{aligned} \tag{4.120}$$

which are practically the same as previously obtained in Case B. Due to the fact that the mode shapes for these frequencies correspond to motions of the cylinder and mooring lines that are essentially the same as for Case B, they will not be shown here.

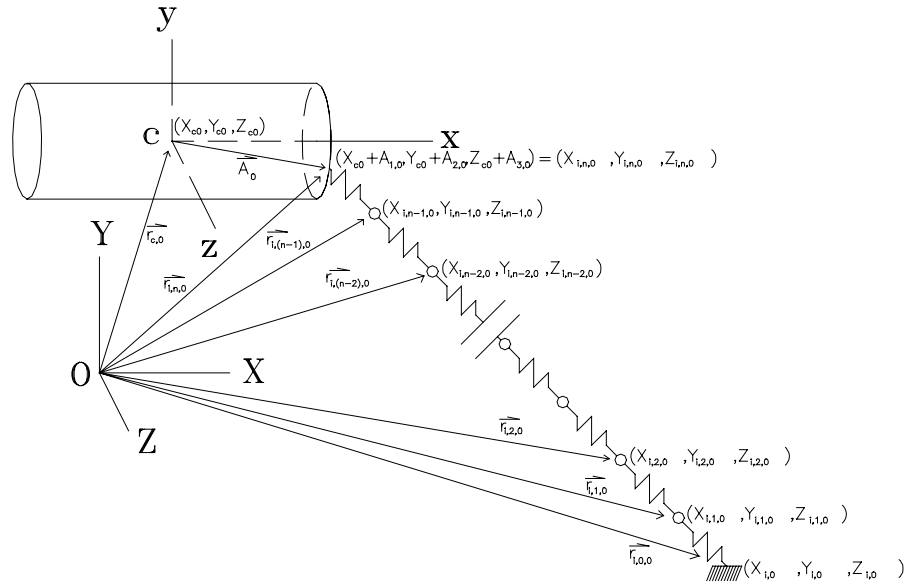


Figure 4.1 – “Unstretched Springs” Configuration – General System

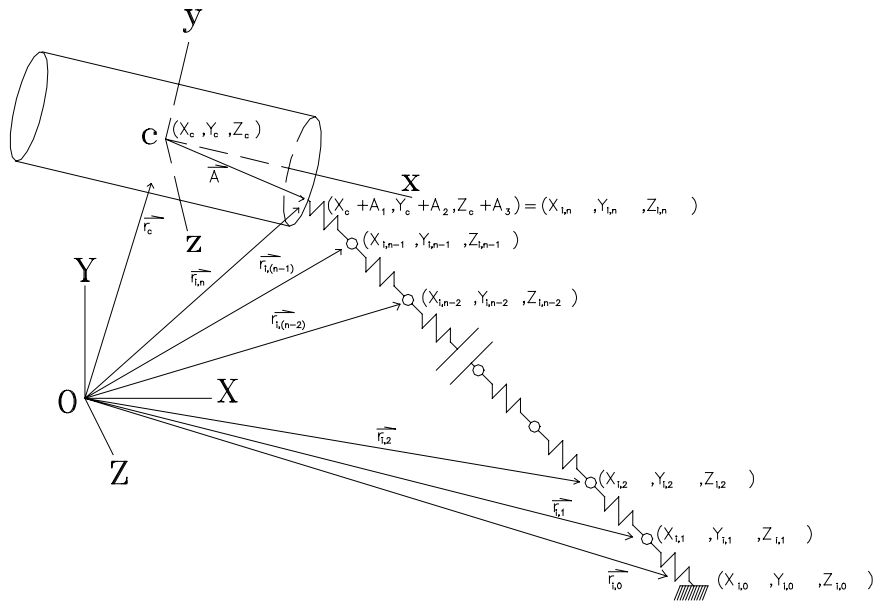


Figure 4.2 – General Configuration During Motion

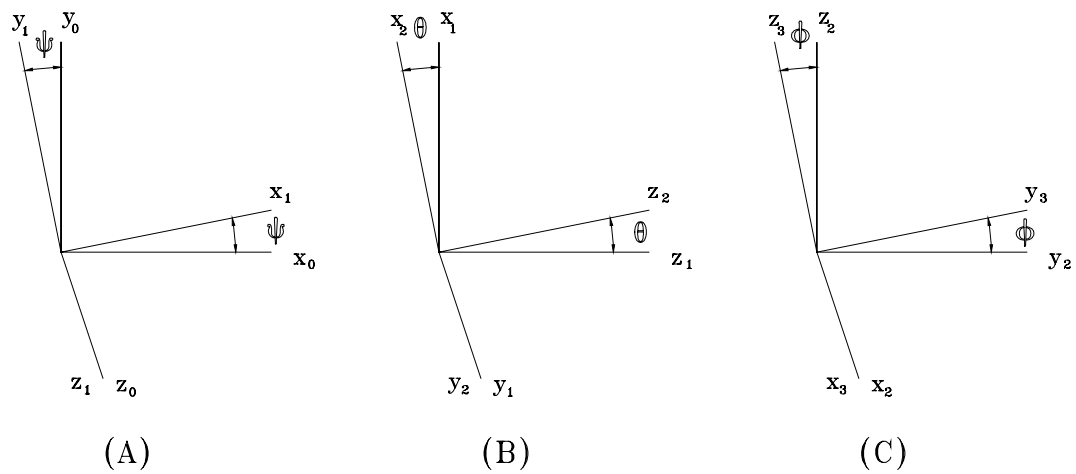


Figure 4.3 – Euler Angles

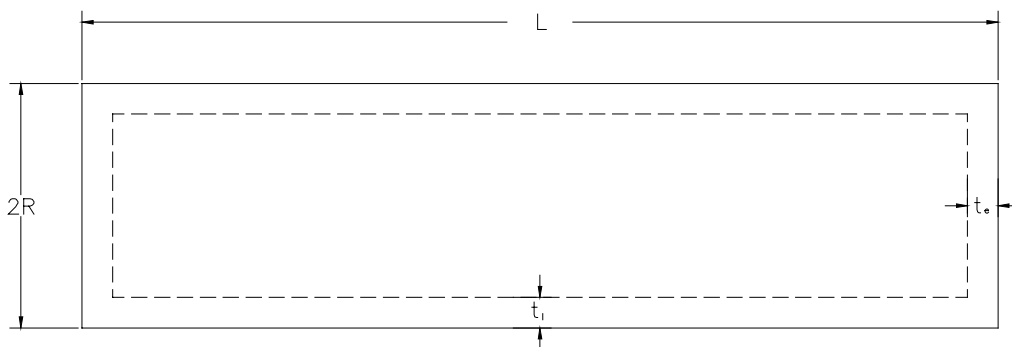


Figure 4.4 – Cylinder Dimensions

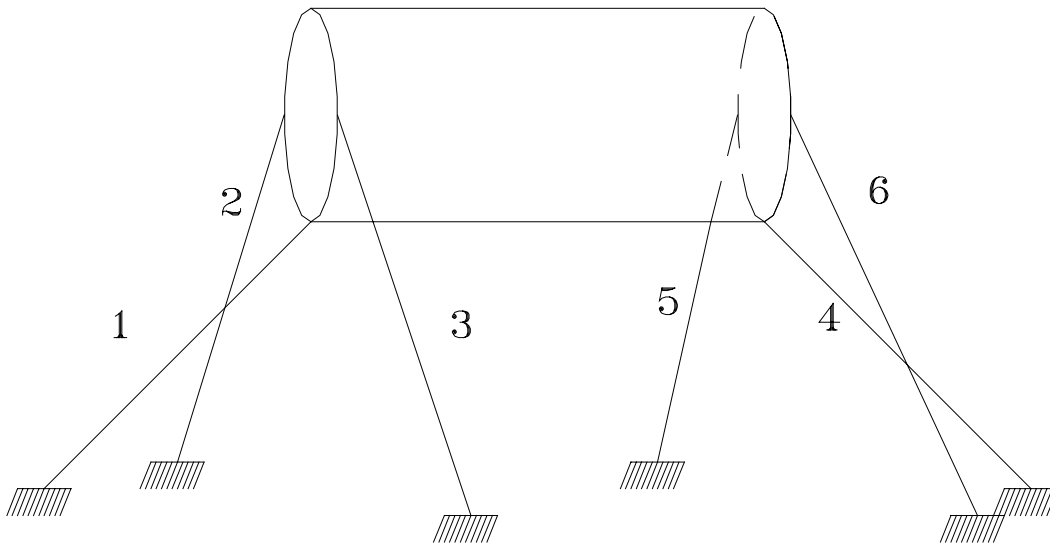


Figure 4.5 – Mooring Line Identification

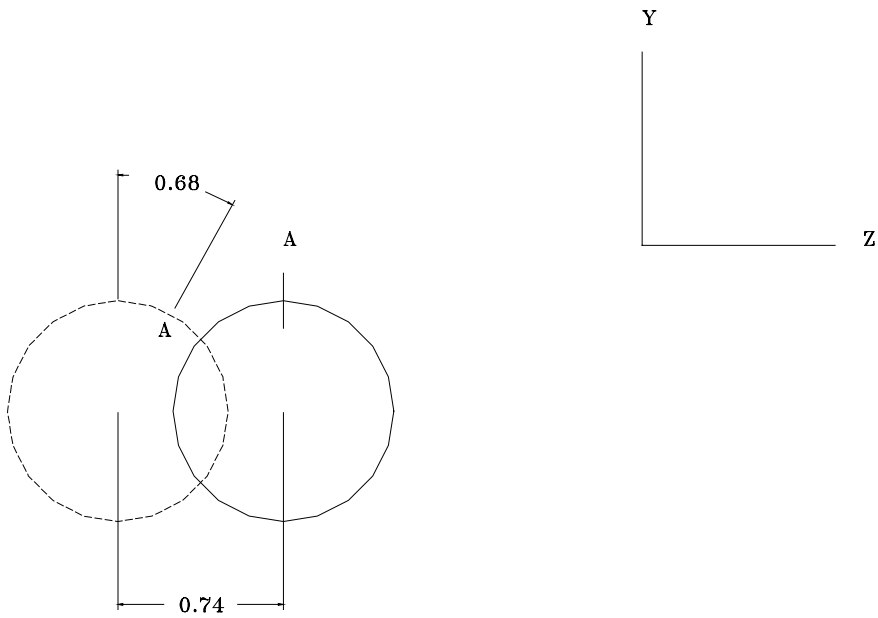


Figure 4.6 – Mode Shape (First Eigenvector – Case A)

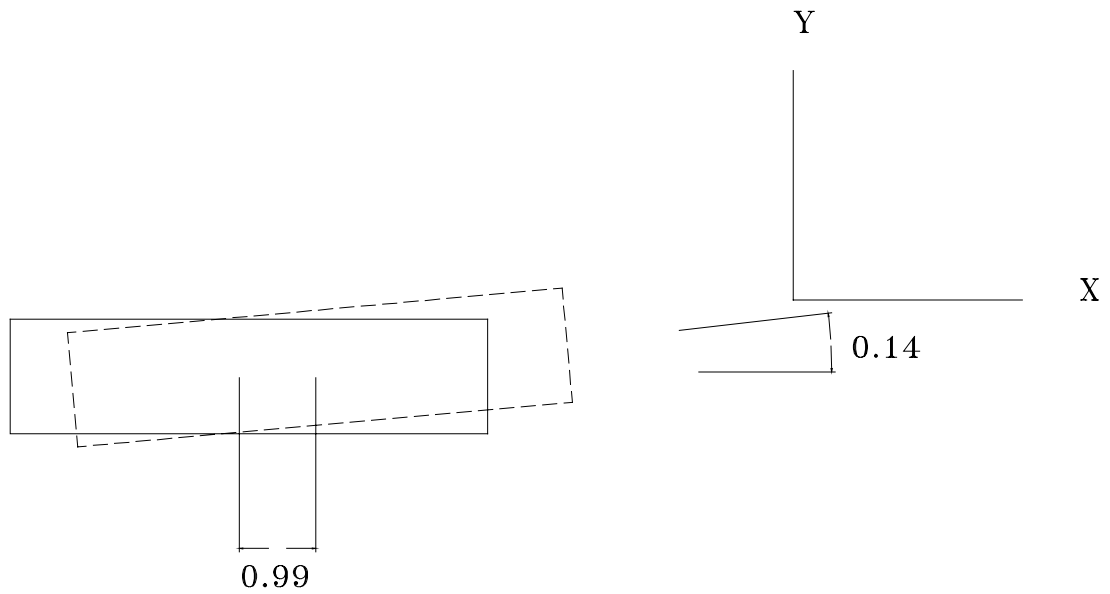


Figure 4.7 – Mode Shape (Second Eigenvector – Case A)

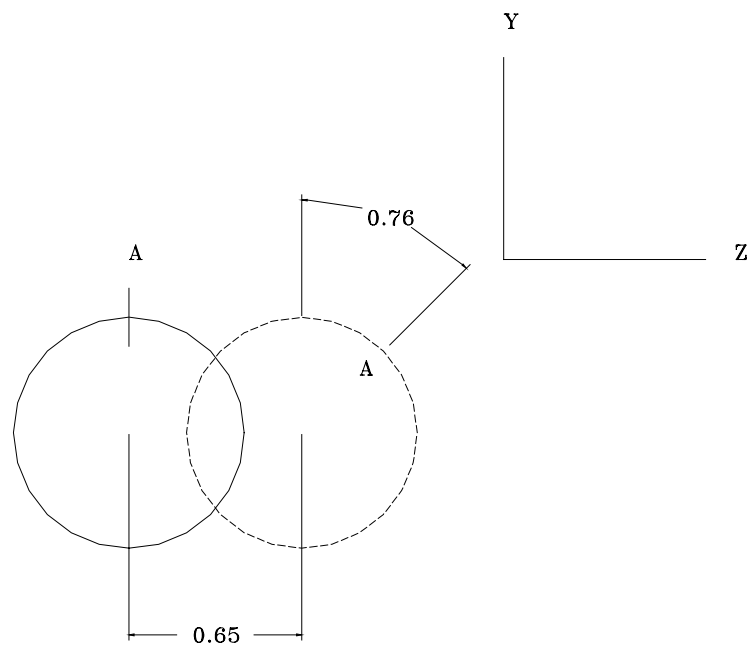


Figure 4.8 – Mode Shape (Fourth Eigenvector – Case A)

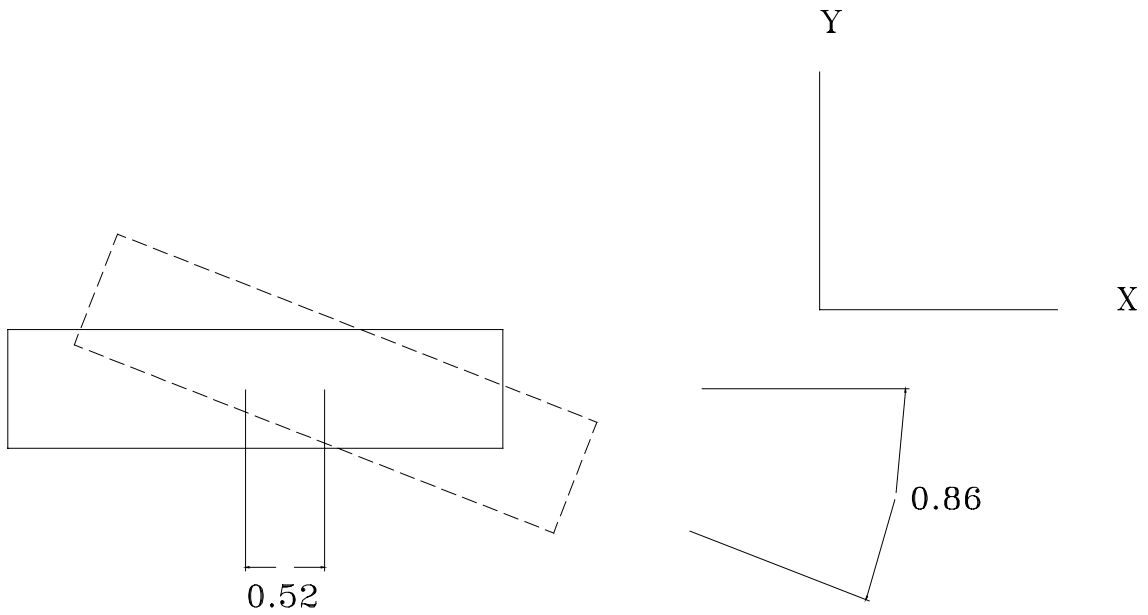


Figure 4.9 – Mode Shape (Sixth Eigenvector – Case A)

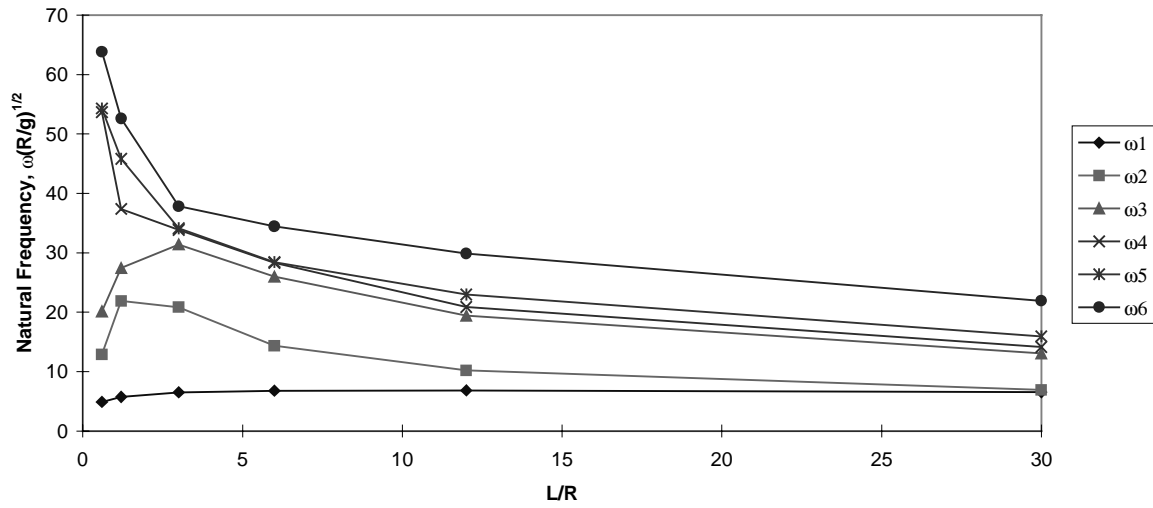


Figure 4.10 – Natural Frequency (Nondimensional) vs. L/R – Case A

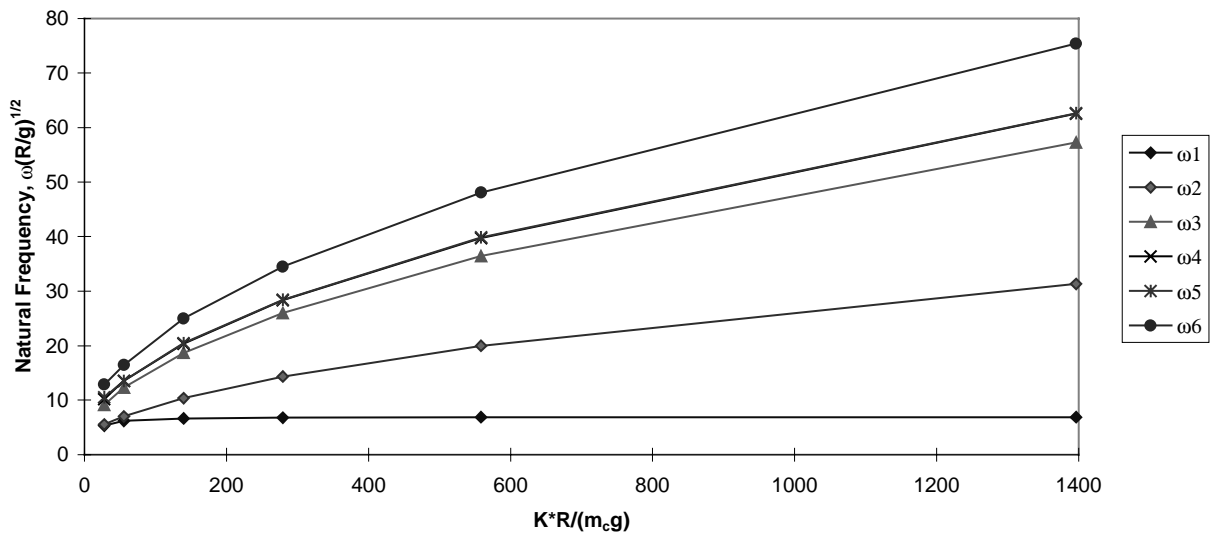


Figure 4.11 – Natural Frequency (Nondimensional) vs. K (Nondimensional)
Case A

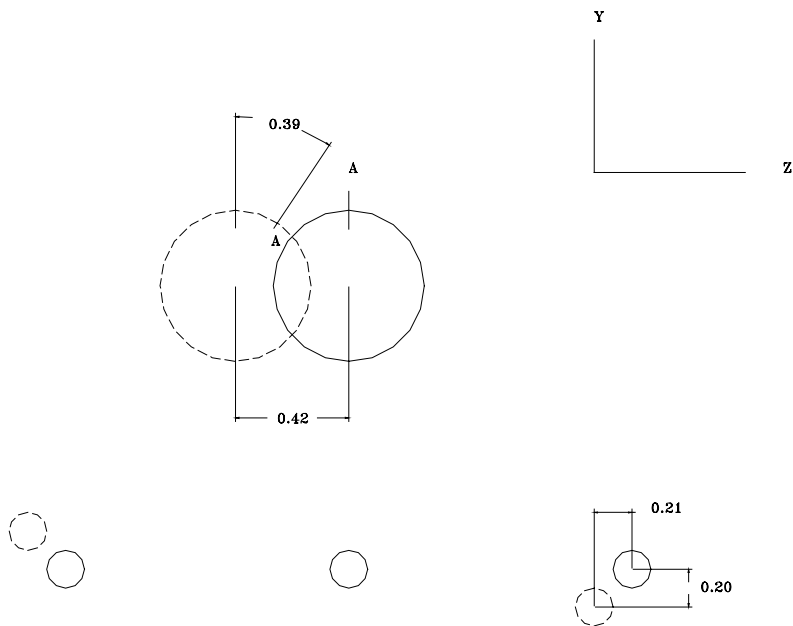


Figure 4.12 – Mode Shape (First Eigenvector – Case B)

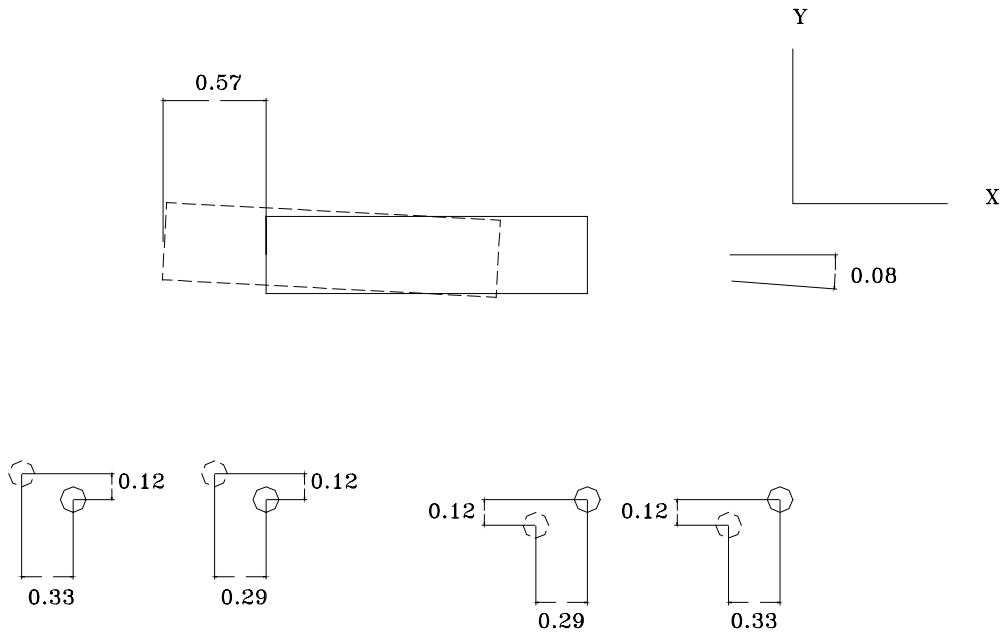


Figure 4.13 – Mode Shape (Second Eigenvector – Case B)

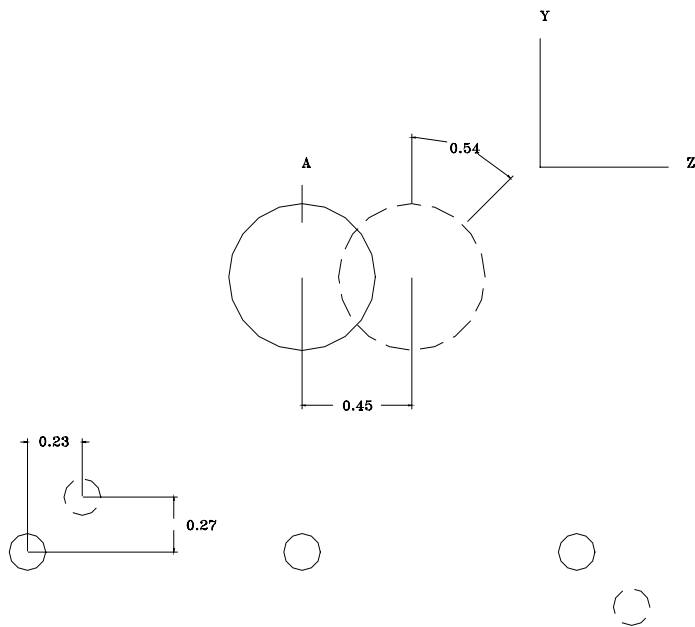


Figure 4.14 – Mode Shape (Fourth Eigenvector – Case B)

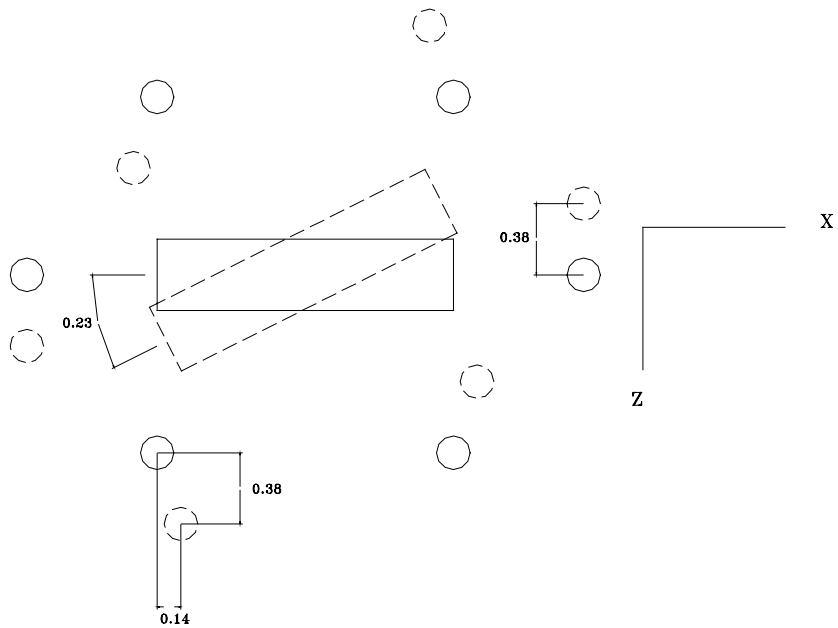


Figure 4.15 – Mode Shape (Fifth Eigenvector – Case B)

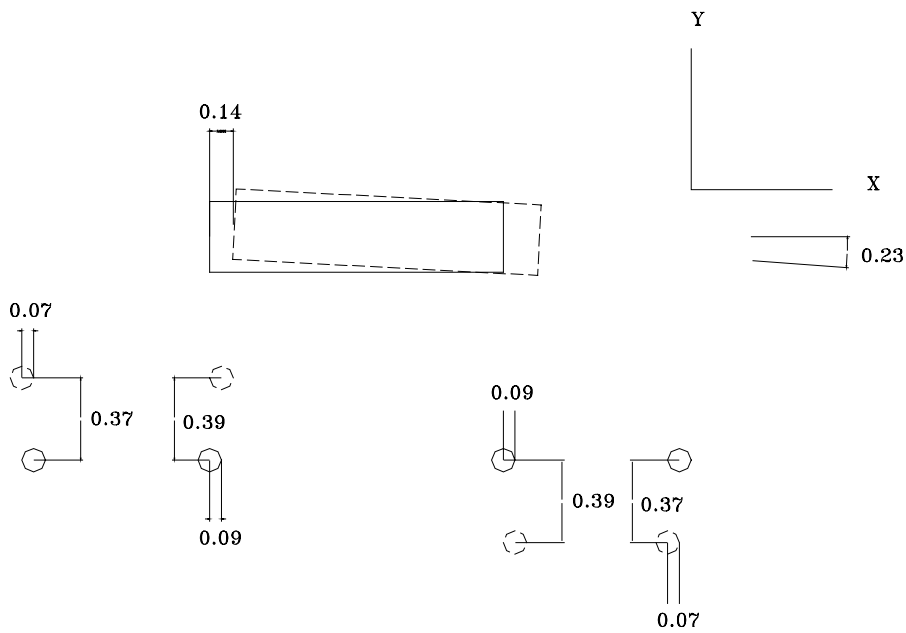


Figure 4.16 – Mode Shape (Sixth Eigenvector – Case B)

wave forces as well as the body motions are proportional to the wave amplitude. In this study, a unit amplitude wave is used for all conditions. Although several important and rare topics such as three-dimensional analysis, oblique waves, and end effects are included in this thesis, there are limitations to its applicability. The primary assumption is that linear theory (small motion) prevails, as evident in the form of (5.1), and that linear wave theory is adequate. However, for regular waves and small motions of the structure, this assumption is very adequate. There is a general exception for moored structures. At very low frequencies, the mooring lines will act much more like catenaries, and the provided stiffness is highly nonlinear (Tsinker 1995). On the other hand, the breakwater of this thesis is an air-filled structure with a very large net buoyant force acting on it and Chapter 3 ensures the mooring lines are taut which causes the lines to respond linearly even at low frequencies.

5.2 LINEAR WAVE THEORY AND FLUID BEHAVIOR

Before proceeding to the question of how to solve for the new elements of (5.1) (M and K are the same as in Chapter 3), the assumptions and wave theory should be considered. It is assumed that the fluid is inviscid and incompressible. It is also assumed that the fluid particle motion is irrotational (i.e., the curl of the velocity vector is zero). Therefore, the velocity field can be written as the gradient of the velocity potential Φ .

For the examination of the moored cylinder as a breakwater, a new coordinate system will be chosen which is in accord with those more common to ocean engineering systems. The global XYZ system is fixed to the ocean floor directly below the center of gravity of the cylinder in its equilibrium configuration. The Z axis is defined as positive upwards, the Y axis is parallel to the cylinder's axis, and the X axis is positive in the direction of wave propagation for $\beta=0$. This new coordinate system is shown in Figure 5.1 with the incidence angle β . In addition to coordinate changes, nondimensional quantities will be dimensionalized and metric units will be used for all figures.

In response to the sinusoidal waves of unit amplitude and frequency ω (rad/s) passing over the structure, the cylinder will be assumed to undergo small steady-state vibrations about its equilibrium position at the driving frequency ω of the waves. The displacement of the structure will involve rigid body motions in each of the six previously established degrees of freedom and defined by

$$\xi_j(t) = \hat{\xi}_j e^{-i\omega t} \quad (5.2)$$

where $j = 1$ to 6 for each of the six degrees of freedom, surge, heave, sway, pitch, yaw, and roll, respectively, and the hat indicates a complex amplitude. Following Newman (1994) and Dewi (1997), the velocity potential can be written in the form

$$\Phi(x, y, z, t) = \text{Re} \left[\left(\phi_I + \phi_D + \sum_{j=1}^6 \phi_j(x, y, z) \hat{\xi}_j \right) e^{-i\omega t} \right] \quad (5.3)$$

where

$\phi_D e^{-i\omega t}$ is the potential of the diffracted waves,

$\phi_j e^{-i\omega t}$ is the radiation potential for mode (degree of freedom) j , and

$\phi_I e^{-i\omega t}$ is the incident wave potential.

The incident wave potential at some position z above the ocean floor is defined by Newman (1994) as

$$\phi_I = \frac{igA_I \cosh(kz)}{\omega \cosh(kd)} e^{ik(x \cos \beta + y \sin \beta)} \quad (5.4)$$

where

A_I is the incident wave amplitude,

d is the water depth,

β is the incidence angle, and

k is the wave number. The wave number can be found from the following dispersion relation (Dean and Dalrymple 1991):

$$\omega^2 = kg \tanh(kd) \quad (5.5)$$

where g is the acceleration of gravity.

5.3 EXTERNAL FLUID CHARACTERISTICS

The motion of the fluid surrounding the air-filled breakwater is defined such that each of the ϕ_j potentials must satisfy Laplace's equation, $\nabla^2 \phi_j = 0$ (Dean and Dalrymple 1991). The following boundary conditions must also be satisfied:

For the free surface:

$$\frac{\partial \phi_j}{\partial z} - \frac{\omega^2}{g} \phi_j = 0 \quad (5.6)$$

For the ocean floor:

$$\begin{aligned}\frac{\partial\phi_D}{\partial z} &= 0 \\ \frac{\partial\phi_j}{\partial z} &= 0\end{aligned}\tag{5.7}$$

For the wet body surface, S_b :

$$\begin{aligned}\frac{\partial\phi_D}{\partial n} &= -\frac{\partial\phi_I}{\partial n} \\ \frac{\partial\phi_j}{\partial n} &= -i\omega n_j\end{aligned}\tag{5.8}$$

where

$$n_j = \bar{s}_j \cdot \bar{n} = u_j n_x + v_j n_y + w_j n_z\tag{5.9}$$

where \mathbf{s}_j denotes the displacement of panel j in the X , Y , and Z directions, respectively, and \mathbf{n} points from the body surface to the external fluid and is normal to the breakwater surface.

A boundary integral method is used to analyze the fluid flow around the structure. Wehausen and Laitone (1960) provide the necessary Green's function for this method, namely

$$\begin{aligned}G(P, Q) &= \frac{1}{\sqrt{R^2 + (z - \zeta)^2}} + \frac{1}{\sqrt{R^2 + (2d + z + \zeta)^2}} \\ &+ 2 \int_0^\infty \frac{\left(k + \frac{\omega^2}{g}\right) \cosh[k(z + d)] \cosh[k(\zeta + d)]}{k \sinh(kd) - \frac{\omega^2}{g} \cosh(kd)} e^{-kd} J_0(kR) dk\end{aligned}\tag{5.10}$$

where

$P=(x,y,z)$ is the coordinate of the field point,

$Q=(\xi,\eta,\zeta)$ is the coordinate of the source point, and

$$R = \sqrt{(x - \xi)^2 + (y - \eta)^2}$$

The application of Green's second identity gives a Fredholm equation of the second kind, which in turn results in values of the potential on the wet body surface. The Fredholm equation can be written as

$$-2\pi\phi_j(P) + \iint_{S_b} \phi_j(Q) \frac{\partial G(P,Q)}{\partial n_Q} dS_Q = \iint_{S_b} \frac{\partial \phi_j}{\partial n_Q}(Q) G(P,Q) dS_Q \quad (5.11)$$

The above integral is solved by approximating the cylindrical breakwater surface by a set of flat, quadrilateral panels with a known centroid for every panel. It is assumed that the potential across a given panel is constant and the value is assigned to the centroid. In order to evaluate Green's function (5.10), the FORTRAN subroutine FINGREEN developed by Newman (1985) is used.

5.4 DETERMINATION OF FORCE, ADDED MASS, AND DAMPING ELEMENTS

Recalling (5.1), $[M_A]$, $[C]$, and $\{F\}$ must be determined for each of the six degrees of freedom the structure undergoes. Following Newman (1994), the added mass terms are found in matrix form from

$$[M_A]_{ij} = \frac{1}{\omega^2} \operatorname{Re} \left(-i\omega\rho_w \iint_{S_b} \phi_j n_i dS \right) \quad (5.12)$$

where $[]_{ij}$ denotes a given matrix element of the square $[6 \times 6]$ matrix. Also, ρ_w is the density of salt (ocean) water. Likewise, the damping matrix $[C]$ is found by

$$[C]_{ij} = \frac{1}{\omega} \operatorname{Im} \left(-i\omega\rho_w \iint_{S_b} \phi_j n_i dS \right) \quad (5.13)$$

and the total hydrodynamic force, which is composed of the incident wave force and the diffracted wave force, is found by

$$F_j^I + F_j^D = -i\omega\rho_w \iint_{S_b} (\phi_I + \phi_D) n_j dS \quad (5.14)$$

for each of the $j=1$ to 6 degrees of freedom. With the previously mentioned assumption dealing with a constant potential across each panel, and verifying convergence and the required number of panels to insure validity of results, each of the integrals above is given by a summation over the surface of the breakwater.

5.5 SOLVING FOR RESPONSE AMPLITUDES OF THE BREAKWATER IN WATER

Now (5.1) can now be solved in the frequency domain by inserting the adequate added mass, damping, and forcing terms for a given wave frequency. The response

amplitudes $\hat{\xi}_j$ as defined earlier can be found by solving six simultaneous equations. The velocity potentials on the free surface are obtained from Green's Theorem (Dewi, 1997) as

$$\phi_j(P) = \frac{1}{4\pi} \iint_{S_b} (\phi_j(Q) \frac{\partial G(P, Q)}{\partial n_Q} - G(P, Q) \frac{\partial \phi_j(Q)}{\partial n_Q}) dS_Q \quad (5.15)$$

and are part of the total velocity potential Φ summation of (5.3).

Finally, it is of prime importance to find the free surface elevation ζ in the proximity of (and especially behind) the breakwater. It can be found from

$$\zeta = -\frac{1}{g} \frac{\partial \Phi}{\partial t} = \frac{i\omega \Phi}{g} \quad (5.16)$$

5.6 PROCEDURE VALIDATION

The FORTRAN program used to solve for the added mass, damping, hydrodynamic forces, and velocity potentials for this breakwater was developed by Dewi (1997). As a result, the program has been previously verified with existing results in the literature for two-dimensional and three-dimensional arches, a rigid hemicylinder attached to the ocean floor, a vertical cylindrical column, and circular plates in contact with fluid. However, given the particular structure of this thesis, a moored, horizontal, rigid, cylindrical breakwater, the FORTRAN program should still be validated. As discussed in detail in Chapter 2, Evans et al. (1979) analyzed a long cylinder in waves using two-dimensional analysis and found that at the "tuning frequency" the transmission coefficient is zero. Creating a 304.8 m (1000 ft) long cylinder, these results have been verified. Although a three-dimensional analysis is used, the structure moves only in sway and heave for normal waves. Since end effects are negligible, the structure's motion can be described accurately in two dimensions. Figure 5.2 shows the magnitude of the waves over the proximity of the structure. The structure is located at X equal to 0 and extends from -152 m to 152 m in the Y direction. The waves advance from -X to +X. Figure 5.2 shows clearly that for a long structure, the magnitude of the waves after the structure is approximately zero. The plot is for a wave frequency ω of 1.25 rad/s which is the wet natural frequency ω_n of the cylinder. Here the term wet natural frequency is analogous to "tuning frequency" and represents the first natural frequency of the structure in water.

Figures 5.3 (a)-(f) show the free surface elevation near the breakwater at fractions of the wave period. The figures are not to scale and the structure appears much larger than it actually is. This is done in order to more specifically show the wave elevations near the structure. The location of the horizontal plane below the structure is not defined by $Z=0$ (ocean floor), but is approximately $Z=3.0$ m (the bottom of the structure). Figure 5.3 (e) seems strange, for the upstream waves are apparently reduced by the breakwater. This is not really the case. It should be recalled that the upstream waves represent the superposition of incident and deflected waves. At this time, the two waves are "out of phase" and somewhat cancel each other out. On closer inspection, it is clear that at some time t , the upstream waves are larger than at other times. Hence, depending on the phase of the incident and deflected waves, amplification or cancellation can take place. Figure 5.3 portrays the structure's effectiveness. Nevertheless, as will be shown in Chapter 6, for a more reasonable "short" breakwater under normal waves, end effects are considerable and the structure is not as effective. In addition, for oblique waves, the structural response is not two-dimensional and its effectiveness varies.

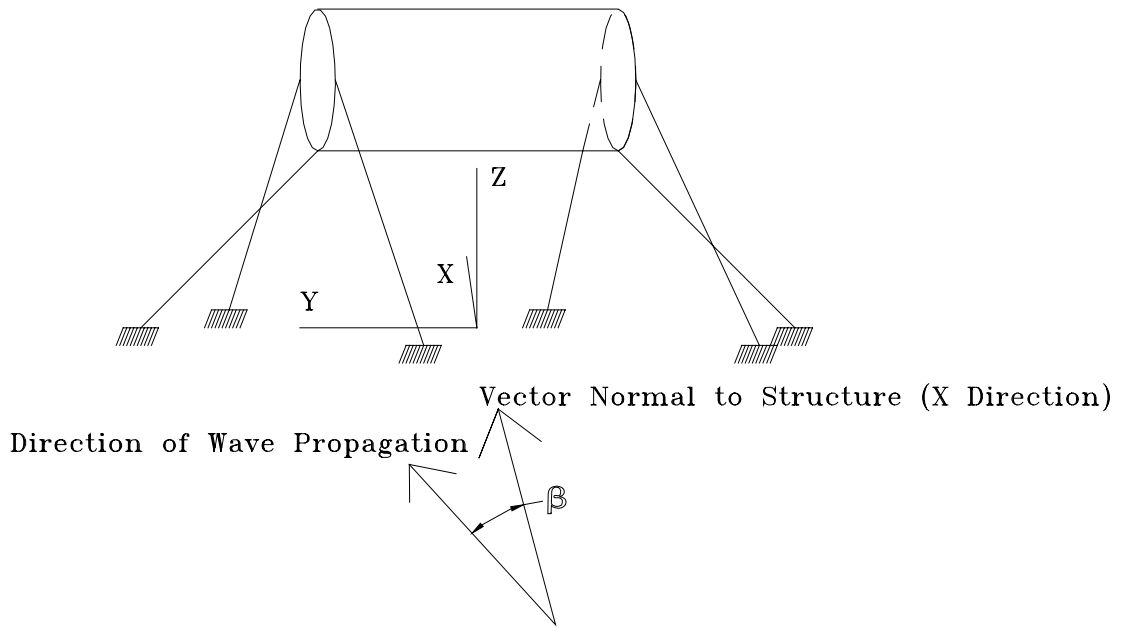


Figure 5.1 – New Coordinate System for Breakwater Showing Incident
Wave Direction β

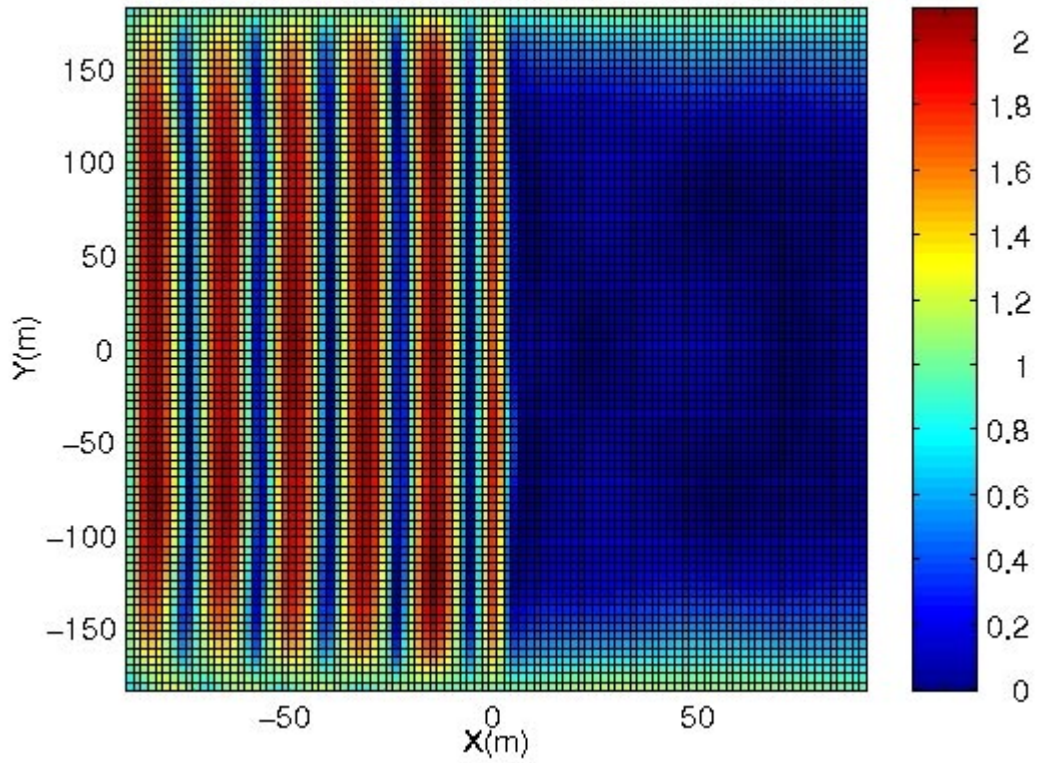


Figure 5.2 – Amplitude of Free Surface Elevation for $\omega=\omega_n=1.25$ rad/s
(304.8 m Breakwater, $\beta=0^\circ$)

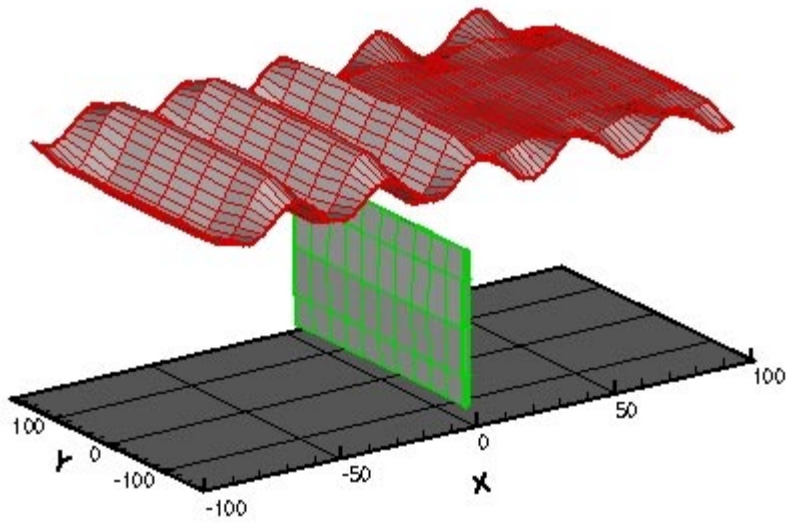


Figure 5.3 (a) - Free Surface Elevation for $\omega=\omega_n=1.25$ rad/s
(304.8 m Breakwater, $\beta=0^\circ$, $t=0$)

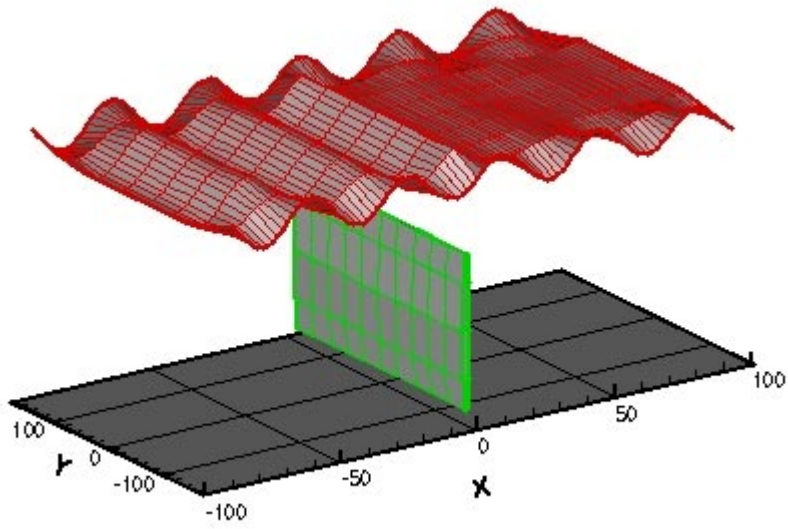


Figure 5.3 (b) - Free Surface Elevation for $\omega=\omega_n=1.25$ rad/s
(304.8 m Breakwater, $\beta=0^\circ$, $t=0.2T$)

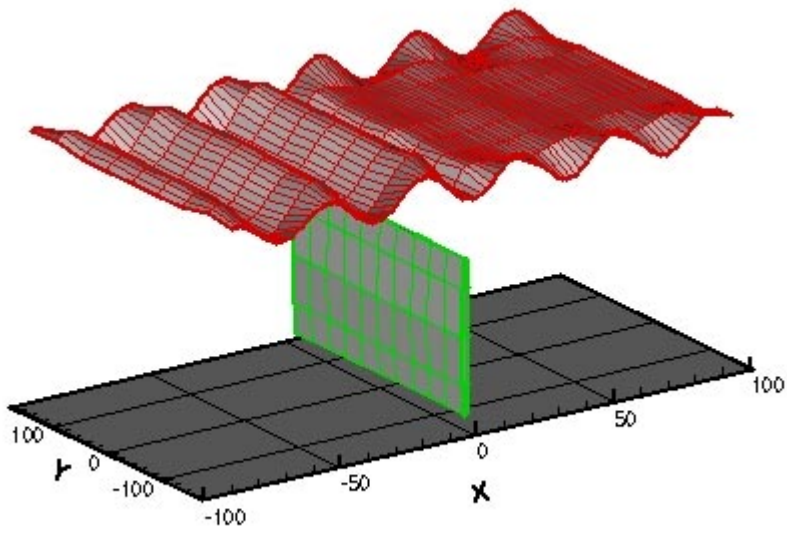


Figure 5.3 (c) - Free Surface Elevation for $\omega=\omega_n=1.25$ rad/s
(304.8 m Breakwater, $\beta=0^\circ$, $t=0.4T$)

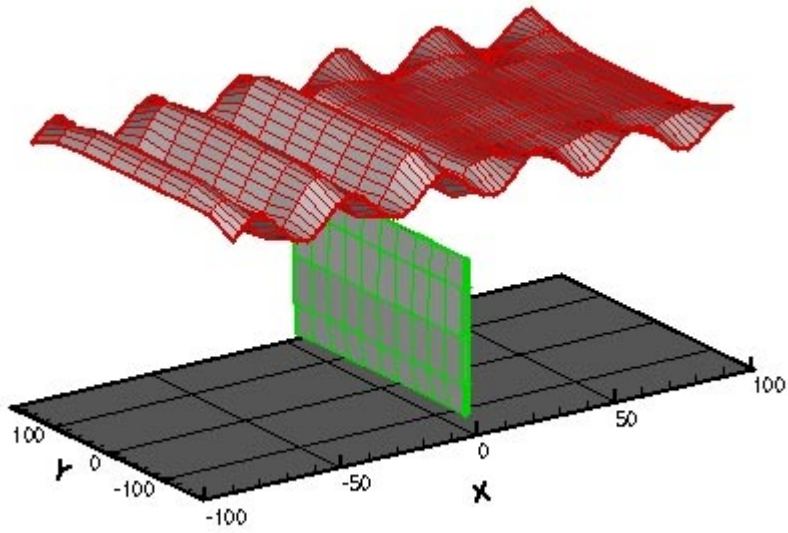


Figure 5.3 (d) - Free Surface Elevation for $\omega=\omega_n=1.25$ rad/s
(304.8 m Breakwater, $\beta=0^\circ$, $t=0.6T$)

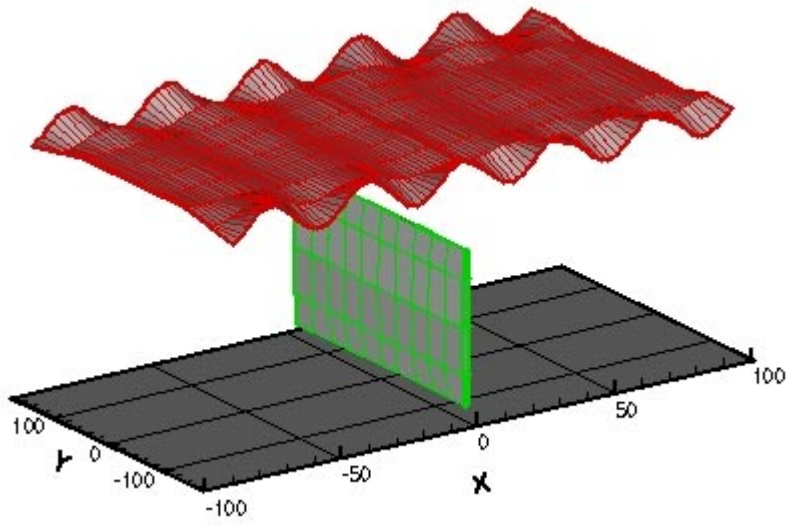


Figure 5.3 (e) - Free Surface Elevation for $\omega=\omega_n=1.25$ rad/s
(304.8 m Breakwater, $\beta=0^\circ$, $t=0.8T$)

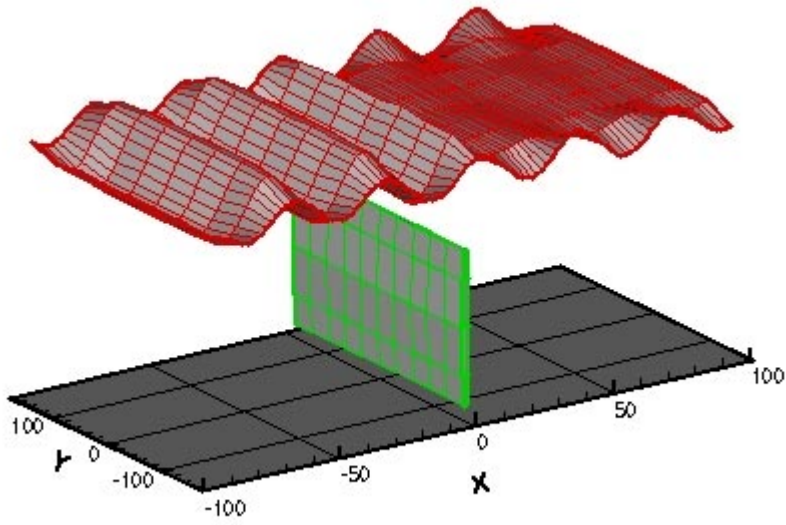


Figure 5.3 (f) - Free Surface Elevation for $\omega=\omega_n=1.25$ rad/s
(304.8 m Breakwater, $\beta=0^\circ$, $t=1.0T$)